

Modelling the Marine Boundary Layer for Offshore Wind Power Utilisation

Vom Fachbereich Physik der Universität Oldenburg zur Erlangung des Grades eines

Doktors der Naturwissenschaften (Dr. rer. nat.)

angenommene Dissertation.

Bernhard Lange

geb. am 27.9.1966

in Bremen

Erstreferent: Prof. Jürgen Parisi
Korreferent: Prof. Søren Larsen
Korreferent: Prof. Joachim Peinke
Tag der Disputation: 11.12.2002

Erklärung

Hiermit versichere ich, daß ich diese Arbeit selbständig verfaßt habe und keine anderen als die angegebenen Quellen und Hilfsmittel benutzt habe.

Bernhard Lange

Thanks

First of all I wish to thank my scientific supervisors at Risø, Jørgen and Søren, for their support the two years I was at Risø and especially for continuing this support thereafter. It is their scientific guidance and overview which directed this work.

The two years I was living in Denmark and working at Risø have a special place in my memory for being two of the most intense years of my life both personally and professionally. This was largely due to the open atmosphere combined with a truly professional work attitude of the group gathered in the Wind Energy Department, which made a large impression on me. I would like to thank all of them for so much fun and such a rewarding work environment! Apart from the research for this study, Risø and here especially Lars are thanked for giving me the opportunity of getting involved in so many other interesting wind energy projects.

Hakeem and Henrik are thanked for hosting me during my stay at DHI Water & Environment and for their support and co-operation ever since. It was a fascinating experience to work there and very much fun indeed to learn about waves and how to model them.

Although the largest part of this work was done at Risø, the last and probably most important part was done in Oldenburg. I wish to thank all my colleagues of the Energy Meteorology group for welcoming me back after the years abroad and especially Detlev and Igor for their wholehearted support for my work. Jürgen and Joachim deserve special thanks for accepting me as an extern PhD student with a topic slightly of their own research interests.

I would like to thank the EU Commission for the Marie-Curie-Fellowship which allowed me to work at this PhD at Risø for two years and Gregor for his example of combining a EC grant with a PhD, which smoothed the way for me. Special thanks to Barry Robertson from the EC for organising the inspiring Marie-Curie Grant Holders Conferences and to the other grant holders for the fun we had.

Working together with scientists from all over Europe has been one of the most interesting experiences of this work. I wish to thank the teams of the two EU funded research projects I was involved in, the POWER and the ENDOW projects, and especially to Rebecca for introducing me into the POWER team.

The work done here heavily relies on the offshore measurement data, especially from the Rødsand site. Many people are necessary to run such a measurement. I wish to thank Jørgen, Rebecca, Peter, Mike, Ole, Anker and Mr. Kobbarnagel for their engagement in collecting these data. Per and Jan from SEAS had an open ear for the requests for additional costly repairs and service of the measurement equipment.

The end of this thesis is the special place reserved for my thanks to Telsche, who went with me all the way from the very beginning of the work to here. Her understanding, support and occasional gentle push helped to make all the difference between work and experience, between exile and adventure, between coping and enjoying. Without her I wouldn't have done it.

Contents

1	GENERAL INTRODUCTION	1
2	EVALUATION OF THE WIND RESOURCE ESTIMATION PROGRAM WASP FOR OFFSHORE APPLICATIONS	4
	Abstract	4
2.1	Introduction	4
2.2	WAsP	5
2.2.1	The wind resource estimation program WAsP	5
2.2.2	WAsP for offshore conditions	5
2.3	Measurements	7
2.3.1	Sites	7
2.3.2	Instrumentation and data analysis	9
2.4	Wind resources	11
2.5	Influence of the sea fetch	13
2.5.1	Methodology	13
2.5.2	Direction dependent wind speed ratios	14
2.6	Wind speed profiles	17
2.7	Sensitivity analysis	20
2.8	Conclusion	23
	Acknowledgements	23
	References	24
3	THE DEPENDENCE OF SEA SURFACE ROUGHNESS ON WIND-WAVES	26
	Abstract	26
3.1	Introduction	26
3.2	The Rødsand field measurement program	28
3.2.1	Site	28
3.2.2	Instrumentation and Measurements	29
3.2.3	Derived measured quantities	31
3.2.4	Data corrections	36
3.2.5	Data selection	40
3.3	Observed trend in sea roughness	42
3.3.1	Trend of sea roughness with wave age	42
3.3.2	Trend obtained from cup anemometer measurements	43
3.3.3	Trend obtained for different fetch lengths	45
3.3.4	Trend obtained for an aggregated data set	46
3.4	Influence of self-correlation	48
3.5	Discussion of analysis method	52
3.5.1	Bin-averaging	52
3.5.2	Rough flow condition	54
3.6	Conclusion	58
	Acknowledgements	60
	References	60
4	THE INFLUENCE OF THERMAL EFFECTS ON THE WIND SPEED PROFILE OF THE COASTAL MARINE BOUNDARY LAYER	63
	Abstract	63
4.1	Introduction	63

4.2	The Rødsand field measurement program	64
4.2.1	Site	64
4.2.2	Instrumentation and Measurements	65
4.2.3	Data processing	66
4.2.4	Air temperature measurements over land	68
4.3	Prediction of wind speed profiles with Monin-Obukhov theory	68
4.3.1	Influence of stability on the vertical wind speed profile	68
4.3.2	Influence of roughness on the vertical wind speed profile	74
4.3.3	Average deviations	76
4.4	The inhomogeneous flow regime in the coastal zone	77
4.4.1	Qualitative description of the flow regime	77
4.4.2	Qualitative comparison with Rødsand data	78
4.4.3	Comparison of the Rødsand data with theoretical approaches	82
4.5	Conclusion	86
	Acknowledgements	87
	References	87
5	IMPORTANCE OF THERMAL EFFECTS AND SEA SURFACE ROUGHNESS FOR OFFSHORE WIND RESOURCE ASSESSMENT	90
	Abstract	90
5.1	Introduction	91
5.2	The Rødsand field measurement program	93
5.3	Extrapolation with Monin-Obukhov theory	95
5.3.1	Derivation of Monin-Obukhov length	95
5.3.2	Sea surface roughness	96
5.3.3	Comparison of predicted and measured wind speed profiles	98
5.4	Correction of the Monin-Obukhov wind speed profile for coastal influence	103
5.4.1	Description of the flow regime	103
5.4.2	Prediction of the inversion height	103
5.4.3	Development of a simple correction method	105
5.5	Predictions of power production	108
5.5.1	Comparison of different methods	108
5.5.2	Comparison with results from a longer time series	112
5.5.3	Comparison with the wind resource estimation program WAsP	113
5.6	Conclusion	114
	Acknowledgements	116
	References	116
6	SUMMARY AND CONCLUSION	119
	CURRICULUM VITAE	122
	PUBLICATION LIST	123

1 General Introduction

Offshore wind power utilisation is developing fast and is expected to make an important contribution to the power production in the European Union and especially in Germany in the near future. The European Union has adopted a directive for the promotion of renewable energy sources as part of its policy on reducing CO₂ emissions. The target set by the directive is to increase the share of renewable energies in the total energy consumption from currently 6% to 12% by 2010. An important share of this increase is expected to come from offshore wind power. In Germany, a sizeable offshore industry is developing. Currently applications for building licences for more than 20 GW offshore wind power capacity are pending.

To build and operate a wind farm offshore is more costly than on land. Only the higher wind resource compared to land sites can make offshore wind farms economically feasible. This wind resource has to be quantified as precisely as possible. An uncertainty in the estimation of the annual mean wind speed of 5% leads to 10% uncertainty in annual energy production – which might make the difference between 10% return on investment and none. On the other hand, measurements at offshore locations are scarce and measurements at heights of prospective wind turbines are particularly rare. Subsequently, actual knowledge about the offshore wind regime is comparatively small.

This thesis is therefore concerned with modelling the structure of the marine atmospheric boundary layer, with focus on effects, which are important for wind resource assessment. Data from the offshore measurement program Rødsand in the Danish Baltic Sea have been analysed. Basic meteorological research has been undertaken in two areas of major importance for marine boundary layer modelling: The aerodynamical roughness of the surface and the influence of atmospheric stability on the flow in the coastal zone.

The sea surface roughness is one of the most important quantities for the description of the physical processes on both sides of the air-sea interface. It describes the momentum transfer from the marine atmospheric boundary layer to the wind driven water waves and currents, which is important for all processes of air-sea interaction such as wind wave growth, storm surges and atmospheric circulation. Unlike land surfaces, the aerodynamic roughness of the sea is not constant, but depends on the wave field present. The standard modelling approach is the Charnock relation, which relates sea surface roughness and friction velocity. Since no direct properties of the wave field are used, this approach requires that wind and waves are in equilibrium. This can often be assumed for the open ocean, but not in coastal waters, where the waves are fetch-limited. During the last 30 years different attempts have been made to establish a relationship between the sea surface roughness and properties of the wave field like wave height, wave steepness or wave age. So far no consensus has been reached. Most often wave age is used as property of the wave field, but also within this approach conflicting parameterisations coexist. It is even unclear if roughness increases or decreases with wave age. Therefore this thesis concentrates on improving the knowledge of the difficulties in finding such parameterisations. Their significance and usefulness, especially for wind power applications, is investigated.

Thermal effects are the second major influence on the coastal marine boundary layer. They are known to have a larger effect on the wind resource offshore than on land.

The reason is that the different thermal behaviour of water together with the low surface roughness allows for a thermally stratified surface layer even at high wind speeds. The influence of moderately stable and unstable stratification on the wind flow is usually described with Monin-Obukhov theory, which predicts a log-linear vertical wind speed profile. Although developed from measurements over land, the theory has been found to be generally applicable over the open sea. In the coastal zone, where the proximity of the coast influences the flow, the situation becomes more complex. The coastline constitutes a pronounced change in roughness and surface heat transfer and causes a strong inhomogeneity to the flow, which may limit the applicability of Monin-Obukhov theory. With airborne measurements and mesoscale modelling it has been shown that thermal effects from the coastal discontinuity can influence the flow field of the complete Baltic Sea. Such mesoscale flow modifications lead to a modified vertical wind speed profile deviating from Monin-Obukhov predictions. Although the existence of such phenomena has been shown in several case studies, their importance for wind power applications is largely unknown. In this thesis the climatological significance of thermal effects is investigated with the use of the Rødsand data. Furthermore, a hypothesis is formulated to explain the findings and a simple correction model is presented.

The structure of the thesis is as follows. Following this introduction, chapter 2 is an evaluation of the state of the art in offshore wind resource modelling for wind power applications.¹ The WASP program is used to estimate the wind climate at three measurement sites in the Danish Baltic Sea. The two main suspects for the observed deviations are sea surface roughness and thermal effects. The models used for these effects in WASP are very simple and more advanced approaches are explored in the basic meteorological research in the following two chapters, which are the core of this thesis.

A more advanced empirical model for the sea surface roughness is investigated in chapter 3.² It extends the Charnock relation by a parameterisation of the Charnock parameter with wave age. Simultaneously measured meteorological and oceanographic data from the Rødsand measurement program are used. An important part of the work is the investigation of the impact of self-correlation (spurious correlation) on the proposed wave age model, which is crucial for the significance and usefulness of this approach.

The influence of thermal stratification on the vertical wind speed profile is studied in chapter 4.³ The measured wind shear at the Rødsand measurement station is compared to the predictions of Monin-Obukhov theory. Thermal effects due to the coastal discontinuity, which limit the applicability of the theory, are identified. Their significance for the wind regime at the Rødsand site is analysed.

¹ This chapter has also been published as: Lange, B. and J. Højstrup: Evaluation of the wind-resource estimation program WASP for offshore applications. *Journal of Wind Engineering and Industrial Aerodynamics*. Vol.89 (2001), issue 3-4; pp.271-291

² This chapter has also been submitted for publication to *Journal of Physical Oceanography* as: Lange, B., H. K. Johnson, S. Larsen, J. Højstrup, H. Kofoed-Hansen: The dependence of sea surface roughness on wind-waves.

³ This chapter has also been submitted for publication to *Boundary-Layer Meteorology* as: Lange B, Larsen S, Højstrup J, Barthelmie R.: The influence of thermal effects on the wind speed profile of the coastal marine boundary layer.

The results of the more basic meteorological research of chapters 3 and 4 are used in chapter 5 in an example application. Here the wind speed at hub height and the wind turbine power production at Rødsand are estimated from the wind measurements at 10 m height. The importance of the different effects is investigated by comparison with the measured wind speed. To quantify the effect of thermally induced flow modifications in the coastal zone a simple correction method for the vertical wind speed profile is developed. Conclusions are drawn in chapter 6.

Chapters 2 to 4 of this thesis have been published or submitted for publication in international journals together with several co-authors. The co-authors contributed with ideas, comments, discussions and by making a large amount of unique measurement data available, while all calculations, analysis and text in this thesis are done by myself.

2 Evaluation of the wind resource estimation program WAsP for offshore applications⁴

Abstract

The increasing interest in harvesting offshore wind energy requires reliable tools for the wind resource estimation at these sites. Most commonly used for wind resource predictions on land as well as offshore is the WAsP program. It has been validated extensively for sites on land and at the coast. However, due to the lack of suitable measurements there is still a need for further validation for offshore sites. Data from ongoing measurements at prospective wind farm sites in the Danish Baltic Sea region are available now. The wind resources estimated from these measurements are compared to WAsP-predictions. They agree well. The only deviation found is for two sites, which are located at about the same distance, but on different sides of the island Lolland. Here the measurements show a difference in the wind resources, which is not predicted by WAsP.

A direction dependent comparison explains this deviation. Wind speed ratios of several pairs of stations are modeled with WAsP for 12 directional sectors and compared with the measurements. Deviations in the directional wind speed predictions were found to correspond with the length of the sea fetch: For smaller sea fetches WAsP seems to slightly over-predict the wind speed, while for long fetches of more than 30 km an under-prediction is found. An analysis of the vertical wind speed profiles at three sites indicates that a combination of different effects is responsible for the correlation between sea fetch and model behavior. Effects of atmospheric stability as well as a fetch dependent sea surface roughness have to be taken into account.

2.1 Introduction

Suitable sites for wind farms on land are scarce in some regions in Europe, while potential areas for offshore sites are huge. Additionally, the wind resource offshore is much better than on land. Therefore the interest in developing offshore sites for wind energy utilization has been growing in recent years and it is expected that an important part of the future expansion of wind energy utilization at least in Europe will come from offshore sites.

However, compared to land sites the economic viability of offshore wind farms depends on the compensation of the additional installation cost by a higher energy production. A reliable prediction of the wind resource at offshore sites is therefore crucial for project planning and siting.

The wind resource prediction model WAsP [2.1] of the European Wind Atlas [2.2] is the standard method for wind resource predictions on land as well as offshore. It has been validated extensively for land conditions. A validation study for coastal stations was performed by inter-comparisons of wind measurements at different heights from high meteorological masts close to the sea [2.3]. No significant deviation was found.

⁴ This chapter has also been published as: Lange, B. and J. Højstrup: Evaluation of the wind-resource estimation program WAsP for offshore applications. *Journal of Wind Engineering and Industrial Aerodynamics*. Vol.89 (2001), issue 3-4; pp.271-291

Only very few measurements are available for a validation of WAsP for offshore sites. A comparison with data taken from the Vindeby offshore wind farm showed reasonable agreement with a slight over-prediction of the wind speed at Vindeby [2.4].

With the new data from offshore masts an evaluation of WAsP is attempted for the use in offshore applications. The aim is to evaluate the limits of applicability of the model. It is not the intention of this study to improve WAsP.

In Denmark plans are going ahead to install 4000 MW offshore wind turbines by the year 2030. In the current planning phase offshore wind measurements are being made at several prospective wind farm sites. Measurements located in the confined Danish waters of the Baltic Sea near the islands of Lolland and Falster at distances of about 10 km from the coast are used to investigate wind characteristics and estimate wind speeds and power productions for planned wind farms [2.5].

The data presently available from these measurements are used in this study together with data from the Vindeby offshore wind farm, which is located about 2 km from the coast. Thus the measurements cover the distances most likely encountered in the planning of bottom mounted offshore wind farms.

2.2 WAsP

2.2.1 The wind resource estimation program WAsP

The Wind Analysis and Application Program WAsP contains models for the vertical extrapolation of wind data taking into account sheltering of obstacles, surface roughness changes and terrain height variations. These models are used twice in the process of predicting the wind resource at a site from wind measurements at a different site. First a regional wind climatology is calculated from a measured time series of wind speed and direction, i.e. wind speed distributions for 12 directional sectors for the geostrophic wind are calculated. It is then assumed that the geostrophic wind climate is representative also for the predicted site. The WAsP models are then used to predict the wind resource for the prediction site from the wind climatology calculated in the first step. The output consists of predictions of Weibull wind speed distributions in 12 directional sectors.

2.2.2 WAsP for offshore conditions

In comparison to land conditions modeling of the wind resource in coastal waters is complicated by a combination of several effects:

The favorable wind resource offshore is mainly caused by the low surface roughness of water areas. Contrary to land conditions, the sea surface roughness is not constant but depends on the wave field present. This in turn is governed by the momentum exchange process between wind and waves which depends on wind speed, water depths, distance from the shore, atmospheric stability, etc.

For fully developed wind waves the dependence on wind speed can be modeled with the Charnock model [2.6]. It describes the sea surface roughness as a function of wind speed, but independent of fetch. In the confined waters around the measurement sites the waves are mainly fetch limited and the length of the upwind sea fetch might also be important for the sea surface roughness [2.7], [2.8]. In the WAsP model this

complex dependency is approximated by an average value of 0.2 mm for the sea surface roughness. No dependency on wind speed or fetch is taken into account. During the development of the WAsP model it was found that the results of this simple approach could not be improved by the use of the Charnock equation [2.2], but very little offshore data was available for verification at the time.

The atmospheric stability is the second parameter, which differs greatly between land and water areas. The main difference is that on land we see a significant daily variation of stability whereas offshore the large heat capacity of the water dampens out the daily variations to a very low amplitude. Instead we see a quite marked yearly variation, because the temperature of the water lags behind the air temperature. The atmospheric stability has an influence on the vertical momentum transport, which is reflected in the vertical wind speed profile (see e.g. [2.9]). It also influences the growth of the internal boundary layer after the land-sea roughness change. In the WAsP model the atmospheric stability is taken into account as a perturbation of the logarithmic wind speed profile. The mean vertical heat flux and its variability are used to characterize the atmospheric stability. Land and water surfaces are distinguished by different values for these quantities. An interpolation between land and sea areas is used in a transition zone of 10km on both sides of the coastal discontinuity. Land and water areas are distinguished in the model by their roughness values.

Roughness changes are described by an internal boundary layer (IBL) approach. The IBL model does not depend on the atmospheric stability, i.e. no difference is made between an IBL over land and over water, although it is well-known that stability plays a major role in the development of the IBL (see e.g. [10]).

The model describes the height of the influence of a roughness change by two limits. Below the lower limit the height profile is determined by the new roughness behind the roughness change, above the higher limit is determined by the old roughness and in between the two limits a transitional profile is assumed.

For the measurement stations used here the fetch is between 1.4 and 100 km and the measurement heights between 10m and 50m. The IBL heights versus distance to the roughness change are shown in Figure 2.1. It can be seen that for offshore stations with a measurement height of 10 m the land influence vanishes at a fetch of 1km in the model. At a measurement height of 50 m this is the case at a fetch of 5km.

This means that roughness changes with a distance to the site of more than 5 km have no influence on the calculations made with WAsP.

A detailed analysis of the influence of the atmospheric stability in the coastal zone has been performed in [2.11] with the Vindeby data. A comparison with WAsP and a discussion of the performance of the atmospheric stability models of WAsP can be found in [2.12]. Modifications of the model parameters of WAsP only lead to small improvements in the prediction accuracy. The focus of the investigation here is laid on the question if the length of the upstream sea fetch has an influence on the prediction accuracy of the WAsP model. With the new measurements now available, a wide range of sea fetch distances is available for this investigation.

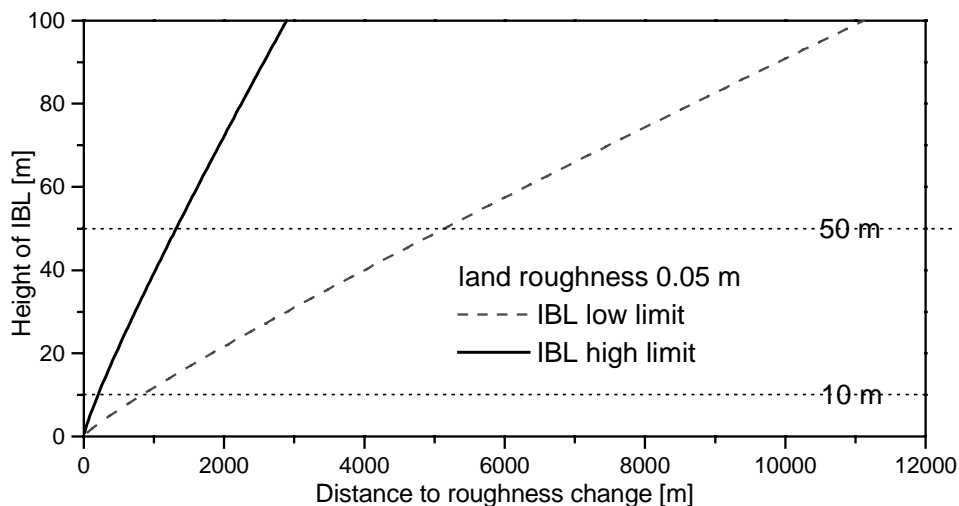


Figure 2.1: Height of IBL behind a roughness change versus the distance to that change as modeled by WAsP

2.3 Measurements

2.3.1 Sites

Measurements are made with several meteorological masts on and around the islands of Lolland and Falster in Denmark. The locations of the sites used here are shown in Figure 2.2 and Figure 2.3. The coordinates are given in Table 2.1. The measurements at Vindeby sea mast west (SMW), Vindeby sea mast south (SMS), Omø Stålgrunde and Rødsand are measurements from offshore meteorological masts. The measurement at Vindeby land mast (LM) is an accompanying measurement at the coastline. Long term meteorological measurements from the station Tystofte on Sjælland are also used.

The Vindeby masts SMW, SMS and LM are situated near the Vindeby offshore wind farm about 1.5 to 2 km off the north coast of Lolland (Figure 2.3). The wind farm consists of 11 Bonus 450 kW turbines. For a detailed description of the wind farm see [2.13].

The sites Omø Stålgrunde (hereafter abbreviated as Omø) and Rødsand are offshore sites located in the southeastern part of Denmark near the island of Lolland. Both sites have a distance of about 10 km to the nearest land. Omø is located to the north of Lolland near the Vindeby site, while Rødsand is situated southeast of Lolland (Figure 2.2).

The meteorological station Tystofte is a land measurement located in the southern part of Sjælland, about 5 km from the coast and 25 km from the Omø measurement site (Figure 2.2).

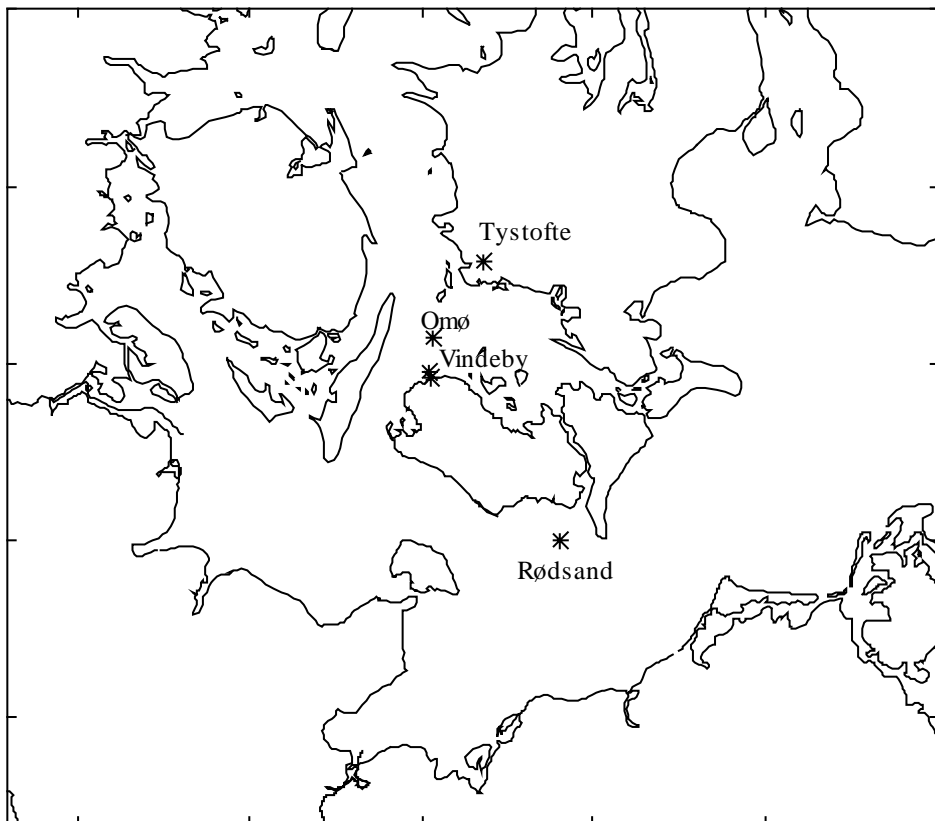


Figure 2.2: Locations of the measurement sites in the Baltic Sea in the southern part of Denmark

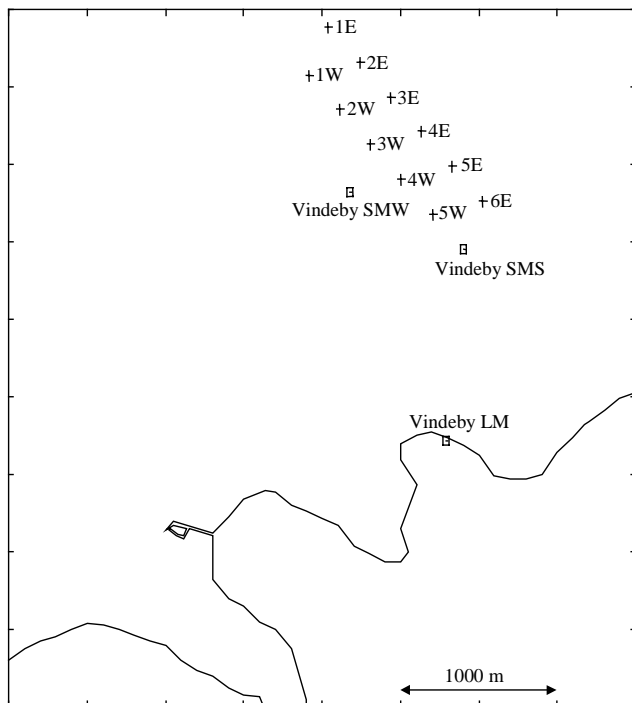


Figure 2.3: Layout of the Vindeby offshore wind farm and the measurement masts Vindeby SMW, SMS and LM.

Table 2.1: Location, time, heights of the measurements and influence of tower shade (the anemometer heights used in this study are marked with *)

Site	Location (UTM-32)	Time period of measurement	Height of anemometers	Sectors with tower shade
Vindeby SMW	636179 m E 6093319 m N	11/93 - 5/96	7, 20, 38, 48*	30, 60
		9/96 – 8/98	10*, 30*, 48*	30, 60
Vindeby LM	636793 m E 6091717 m N	5/93 - 5/96	7, 20, 38, 46*	150, 180
		9/96 – 9/98	10*, 30*, 46*	330, 0
Omø	636080 m E 6102600 m N	8/96 – 8/98	10*, 30*, 50*	90
Rødsand	677900 m E 6048300 m N	10/96 – 5/98	10*, 30*, 50*	60, 90

2.3.2 Instrumentation and data analysis

Wind speeds are measured by cup anemometers at different heights, which are listed in Table 2.1 along with the locations and measurement periods used. All anemometers are mounted on booms and wind direction sectors disturbed by tower shading are also given in Table 2.1. Data from these wind directions have been omitted. All data have been quality controlled by visual inspection of the time series. The estimated accuracy of the wind speed measurement is about 2%. Data logging has been made with 5 Hz sampling rate. All data have been averaged to half hourly mean values.

Wind speed measurements at the Vindeby masts are disturbed for some wind direction sectors by wakes of the turbines of the nearby wind farm. The measured wind speeds are therefore corrected for the shading effect of the turbines when they are bin-averaged for 30° wind direction sectors. Correction factors for the mean wind speeds are estimated with the wind farm modeling program FCalc [2.14]. Reductions of up to 7% for the SMW and 2% for the LM are predicted.

Figure 2.4 shows wind roses and wind speed histograms from the 4 measurement stations used.

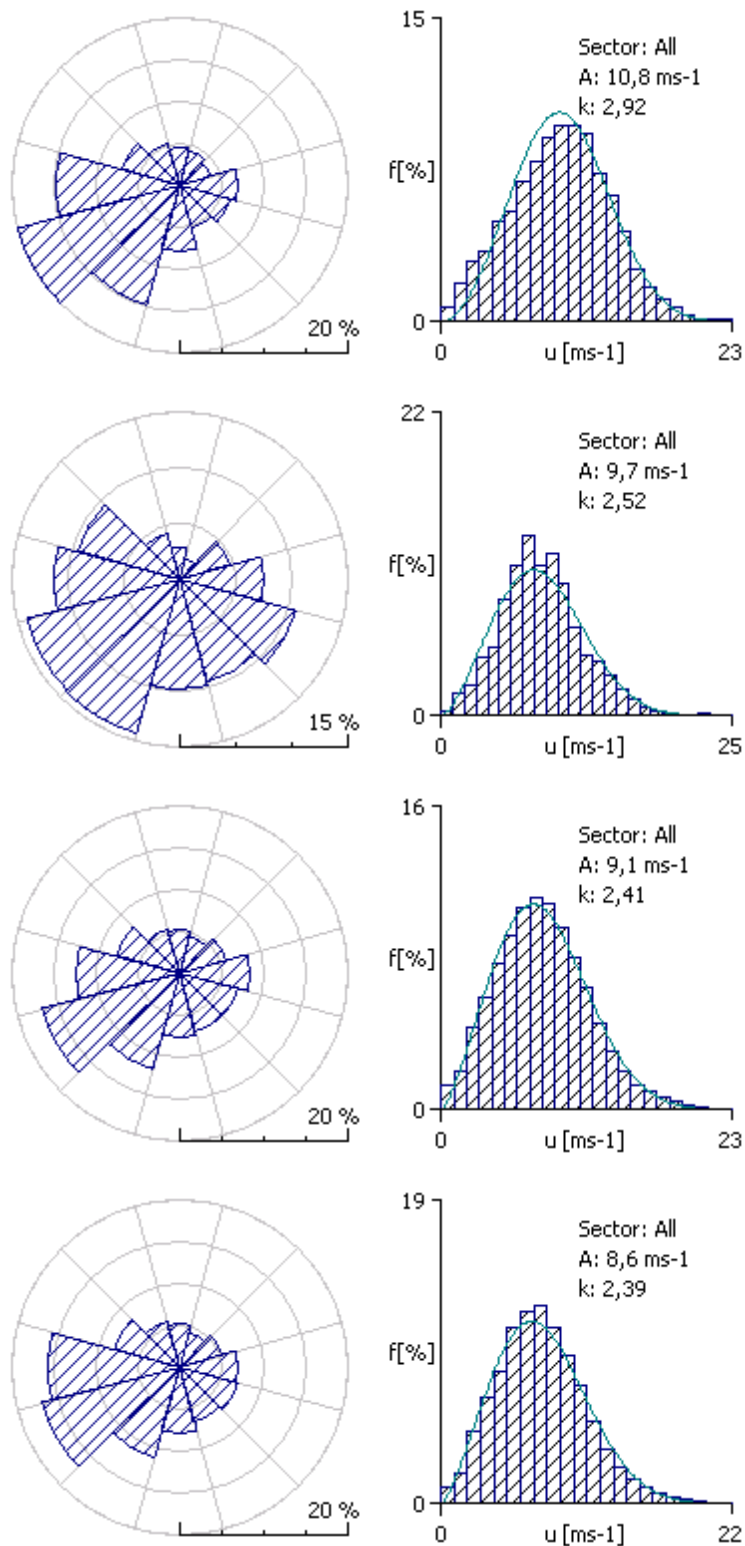


Figure 2.4: Wind roses and wind speed histograms (with fitted Weibull distributions) for (from top): Rødsand, Omø Stålgrunde, Vindeby SMW and Vindeby LM

2.4 Wind resources

The wind resource, i.e. the long-term mean wind speed, is estimated from the onsite measurements and compared to WASP-predictions. Deviations between the wind resource during the measurement period and the long-term average were corrected by correlation with the 14 year long time series from the station Tystofte. The estimation of the long term mean wind speeds from the measurements was done by a combination of different methods using all available measurements (see [2.5]).

It has to be kept in mind, however, that the measurements at Omø and Rødsand run intermittently with a total data set equivalent to only about 8 and 12 months, respectively. Even though they were corrected, this leaves some uncertainty of the estimated mean wind speeds. The uncertainty in the estimated long term average wind speed was judged to be +/- 5% for Omø and Rødsand and +/-2% for the other stations.

All stations are located either offshore or in very flat terrain. Height variations could therefore be neglected. Also, for none of the measurement sites a correction due to obstacles was necessary. Therefore only the roughness model has been used in this study. A roughness map with a simple roughness classification has been made for large areas surrounding the measurement sites. Three roughness classes are distinguished: water areas with roughness 0.0002m, predominantly agricultural areas with roughness 0.05m and woods and cities with roughness 0.4m. As an example the roughness map of the Vindeby site is shown in Figure 2.5.



Figure 2.5: Map of roughness change lines around the Vindeby and Omø Stålgrunde sites; the distance between the grid lines is 10km; roughness values used: 0.0m for water, 0.05m for agricultural areas and 0,4m for cities and forests

WAsP estimations were calculated using two different measurement stations as input:

- The Vindeby land mast, which is a coastal measurement at the Vindeby site. The predictions made with these measurements were corrected for deviations from the long-term average.
- The Tystofte station, which is a long term land measurement.

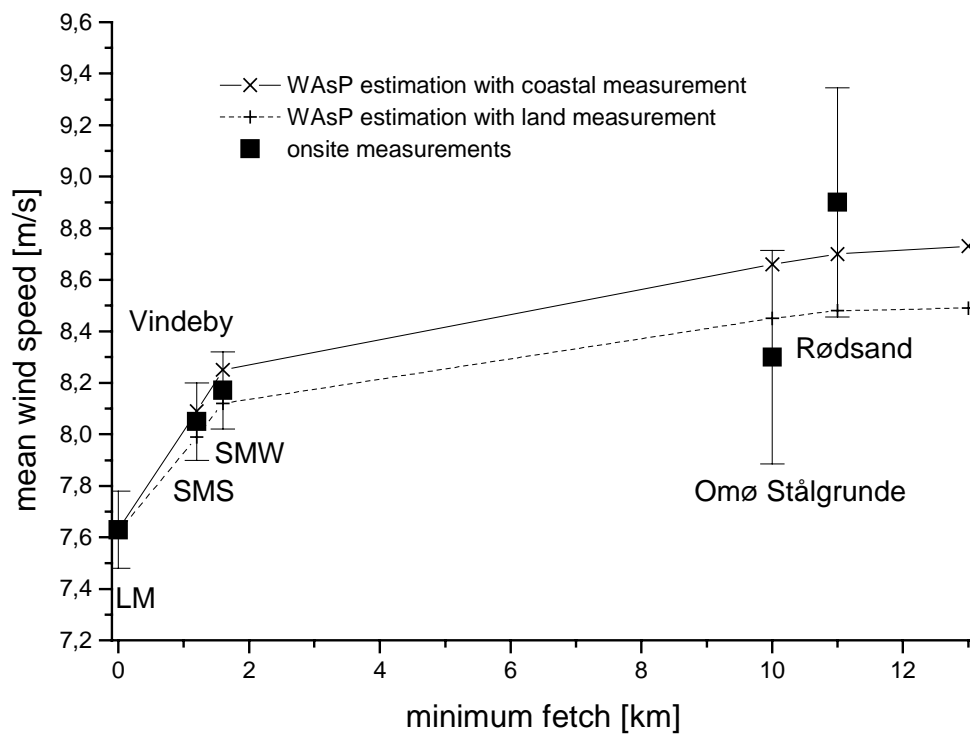


Figure 2.6: Long term mean wind speeds for a coastal and 4 offshore sites at 48 m height estimated from onsite measurements and predicted by WAsP on the basis of a coastal and a land measurement; additional points are shown (at maximum fetch) for WAsP predictions far offshore

Figure 2.6 shows the mean wind speeds of the sites versus their distances to the nearest coast, i.e. their minimum fetches. The points connected with lines are WAsP predictions; the squares are the estimations from the onsite measurements. The error bars indicate the estimated maximum uncertainties of the wind resource estimated from the measurements.

Deviations of the WAsP predictions from the estimations based on the onsite measurements are generally small, up to 5%. They are in the same range as the uncertainties in the wind speed estimations based on the onsite data. As expected, the mean wind speed rises with increasing distance to the coast. The largest increase in wind speed when going offshore from the coast is found for the first kilometers. The increase in wind speed between the coastal station (Vindeby LM) and the offshore sites in 10 km distance is about 10-15%.

For comparison WAsP predictions have also been made for conditions far away from any land. They are shown as additional points at maximum fetch in Figure 2.6. It can be seen that WAsP predicts only a very small influence of land for distances larger than about 10 km. The two sites Rødsand and Omø already almost reach that limit.

The WAsP predictions based on the coastal and the land measurements coincide at the site of the coastal station. For stations further away from the coast the predictions differ up to about 3% with the prediction based on the land measurement being lower than that based on the coastal measurement. For sites near the shore both predictions are very close to the measurement. Differences are only 1-2% and lie within the uncertainty range of the measured data. For the sites Omø and Rødsand, which have larger distances to the shore, the differences are still small (1-5%). However, a difference between these two sites is found in the measurements while WAsP predicts almost equal values.

2.5 Influence of the sea fetch

2.5.1 Methodology

The WAsP method uses measurements from one site (predictor) to estimate the wind resource at the predicted site. Within the model the measured directional wind speed distributions are described by Weibull functions. For short time series this procedure introduces an error due to deviations of the measured distribution from Weibull curves. To avoid this error the comparison is made for wind speed ratios rather than wind speeds. In this way the results are also largely insensitive to other wind direction dependent properties like the atmospheric stability, since such influences would be present at both stations under investigation.

Ratios of measured wind speeds from two different stations are made for 12 wind directional sectors. These are compared with the respective ratios from WAsP estimated wind speeds. With different fetches for the two stations the influence of the sea fetch can be investigated in its measured and modeled influence on the wind speed.

An example of the directional dependence of the wind speed ratio is given in Figure 2.7. The ratio is obtained by dividing the measured mean wind speed of Vindeby SMW by that measured at Vindeby LM. It is plotted versus the wind direction measured at Vindeby SMW. No corrections for wind farm shading have been applied here and the directional resolution is 3°.

The directions with mast shading are shown and the disturbance can clearly be seen. Also indicated are the directions of the 11 turbines from the Vindeby wind farm. The reduction of the wind speed due to the influence of the wakes can be identified.

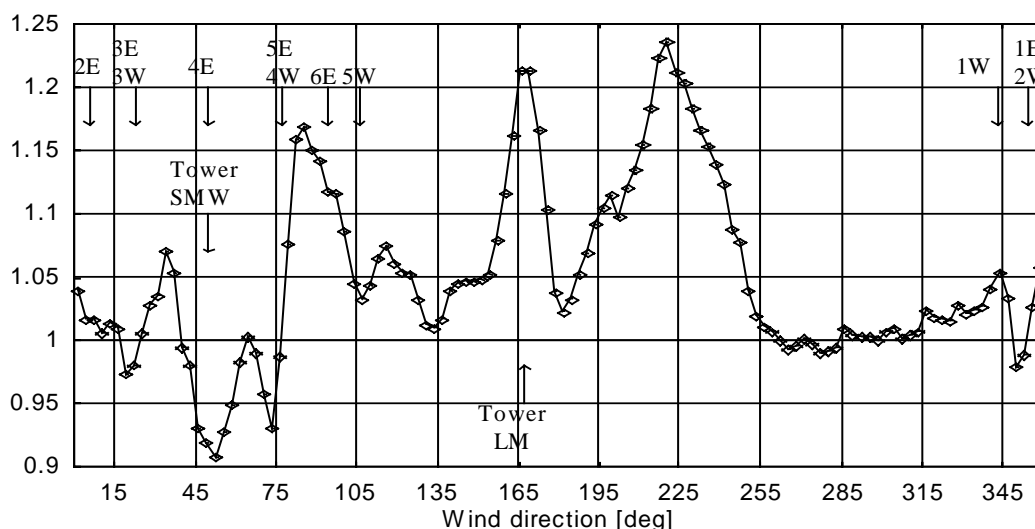


Figure 2.7: Measured ratios of mean wind speed Vindeby SMW / Vindeby LM; directional resolution 3°; directions of the turbines and measurement masts are shown with arrows

For the WAsP estimations of the wind speed ratios a common time series of wind speeds and directions is compiled for both stations. The measured data of one site are taken as input to WAsP to derive a wind climatology of the station itself and of the second measurement station. This is used to predict the sector-wise mean wind speeds for both sites. Subsequently the predictor and predicted station are exchanged and a new ratio calculated. The average ratio is used for comparison with the measurement (see Figure 2.8 to Figure 2.10). Differences between the two ratios were found to be negligible (<0.8%).

The ratios of the measured data are derived from the same time series as used for the WAsP predictions. The wind speeds of both stations are bin averaged in 30° bins with respect to the wind speed of one station. This is repeated with the wind direction of the other station and the average ratio is used for comparison. Wind direction sectors where the measurement is disturbed by mast interference are omitted. Uncertainties of the measured ratios are estimated as the average standard deviation of the means plus half of the difference of the two ratios calculated.

2.5.2 Direction dependent wind speed ratios

Examples for measured and WAsP estimated direction dependent wind speed ratios are shown in Figure 2.8, Figure 2.9 and Figure 2.10 along with the lengths of the sea fetches of the respective stations. The solid lines show the measured ratios and the dashed lines are WAsP predictions. Measured data with possible mast interference have been omitted.

Figure 2.8 shows the ratios of Vindeby SMW and LM. Vindeby SMW is located 1.6 km off the north coast of Lolland (Figure 2.3). Here the behavior of WAsP for small fetches can be investigated.

The measurements show two distinct maxima of the ratio, in directions which are roughly along the coastline. This situation leads to a large fetch difference since the SMW has long sea fetches while the LM has mainly land fetch. In between these maxima (sectors 120°-180°) SMW has a short sea fetch of only 1.4 to 3 km. For the

other directions both stations have similar long sea fetches and the ratio is close to one.

The WASP-predictions show generally the same directional pattern as the measurements. In most cases the deviations between measurements and WASP-predictions are small and the general behavior of the directional wind speed difference between the two stations is modeled well. Significant deviations are found only for the case with land fetch for LM and short sea fetch for SMW where WASP seems to over-predict the difference between the wind speeds on land and at sea.

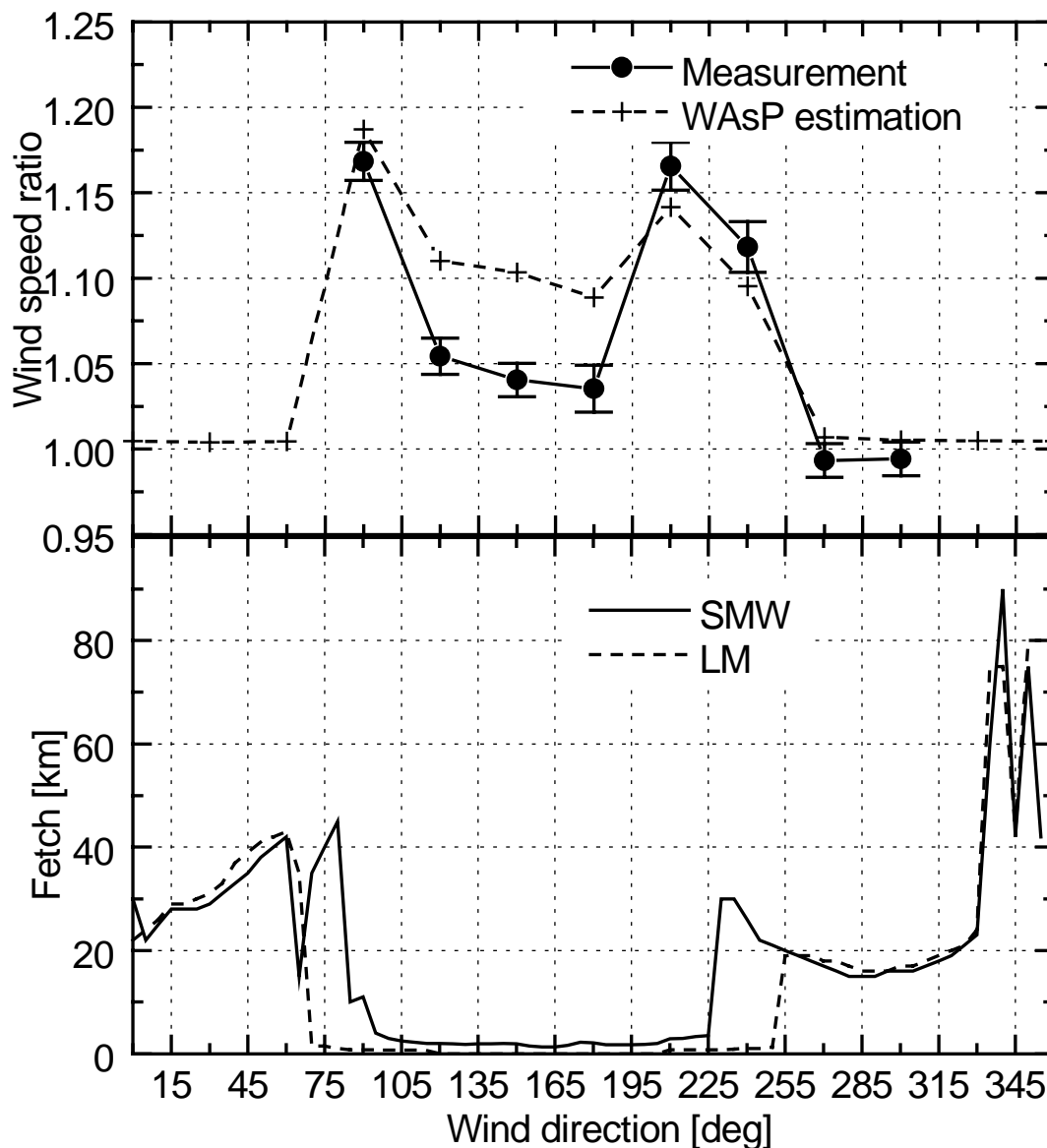


Figure 2.8: Vindeby SMW / Vindeby LM: Measured and WASP-predicted wind speed ratios (top) and sea fetches (bottom) versus wind direction

Figure 2.9 shows the results for the ratio between Omø and Vindeby LM. The overall situation at these sites is quite similar to the one for Vindeby SMW and LM, only that Omø is located about 10 km further offshore (Figure 2.3). 150° and 180° are the sectors with wind from Lolland and a sea fetch of about 10-15 km. Here WASP again over-predicts the difference between sea and land. The very rapid change of sea fetch length from 15 to more than 80 km at 200° seems to have an influence also on the

wind direction sector 180°. For the very long fetches at Omø at 120° and to a lesser extent at 210° and 240° WAsP under-predicts the difference.

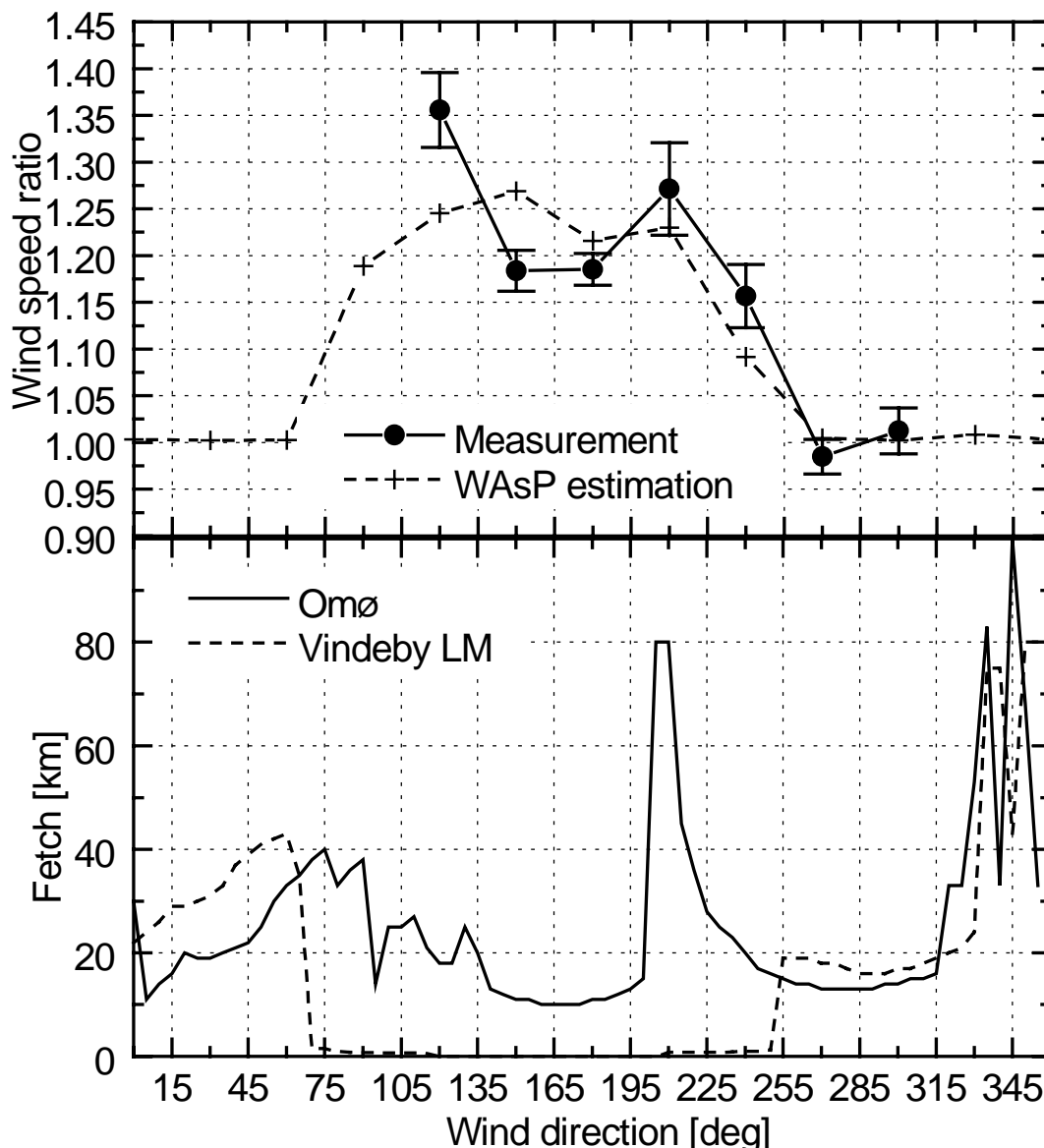


Figure 2.9: Measured and WAsP-predicted wind speed ratios versus wind direction from Omø / Vindeby LM (top) and sea fetches of Omø and Vindeby LM versus wind direction

In Figure 2.10 the ratios of the two offshore stations Omø and Rødsand are shown. Rødsand is located 11 km off the south coast of Lolland and the two sites are about 60 km apart from each other (Figure 2.2). A comparison of these sites gives the opportunity to study the measured and predicted differences for two offshore stations with very different fetches situations. The measurements show a minimum in the ratios at wind direction sectors 270° and 300° and a maximum at 330°. This corresponds closely to the very large sea fetches at Rødsand in directions 260° to 290° and at Omø at 330° to 350°. For the other directions the ratio does not deviate much from one.

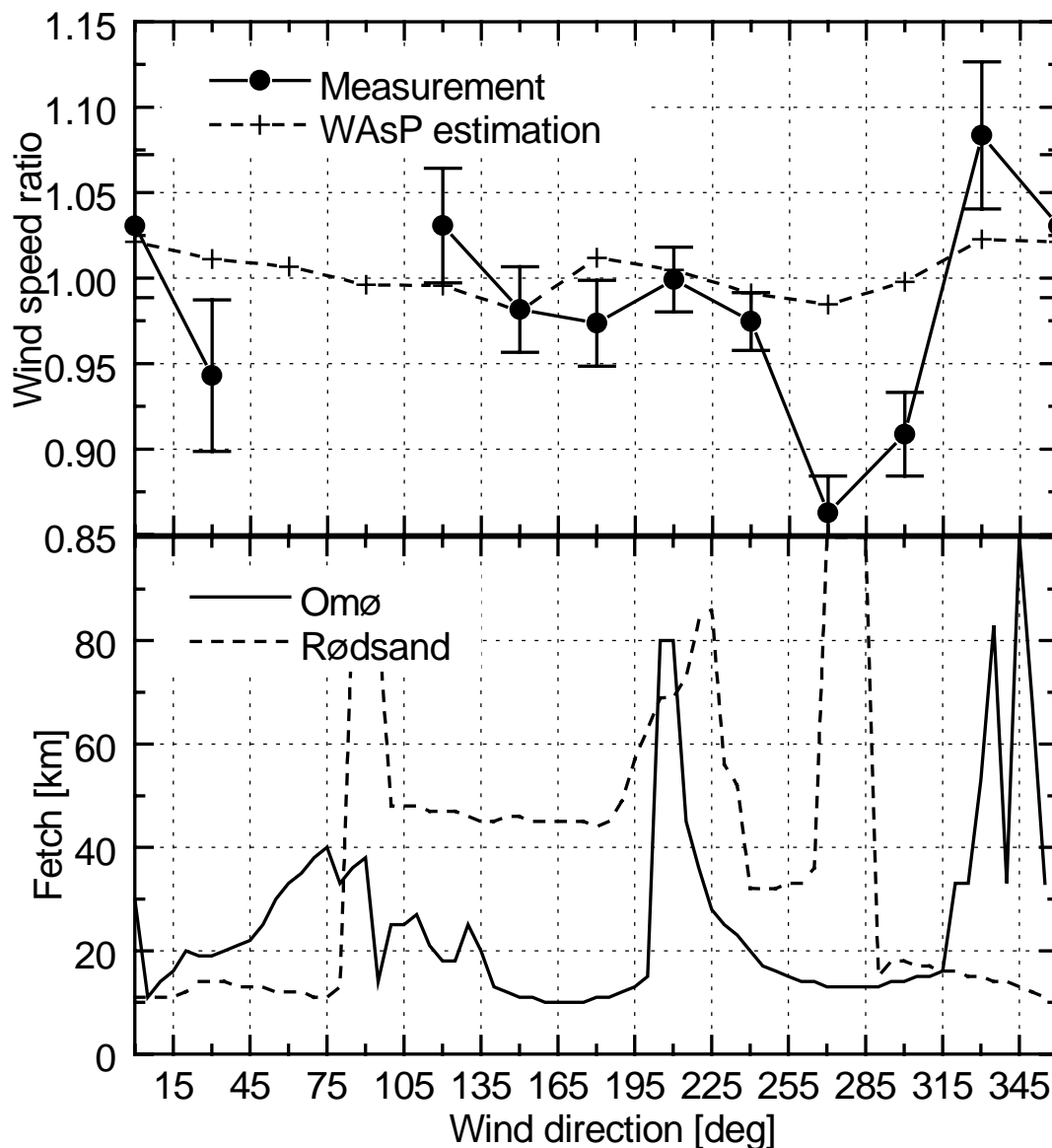


Figure 2.10: Omø / Rødsand: Measured and WAsP-predicted wind speed ratios (top) and sea fetches (bottom) versus wind direction

The WAsP-predictions show only very small deviations from unity. This leads to significant deviations of 6-12% from the measurements for the two cases mentioned. For the 30° sector a smaller deviation can be seen which can not easily be assigned to a fetch difference. For all other wind directions the deviations are in the order of the measurement uncertainty.

2.6 Wind speed profiles

To investigate possible causes for the deviations of the WAsP model measured and modeled vertical wind speed profiles are compared. Two pairs of stations have been used: Vindeby LM and SMW as well as Vindeby LM and Omø. Measurements are available at three heights: 10m, 30m and 50m (46m at LM, 48m at SMW). The wind speed measurements have been corrected for the effect of flow distortion caused by the measurement towers. The correction has been made with a procedure developed

for the Vindeby towers (see [2.15]). Data for wind directions where the tower was upwind of the anemometer were omitted.

WAsP calculations are made with the measured time series at Vindeby SMW at 48m and Omø at 50m height as input. Estimations are made for both sites at all heights.

In most cases WAsP predictions of the mean wind speeds as well as estimations of vertical wind speed profiles agree well with the measurements. Some examples of measured and modeled profiles are shown in Figure 2.11 and Figure 2.12.

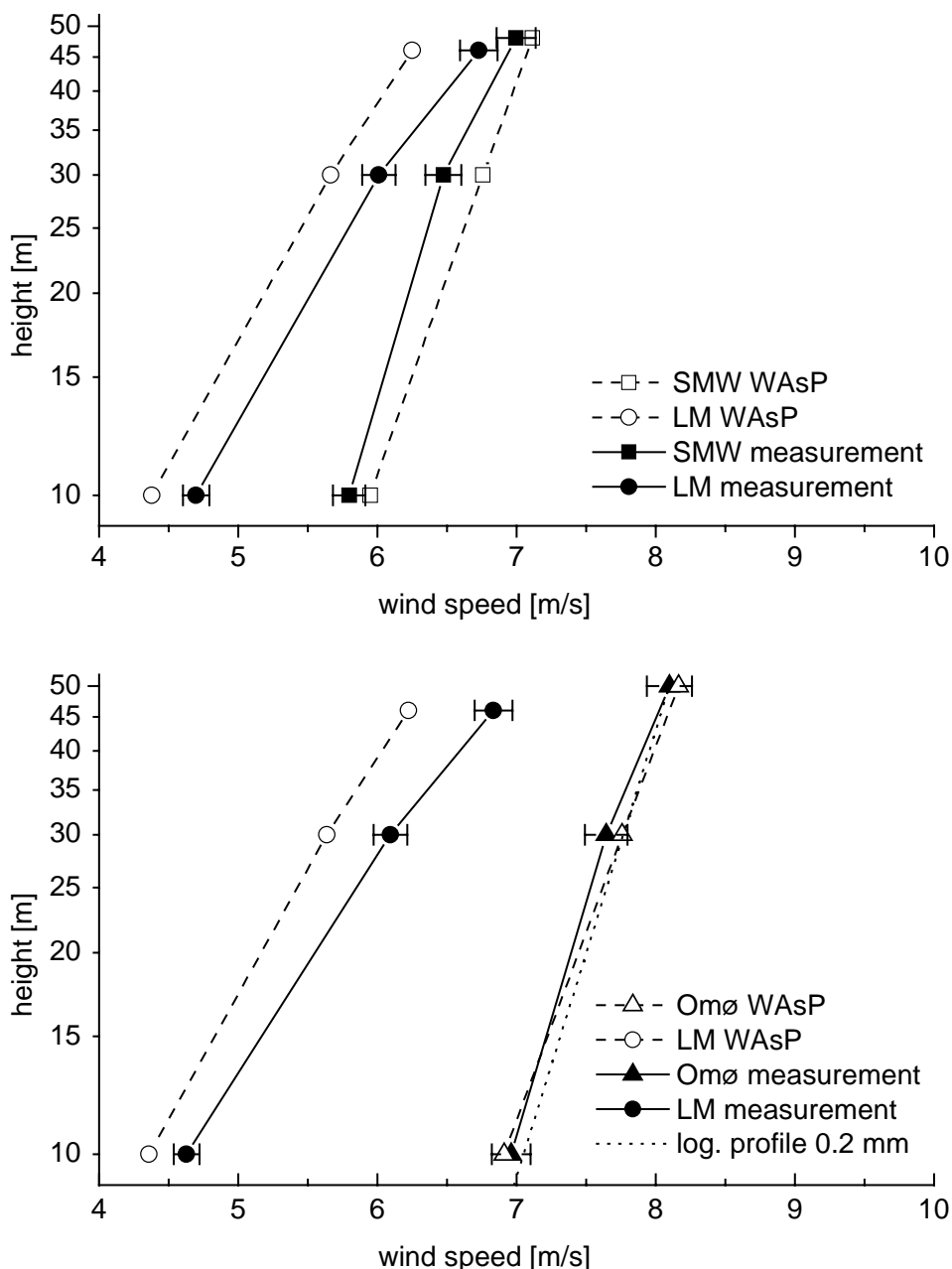


Figure 2.11: Measured and WAsP-predicted mean wind speeds for wind directions with land fetch situations (150° and 180° sectors) versus measurement heights (in logarithmic scale) for the two sites Vindeby LM and SMW (upper graph) and Vindeby LM and Omø (lower graph); the error bars show the 2% estimated uncertainty in the wind speed measurement

Figure 2.11 shows the case with wind blowing from land, i.e. Vindeby LM has land fetch, Vindeby SMW has about 1.6 km sea fetch and Omø has about 10 km sea fetch. The earlier comparison of the wind speed ratios showed that WAsP over-predicts the difference between LM and the offshore masts at 50 m height (Figure 2.8 and Figure 2.9). This is repeated in the profiles shown in Figure 2.11.

The profiles for the offshore stations are steeper (larger slope) than for the LM due to the difference in land and sea roughness. A comparison of the profiles from Vindeby SMW and LM clearly shows a wind speed difference that decreases with height. At the highest anemometer at 48 m the difference is only about 3%. This shows that at 1.6 km distance the influence of the land is still dominant at this height.

Comparing the wind speed profiles of Vindeby LM and Omø the same tendency can be seen, though to a lesser extent. As expected, the wind speed difference at the highest anemometer is larger than for the SMW, which shows that the internal boundary layer from the land-sea transition is higher and the wind is much less influenced by the land roughness.

Comparing the shape of the profiles, it can be seen that the WAsP-calculated profiles differ in steepness as well as curvature from the measured ones. This can also be seen in Figure 2.12, which shows the situation of land fetch for the LM and long sea fetches for both of the offshore masts (240° sector).

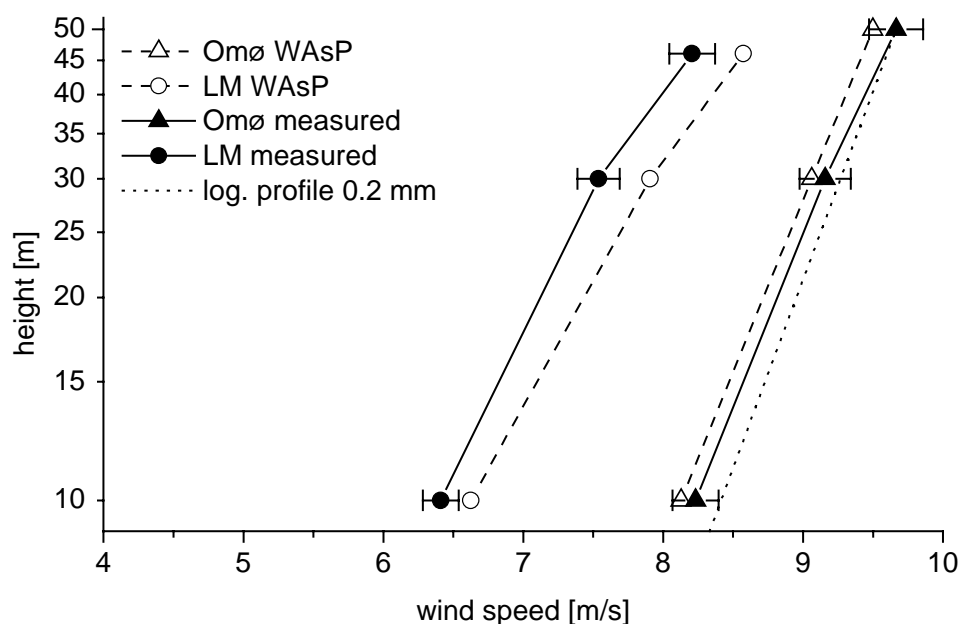


Figure 2.12: Measured and WAsP-predicted mean wind speeds for wind directions with different fetch situations (240° sector) versus measurement heights (in logarithmic scale) for the two sites Vindeby LM and SMW (upper graph) and Vindeby LM and Omø (lower graph); the error bars show the 2% estimated uncertainty in the wind speed measurement

2.7 Sensitivity analysis

For WAsP calculations only the measured data and roughness maps are needed as input. The roughness maps have to be made by estimating the roughness of the terrain. This roughness classification is to some extent subjective. Since different roughness estimates will have an influence on the calculations it is important to make a sensitivity study. The aim is to investigate if a different roughness estimation also qualitatively changes the results found.

Example calculations of direction dependent wind speed ratios and profiles have been made using different roughness maps. Two extreme roughness maps with very high and with very low – but still not completely unrealistic – roughness values for land areas have been prepared. The results of the WAsP calculation with these maps are compared with the results obtained with the original maps. The roughness length of water can not be changed in the WAsP model since here the value (0.0) is used as an indicator not only for the roughness (which is fixed as 0.2mm), but also for the heat fluxes over water.

For the wind direction dependent wind speed ratios the case of Vindeby LM and Vindeby SMW has been chosen as example. The roughness estimations for the two extreme roughness maps are shown in Table 2.2. The result of the calculations are shown in Figure 2.13.

Table 2.2: Roughness estimates for the sensitivity analysis of WAsP results on roughness map for wind speed ratio

original roughness lengths	low estimate	high estimate
0	0	0
0.05	0.03	0.1
0.4	0.2	0.5

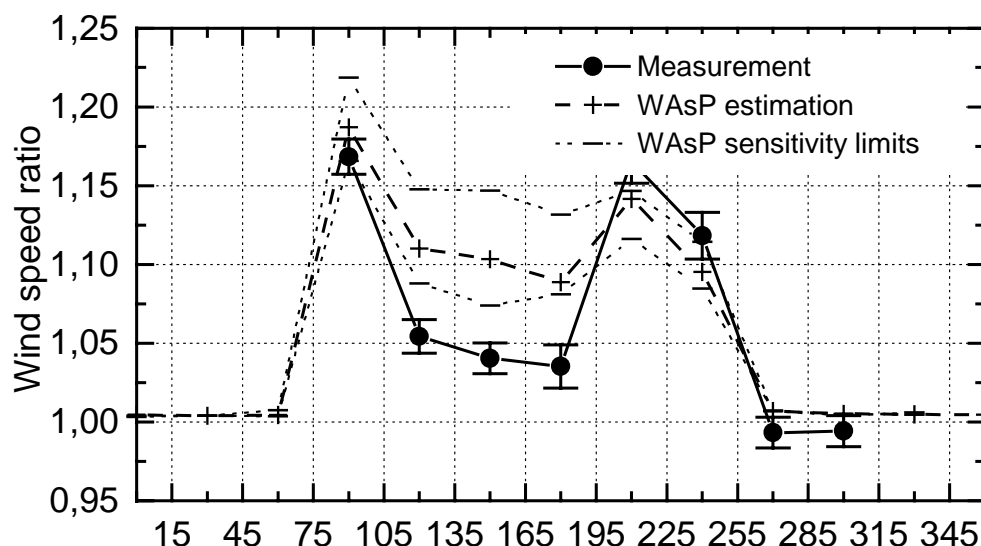


Figure 2.13: Sensitivity analysis: Measured and WAsP-predicted wind speed ratios versus wind direction from Omø / Vindeby LM; the calculations with WAsP were made with the original roughness description and two extreme high and low roughness estimates

The WAsP-predictions with all three maps show generally the same directional pattern. The significant deviations from the measurements found with the original maps for the land sectors (150°-210°) are also present for the calculations using the high and low roughness maps. The conclusion that WAsP seems to over-predict the difference between the wind speeds on land and at sea is qualitatively not questioned by a variation in roughness within the limits shown in Table 2.2. However, the choice of roughness has of course an influence on the magnitude of the over-prediction.

For the comparison of wind profiles the case of Omø Stålgrunde and Vindeby LM with wind from land (150° and 180°) has been chosen (see Figure 2.14). For the wind profile calculations a detailed map around the Vindeby stations was used. The roughness in this map has been changed as shown in Table 2.3.

Table 2.3: Roughness estimates for the sensitivity analysis of WAsP results on roughness map for wind profiles

original roughness lengths	low estimate	high estimate
0	0	0
0.01	0.005	0.02
0.05	0.03	0.1
0.1	0.05	0.15
0.15	0.1	0.25
0.25	0.15	0.3
0.3	0.2	0.5

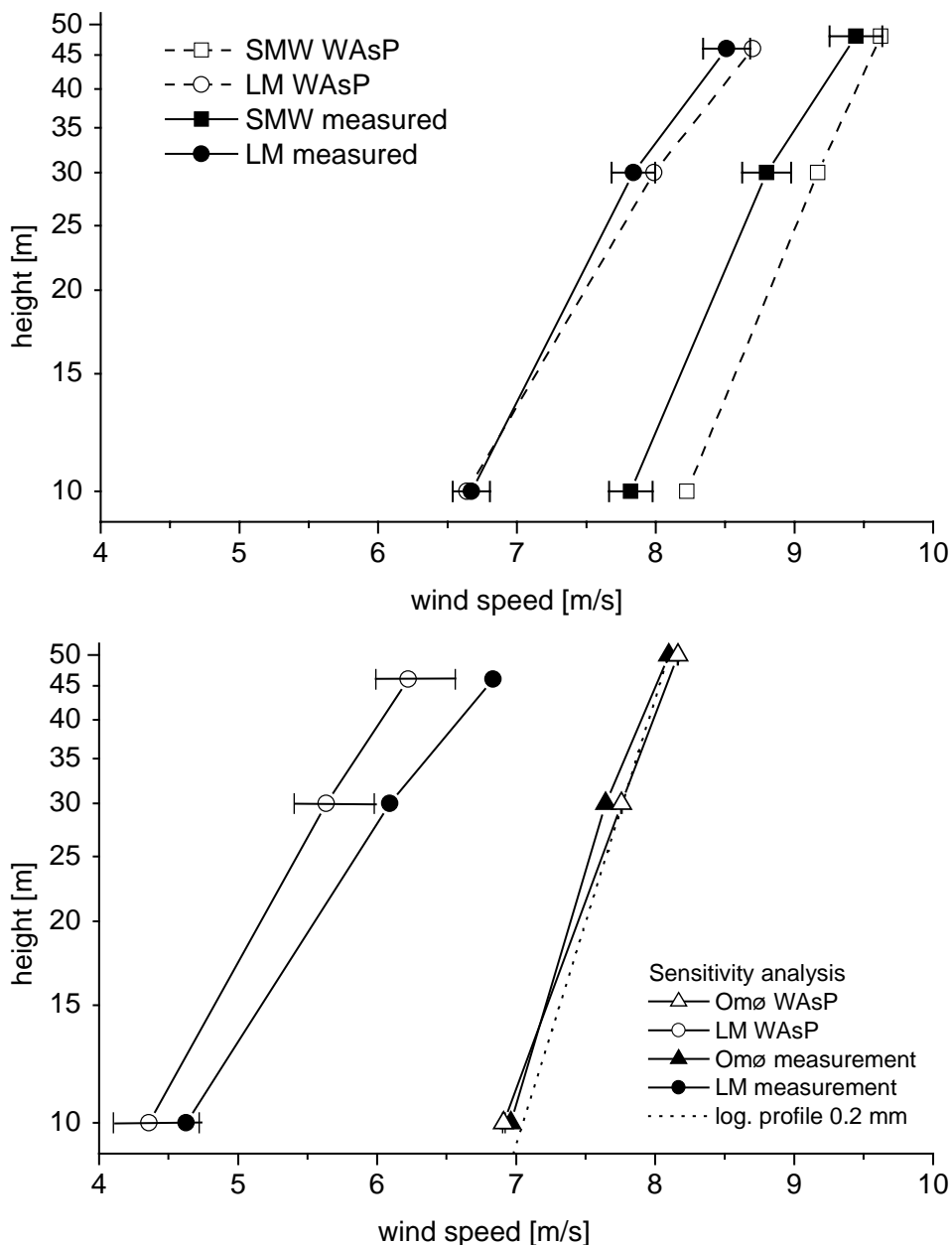


Figure 2.14: Sensitivity analysis: Measured and WAsP-predicted mean wind speeds for wind directions with land fetch situations (150° and 180° sectors) versus measurement heights (in logarithmic scale) for the two sites Vindeby LM and Omø; the error bars show the WAsP calculations with the two extreme high and low roughness estimates; measurement uncertainties are not shown here

It can be seen that the variation in roughness has a large influence on the calculations for Vindeby LM, while Omø Stålgrunde is not influenced. This reflects the fact that WAsP is not influenced by roughness changes at such large distances from land ($>10\text{km}$ for Omø Stålgrunde).

Comparing the different WAsP-calculated profiles of the Vindeby LM with the measured one reveals again that the wind speed quantitatively is influenced by the choice of roughness. However, the deviations both in steepness and curvature between measured and calculated profile do not depend on the choice of roughness map.

2.8 Conclusion

The data presently available from ongoing measurements in the Danish Baltic Sea have been analyzed and compared with predictions made with the wind resource estimation program WAsP. Measurements of a coastal and an inland station have been used for the predictions. It was found that the predictions of the long-term average wind resource are in good agreement with measurements.

The measurement indicates a small difference in wind resources between the stations Rødsand and Omø, which is not predicted by WAsP. A possible reason for this is the difference in the fetch situation. Omø is surrounded by land about 10 km distance to the south, west and northeast directions, while Rødsand has land at this distance only in the northern and north-eastern directions. The probability of wind from this direction is low (Figure 2.5). It also has long sea fetches in the most frequent westerly wind directions (Figure 2.2).

A direction dependent comparison of measured and predicted wind speeds allows comparisons between the different fetch situations. The investigation of the direction dependent wind speed also shows a generally good agreement between WAsP-predictions and measurements. However, for single wind directions significant deviations were found. These deviations show some correlation with the length of the upwind sea fetch. WAsP tends to over-predict the wind speed for situations with short sea fetches and under-predict it for long fetches. This effect explains the measured differences between the Omø and Rødsand sites. The very long fetches at Rødsand, which also occur in the prevailing wind direction lead to higher wind speeds compared to Omø. Since WAsP does not take these long fetches into account it under-predicts the wind resource at Rødsand. Fetches of more than 10 km (transition around coastal discontinuity) have no influence on the calculations (see chapter 2.2.2).

The comparison of measured and predicted height profiles shows deviations between modeled and measured profiles both in steepness and in curvature. This indicates that a combination of different causes is responsible for the deviations found for some wind directions. The modeled sea surface roughness can not solely be held responsible for the deviations. The growth of the internal boundary layer and the influence of the atmospheric stability also seem to play an important role.

In a sensitivity analysis WAsP results were tested for the dependency on the estimation of the terrain roughness description. Comparative calculations were performed for two examples with extremely high and low roughness estimates. For the direction dependent wind speed ratios as well as the wind profiles quantitative differences were found, but the qualitative result is not affected.

A detailed model is needed to find an explanation for these findings. It might have to include several effects like the dependence of the sea surface roughness on wind speed and fetch (see e.g. [2.8]) as well as the influence of the atmospheric stability on the height profile of the wind speed and on internal boundary layers due to roughness changes (see e.g. [2.4]).

Acknowledgements

The original instrumentation and maintenance of the Rødsand measurement station were funded by the EU-JOULE program and the Danish Energy Ministry's UVE program 'Offshore Wind Resources'. Subsequent instrumentation, operation and

maintenance were funded by SEAS Distribution A.m.b.A. The technical support team at Risø, particularly Ole Frost Hansen, are acknowledged for their contribution to the data collection. Mr Kobbernagel of Sydfalster-El performed the maintenance and data collection at Rødsand. The authors wish to thank the referees for their useful comments. The work of one of the authors (B. Lange) is funded by the European Commission through a Marie Curie Research Training Grant (JOR3-CT98-5005).

References

- [2.1] Mortensen, N.G., L. Landberg, I. Troen & E.L. Petersen: Wind Atlas Analysis and Application Program (WAsP). Risø National Laboratory, Roskilde, Denmark, (1993)
- [2.2] Troen, I. & E.L. Petersen: European Wind Atlas. Risø National Laboratory, Roskilde, Denmark, (1989)
- [2.3] Petersen, E.L.: Wind Resources Part I, The European Wind Climatology. Proceedings of the European Wind Energy Conference, Lübeck-Travemünde; 1993 (1993) p. 663-668,
- [2.4] Barthelmie, R.J., M.S. Courtney, J. Højstrup & S.E. Larsen: Meteorological aspects of offshore wind energy: Observations from the Vindeby wind farm. Journal of Wind Engineering and Industrial Aerodynamics Vol. 62 (1996) p. 191-211,
- [2.5] Barthelmie, R.J.; Courtney, M.S.; Lange, B.; Nielsen, M.; Sempreviva, A.M.; Svenson, J.; Olsen, F.; Christensen, T., Offshore wind resources at Danish measurement sites. In: Wind energy for the next millennium. Proceedings. 1999 European wind energy conference (EWEC '99), Nice (FR), 1-5 Mar 1999. Petersen, E.L.; Hjuler Jensen, P.; Rave, K.; Helm, P.; Ehmann, H. (eds.), (1999) p. 1101-1104
- [2.6] Charnock, H., Wind stress over a water surface. Quarterly Journal of the Royal Meteorological Society, Vol. 81 (1955) p. 639-640
- [2.7] Frandsen, S. (ed.), L. Chacón, P. Enevoldsen, R. Gómez-Elvira, J. Hernández, J. Højstrup, F. Manuel, K. Thomsen & P. Sørensen, Measurements on and Modelling of Offshore Wind Farms. Risø Report R-903 (EN), (1996)
- [2.8] Johnson, H.K., J. Højstrup, H.J. Vested, & S.E. Larsen, On the Dependence of Sea Surface Roughness on Wind Waves. Journal of Physical Oceanography. Vol.28 (1998) p. 1702-1716
- [2.9] Garratt, J.R.: The atmospheric boundary layer. Cambridge atmospheric and space sciences series. 1994
- [2.10] Rao, K.S., Effect of Thermal Stratification on the Growth of the Internal Boundary Layer. Boundary-Layer Meteorology. Vol.8 (1975) p. 227-234
- [2.11] Barthelmie, R.J., The Effect of Atmospheric Stability on the Temporal and Spatial Variability of Offshore Wind Resources. Proceedings of the OWEMES European Seminar: Offshore Wind Energy in Mediterranean and other European Seas, (1997)
- [2.12] Barthelmie, R.J., N.G. Mortensen, L. Landberg & J. Højstrup, Application of the WAsP Model to Determine the Wind Resource in Non-neutral Conditions in Coastal Areas. Proceedings of the European Union Wind Energy Conference, Göteborg, Sweden (1996)

[2.13] Barthelmie, R.J., M.S. Courtney, J. Højstrup and P. Sanderhoff, The Vindeby Project: A Description. Risø Report R-741(EN). Risø National Laboratory, Roskilde, Denmark, (1994)

[2.14] Fcalc, Farm Calculation program. University of Oldenburg, Germany, (1996)

[2.15] Højstrup, J., Vertical Extrapolation of Offshore Windprofiles. In: Wind energy for the next millennium. Proceedings. 1999 European wind energy conference (EWEC '99), Nice (FR), 1-5 Mar 1999. Petersen, E.L.; Hjulær Jensen, P.; Rave, K.; Helm, P.; Ehmann, H. (eds.), (1999) p. 1220-1223

3 The dependence of sea surface roughness on wind-waves⁵

Abstract

The wave age dependency of the non-dimensional sea surface roughness (also called Charnock parameter) is investigated with data from the new field measurement program at Rødsand in the Danish Baltic Sea. An increasing Charnock parameter with inverse wave age is found, which can be described by a power law relation of the form proposed by Johnson et al. (1998) and others.

Friction velocity is a common quantity in both Charnock parameter and wave age. Thus self-correlation effects are unavoidable in the relation between them. The significance of self-correlation is investigated by employing an artificial 'data' set with randomised wave parameters. It is found that self-correlation severely influences the relation. For the Rødsand data set the difference between real and randomised 'data' was found to be within the measurement uncertainty. By using a small sub-set of the data it was found that the importance of self-correlation increases for a narrower range of wave age values. This confirms the conclusion of Johnson et al. (1998), that due to the scatter and self-correlation problems the coefficients of the power law relation can only be obtained from the analysis of an aggregated data set with a wide wave age range combining measurements from several sites.

The dependency between wave age and sea roughness has been discussed extensively in the literature with different and sometimes conflicting results. A wide range of coefficients has been found for the power law relation between Charnock parameter and wave age for different data sets. It is shown that self-correlation contributes to such differences, since it depends on the range of wave age values present in the data sets. Also, data are often selected for rough flow conditions with the Reynolds roughness number. It is shown that for data sets with large scatter this can lead to misleading results of the relation of wave age and Charnock parameter. Two different methods to overcome this problem are presented.

3.1 Introduction

The momentum transfer from the marine atmospheric boundary layer to the wind driven water waves is important for all processes of air-sea interaction, such as wind wave growth, storm surges and atmospheric circulation. It depends on the aerodynamic sea surface roughness, which is therefore one of the most important quantities for the description of the physical processes on both sides of the air-sea interface.

Using dimensional arguments, Charnock (1955) suggested that the dimensionless sea roughness gz_0/u_*^2 (also called Charnock parameter z_{ch}) is constant, where g is the gravitational acceleration, z_0 the sea surface roughness and u_* the friction velocity. Various field measurements showed that this concept works well for open ocean sites,

⁵ This chapter has also been submitted for publication to *Journal of Physical Oceanography* as: Lange, B., H. K. Johnson, S. Larsen, J. Højstrup, H. Kofoed-Hansen: The dependence of sea surface roughness on wind-waves.

except for very low wind speeds (<3-4 m/s), while for sites near the coast the Charnock parameter varies from site to site. Thus, z_{ch} is not a constant, but depends on other geophysical parameters.

It has been argued that these other parameters are properties of the wave field, i.e. that the sea surface roughness is not only dependent on wind speed, but also on the wave field present, which in turn is governed by wind, fetch and water depth. Different attempts have been made to establish a relationship between the sea surface roughness and different properties of the wave field like wave height, wave steepness or wave age (e.g. Hsu, 1974, Donelan, 1990, Smith et al., 1992, Taylor and Yelland, 2001). However, though it is general consensus that the sea surface roughness depends on the wave field, the quantities suitable for description of this dependence are still a subject of controversy.

Most authors tried to improve the description of the sea surface roughness by a parameterisation of the Charnock parameter with wave age⁶ (e.g. (Smith et al., 1992), (Donelan et al., 1993), (Johnson et al., 1998)). The latter group (hereafter called JHVL98) showed that under specific conditions (discussed in section 3.2.5) the Charnock parameter depends only on wave age. They describe this dependence with a power law between the Charnock parameter (or normalised sea surface roughness), z_{ch} , and the inverse wave age, u_*/c_p , in the form

$$z_{ch} = A \left(\frac{u_*}{c_p} \right)^B \quad (3.1)$$

From an empirical fit to measurements from RASEX together with other previously measured data sets they find the coefficients $A=1.89$ and $B=1.59$. One of the main problems in the findings was the conflicting, apparent trend of decreasing Charnock parameter with inverse wave age in the RASEX data set taken alone (see also Taylor and Yelland (2001)).

The problem in this kind of scaling is that the two quantities z_{ch} and wave age, between which a functional relationship is proposed, are not independent of each other. This can lead to self-correlation problems, i.e. the functional relationship might be distorted or even determined by the common scaling variable. A theoretical analysis of the self-correlation problem has been presented by Hicks (1978) and specifically for the question of wave age dependent Charnock parameter by Smith et al. (1992). The latter group concluded that self-correlation had an influence on the results of the HEXOS data. JHVL98 generalised that this will always be the case for a given site, where the fetch range is limited. They concluded that the combination of data from several sites is necessary to minimise self-correlation.

In the present paper we follow the JHVL98 approach with three principal aims:

1. To test the relation proposed by JHVL98 with a new, independent data set.
2. To investigate the influence of self-correlation on the relation.

⁶ The ratio between friction velocity and phase speed of the peak wave component is defined as wave age. When waves mature, their speed - here represented as the peak phase speed c_p - increases gradually until it reaches equilibrium conditions. This equilibrium sea state depends on the momentum transfer from the atmosphere to the waves, here represented by the friction velocity u_* . Therefore the ratio between u_* and c_p can be interpreted as a measure for the state of the wave development in relation to the equilibrium (or fully developed) state.

3. To contribute to an understanding of the reasons for the conflicting results found by JHVL98 and in the literature (see e.g. Toba et al. (1990), Drennan et al. (2000), Maat et al. (1991)) by investigating how self-correlation and the data analysis method could influence the resulting trend.

The plan of the paper is as follows: In section 3.2 the Rødsand field measurement program is presented and the preparation of the measured data described. In section 3.3 these data are analysed in different ways. The results are compared with each other and with published results. The influence of self-correlation on the relation is investigated in section 3.4. The data analysis method is discussed in section 3.5 to gain a better understanding of the relationship between Charnock parameter and wave age. In the final section 3.6 the conclusions of the paper are summarised.

3.2 The Rødsand field measurement program

3.2.1 Site

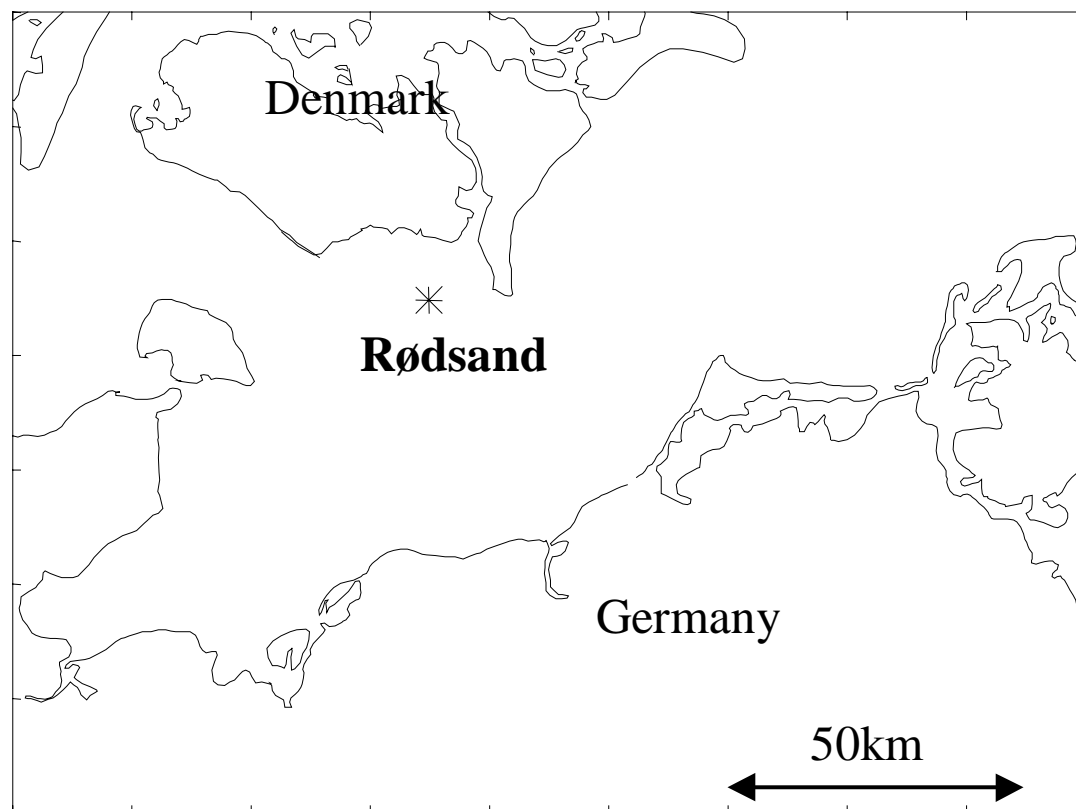


Figure 3.1: Rødsand measurement site

A 50 m high meteorological measurement mast has been established at Rødsand in October 1996 as part of a Danish study of wind conditions for proposed offshore wind farms. Simultaneous wind and wave measurements are performed since April 1998. The mast is situated about 11 km south of the island Lolland in Denmark (11.74596°E , 54.54075°N). The location of the mast is shown in Figure 3.1. The mast is located in 7.7 m mean water depth with an upstream fetch of 30 to 100 km (and above) from the SE to WNW sector (120°N to 290°N). The average upstream water depth in this sector is about 25 m. In the NW to N sector (300°N to 350°N), the water

depth is relatively shallower (from 1 m to 7 m) and the fetch is smaller (about 10 km to 20 km).

3.2.2 Instrumentation and Measurements

The instrumentation of the measurement mast is listed in Table 3.1. Wave and current data are collected simultaneously with several atmospheric parameters. About 5900 half-hourly records with simultaneous wind and wave measurements have been recorded. A more detailed description of the instrumentation and data can be found in Lange et al. (2001).

Table 3.1: Instrumentation of the Rødsand measurement

	height above mean sea level	instrument	sampling rate
Wind speed	50.3 m	cup anemometer	5 Hz
	29.8 m	cup anemometer	5 Hz
	10.2 m	cup anemometer	5 Hz
Wind direction	29.7 m	wind vane	5 Hz
3 axis wind speed and temperature	46.6 m (42.3 m from 12.5.99)	ultrasonic anemometer	20 Hz
Air temperature	10.0 m	Pt 100	30 min mean
Temperature difference	49.8 m – 10.0 m	Pt 500	30 min mean
Sea temperature		Pt 100	30 min mean
Sea level		DHI AWR201 acoustic wave recorder	8 Hz
Sea current		GMI current meter	8 Hz

Cup anemometers

Mean wind speeds and variances are derived from cup anemometers located at three heights (see Table 3.1). Calibrated instruments of the type Risø P2546a are used. The calibration accuracy is estimated to be +/- 1%. Data are corrected for flow distortion errors due to the structure on which the anemometer is mounted, i.e. the mast and the booms (see section 3.2.4.2). However, a correction uncertainty remains, and the overall uncertainty of the wind speed measurement with cup anemometers is estimated to be +/- 3%.

Wind vane

A wind vane of the type Risø Aa 3590 is used. The uncertainty of the instrument itself is negligible. However, the adjustment of the orientation of the instrument is difficult in the field and the absolute accuracy is estimated to be about +/-5°.

Sonic anemometer

The sonic anemometer is of the type Gill F2360a and is mounted at 46.6m height (42.3m from 12/May/99) above MSL. It measures wind speed in three components (x,y,z) and air temperature with a resolution of 20 Hz. The mean bias in the vertical component of the sonic anemometer was found to be below 1 cm/s. This is considered small in comparison to other errors and was not corrected for.

Errors due to flow distortion of the measuring mast have been corrected for (see section 3.2.4.2). Additionally, sonic anemometers experience an array flow distortion, since transducers and struts of the instrument distort the wind flow in the measurement volume. For the horizontal wind speed component flow distortions are corrected with an individual calibration curve supplied by the manufacturer. This is not the case for the vertical wind component. Mortensen and Højstrup (1995) report systematic differences in a field experiment of typically 5% in mean wind speed and 10-15% in friction velocity between different sonic anemometer types. From wind tunnel measurements they find that the errors are dependent on temperature and mean wind direction. However, they state that further investigations are necessary before a correction method can be established. Therefore no attempt has been made to correct the measurements of the sonic anemometer for array flow distortion. The estimated accuracy for the horizontal wind speed component is about +/- 5%. For the friction velocity derived by eddy-correlation it is +/- 10%. Both errors are expected to contain a wind direction dependent bias.

Additionally statistical errors due to sampling variability have to be considered, which are responsible for the scatter in the data. Using the approximation of Wyngaard (1973) derived from the Kansas data, the expected accuracy for the u_* measurements is about 10% for an eddy-correlation measurement at 45 m height with an averaging time 30 minutes and a mean wind speed of 10 m/s. It is mainly this sampling variability, which is responsible for the unavoidable scatter in the u_* data.

Acoustic wave recorder

Waves are measured by an acoustic wave recorder (AWR), which is a SONAR-type instrument positioned under water on a support structure. The type is the HD-AWR201 from DHI Water & Environment.

The instrument is located about 100 m south-west of the offshore meteorological mast at Rødsand since March 1998. The instrument was placed 3.74 m above the sea bottom; the average water level during the measurement was 7.7 m. The instrument measures the distance from the acoustic transducer to the water surface with a sampling rate of 8 Hz.

The cut-off frequency of the instrument is determined by its spatial resolution (area sampled by the acoustic transducer at the surface) rather than its sampling rate. It is estimated to be about 0.8 Hz. The measured time series of water level fluctuations was passed through a simple filter in order to remove local spikes in the data. A fixed speed of sound (1475 m/s) is used independent of actual water temperature and salinity. Water temperature and salinity ranges have been estimated for the site. They lead to a maximum measurement error of -4% to +1% in the water level value and wave height.

Water current measurement

The water current sensor is a two dimensional electromagnetic sensor measuring the water velocity in x- and y-direction, manufactured by GMI (Geophysical and Marine

Instrumentation, Denmark). It is located 5.3 m above the sea bottom. The measurement accuracy of the sensor is estimated to be +/- 2%.

3.2.3 Derived measured quantities

3.2.3.1 Friction velocity

Co-variances are calculated from the sonic anemometer measurements. Linear trends remaining in the time series after selection for stationary conditions (see section 3.2.5) are removed before calculation of the co-variances. Friction velocity is calculated with the eddy-correlation method as⁷:

$$u_* = \left(\overline{u'w'}^2 + \overline{v'w'}^2 \right)^{0.25} \quad (3.2)$$

The uncertainty in the friction velocity measurement is estimated to be about +/- 10% as a combination of the general measurement uncertainty of the instrument and a direction dependent error due to flow distortion.

If the direction dependent error coincides with a wind direction depended distribution of wave ages in the data, this error can distort the trend of sea surface roughness with wave age. This is investigated by comparing the observed trend with the one found in an analysis without using the sonic anemometer, where the friction velocity is derived from the wind speed variance measurement of a cup anemometer.

For near neutral atmospheric stability, friction velocity u_* and standard deviation of the wind speed σ_u are proportional:

$$u_* = \frac{\sigma_u}{C} \quad (3.3)$$

The constant C is estimated for the Rødsand data set by comparing the standard deviation measured with the cup anemometer at 50 m height and the friction velocity derived from the sonic anemometer at 46.6 m (42.3 m) height. The ratio of both is plotted versus the stability parameter $50/L$ in Figure 3.2. No dependence on atmospheric stability can be found for the near neutral stability range used. A possible dependence of C on wave age, which could distort the trend of Charnock parameter versus wave age, is investigated in Figure 3.3. Also here no significant dependence can be found. The mean value for C is 2.42 with a standard deviation of 0.51, which is about 20%. This is in the range of commonly used values: Garratt (1992) quotes 2.4 for flat terrain, Stull (1988) lists values from 2.47 to 2.57.

The measured value for C is used to derive friction velocities from the three cup anemometer measurements. They provide complementary indirect measurements of the friction velocity, which are expected to have no wind direction dependent error.

⁷ The total wind stress consists of the components of the stress in wind direction $\sqrt{u'w'}$ and the component perpendicular to the mean wind direction $\sqrt{v'w'}$. In ideal conditions, i.e. stationary, homogeneous conditions and unlimited averaging time, the second component should vanish. For the determination of the total wind stress from field measurements it has to be included.

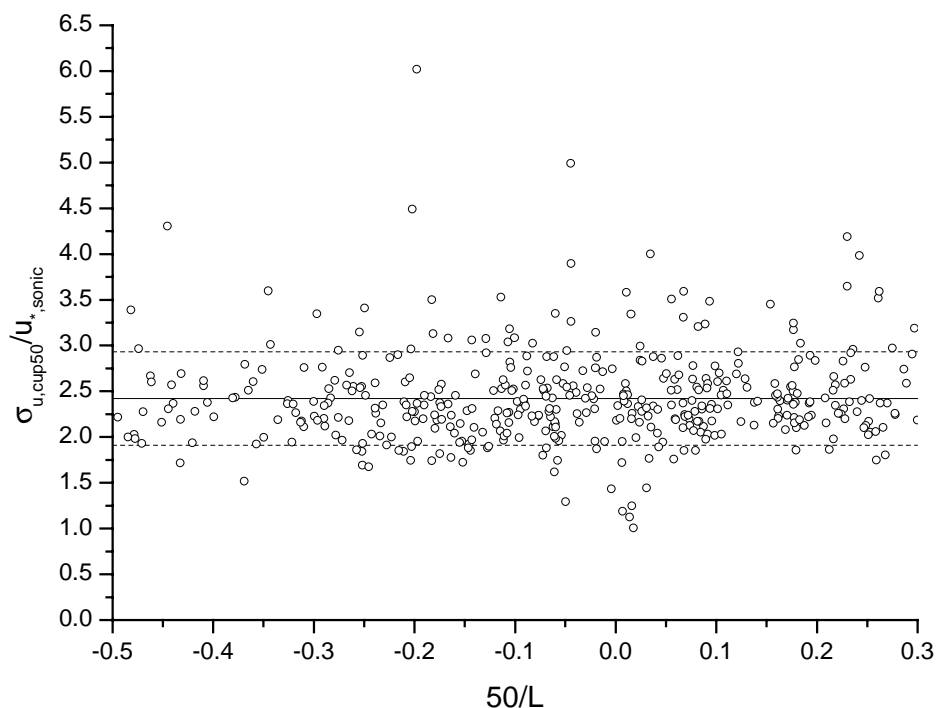


Figure 3.2: Ratio of standard deviation measured with the cup anemometer at 50 m height and friction velocity derived from the sonic anemometer at 46.6 m (42.3 m) height versus stability parameter $50/L$; horizontal lines show the mean ratio (2.42) and its standard deviation (0.51)

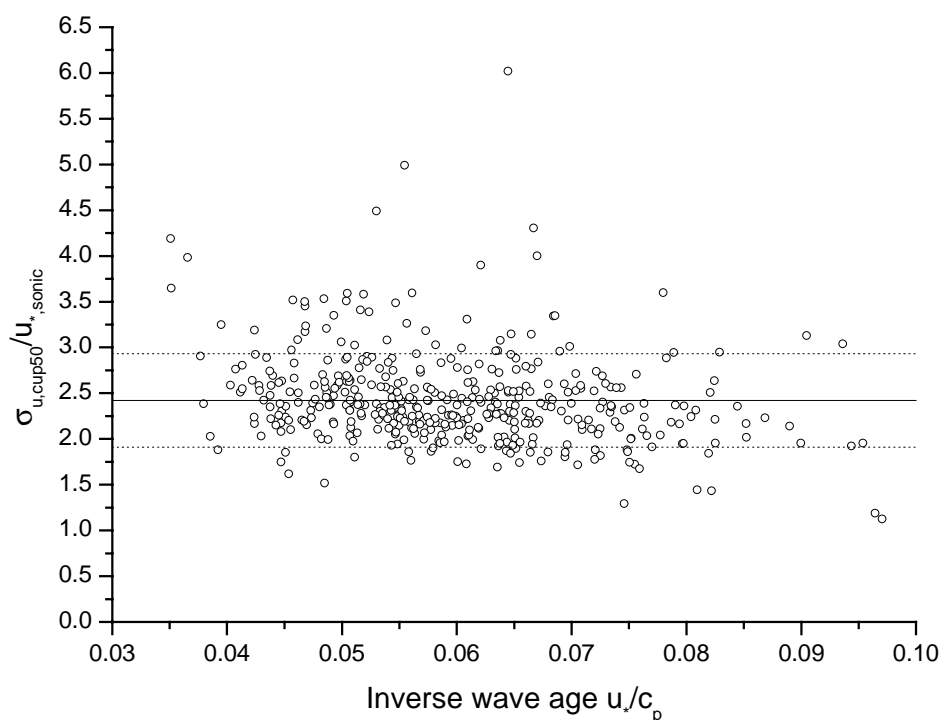


Figure 3.3: Ratio of standard deviation measured with the cup anemometer at 50 m height and friction velocity derived from the sonic anemometer at 46.6 m (42.3 m) height versus inverse wave age u^*/c_p ; horizontal lines show the mean ratio (2.42) and its standard deviation (0.51)

3.2.3.2 Neutral wind speed at 10 m height

The measured mean wind speed has been corrected for influences of the atmospheric stability, described by the Monin-Obukov-length L . L has been determined from the measurements of the friction velocity, u_* , the heat flux, $\langle w'\Theta' \rangle$, and the potential temperature at 10 m, Θ :

$$L = - \frac{u_*^3}{\kappa \frac{g}{\Theta} \overline{w'\Theta'}} \quad (3.4)$$

The von Karman constant κ is taken as 0.4 and the gravitational constant g as 9.81 m/s². The error in L due to humidity can be neglected since the humidity influence is to a large degree included in the heat flux measurement of the sonic anemometer, which measures the sound virtual temperature (see e.g. Schotanus, 1983). The stability function Ψ is calculated by the standard approach (see e.g. Geernaert et al., (1986), JHVL98) and the neutral wind speed u_{10n} is derived from the measured wind speed u_{10} by:

$$u_{10n} = u_{10} + \frac{u_*}{\kappa} \Psi\left(\frac{10}{L}\right) \quad (3.5)$$

Deviations of the measurement height from 10 m due to water level variations have been accounted for by a log-linear wind profile with Charnock sea surface roughness (with $z_{ch}=0.018$) and the measured stability parameter.

3.2.3.3 Sea surface roughness

For the calculation of sea surface roughness the measurements of friction velocity u_* , either from sonic or cup anemometer measurements (see section 3.2.3.1), and of the neutral wind speed at 10 m height u_{10n} have been used. The friction velocity has been corrected to its surface value (see section 3.2.4.1). The roughness length is calculated from the logarithmic wind profile:

$$z_0 = \frac{z}{\exp\left(\frac{u_n(z)\kappa}{u_*}\right)} \quad (3.6)$$

The dimensionless sea surface roughness or Charnock parameter is defined as:

$$z_{ch} = \frac{z_0 g}{u_*^2} = \frac{g z}{u_*^2 \exp\left(\frac{u_n(z)\kappa}{u_*}\right)} \quad (3.7)$$

3.2.3.4 Wave height, wave periods and wave spectrum bandwidth

All wave parameters have been derived from the time series of water elevation measured by the AWR. The significant wave height H_s is derived from the standard deviation of the water level σ by:

$$H_s = 4\sigma \quad (3.8)$$

Three different wave periods and the bandwidth of the spectrum are derived from the wave spectrum calculated for each 30 minute wave record measured at Rødsand. The wave period at 50% accumulated variance T_{50} has been calculated as

$$T_{50} = 1/f_{50} \quad (3.9),$$

the mean period T_m as

$$T_m = m_0/m_1 \quad (3.10)$$

and the mean period based on zero crossing frequency T_z as

$$T_z = \sqrt{m_0/m_2} \quad (3.11).$$

The bandwidth of the wave spectrum has been found from

$$bw = \log_{10}(f_{75}/f_{25}) \quad (3.12)$$

In the equations m_n denotes the n 'th moment of the spectrum and f_n the frequency at n % variance.

3.2.3.5 Wave phase speed at peak frequency

The spectral peak frequency f_p is determined from the measured wave spectra. The direct way of finding f_p would be to search for the frequency corresponding to the maximum spectral density. However, this method is very sensitive to noise. Therefore, following JHVL98, the statistically more stable frequency at 50% accumulated variance f_{50} is determined first and the measured f_{50} is then converted to f_p by using a mean wave spectrum shape.

The JONSWAP spectral model (Hasselmann, et al., 1973) is used as shape function to find the average ratio f_{50}/f_p , which best fits the measured spectra. The average values of the parameters for the fitted spectrum are $\gamma=1.58$ (the peakedness parameter), $f_{50}/f_p=1.11$, $bw=0.153$ and $T_m/T_z=1.081$. These compare well with the measured bandwidth and timescale ratio as shown in Figure 3.4 and Figure 3.5, respectively.

The phase speed at peak frequency c_p is calculated using the measured water depth and spectral peak frequency f_p in the linear dispersion relation.

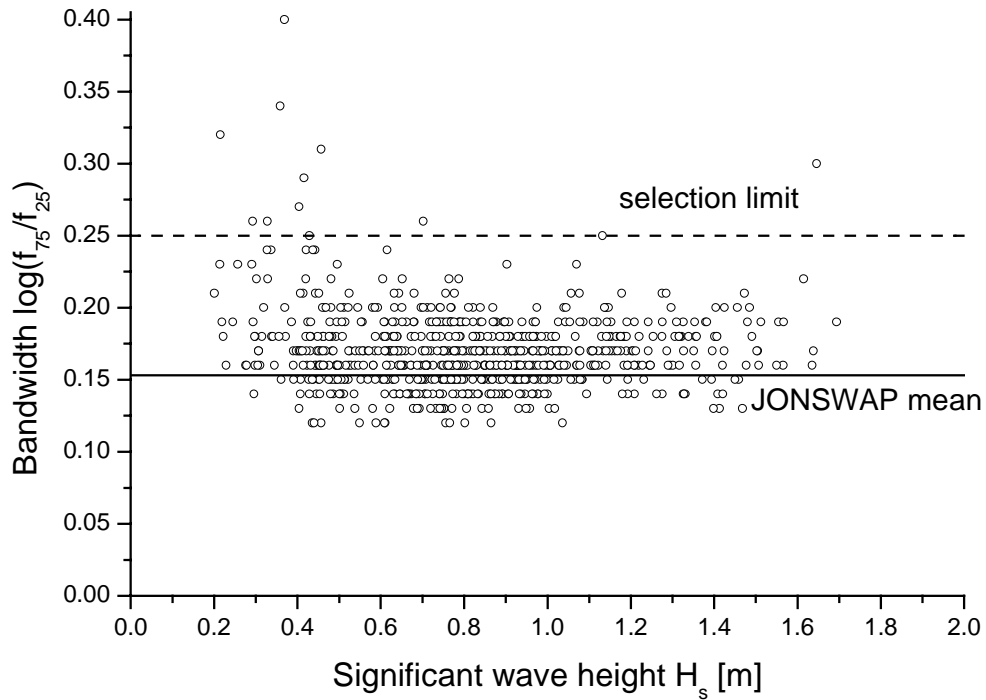


Figure 3.4: Bandwidth of the measured data at Rødsand versus significant wave height; also shown is the bandwidth of the fitted JONSWAP spectrum (0.15) and the bandwidth limit used to select single peaked spectra (0.25)

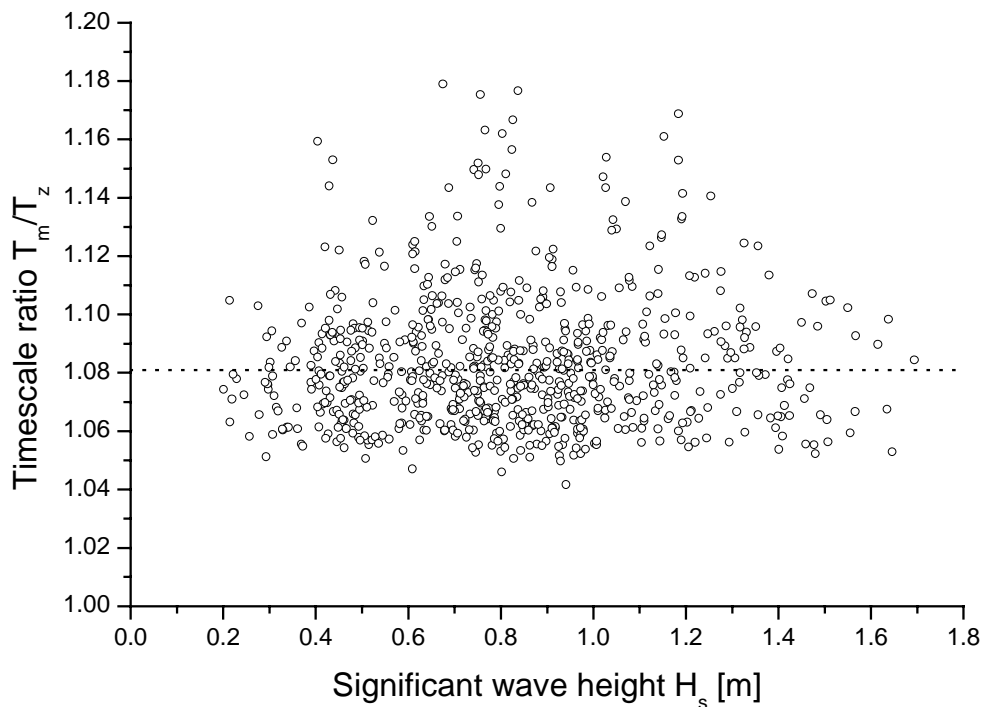


Figure 3.5: Ratio of mean period and wave period based on zero crossing frequency of the measured data at Rødsand versus significant wave height; also shown is the timescale ratio of the fitted JONSWAP spectrum

3.2.4 Data corrections

3.2.4.1 Correction of the wind stress measurement for elevation

To a first approximation it is usually assumed that the flux in the surface layer is independent with height, implying that the friction velocity is constant. However, this assumption is not entirely correct and for near-neutral and stable conditions the friction velocity decreases slightly with height. Since the determination of the sea surface roughness is very sensitive for the value of the friction velocity, this deviation is accounted for in the determination of the surface friction velocity.

Donelan (1990) derives the following expression from an analysis of the horizontal momentum equation at the surface and the top of the boundary layer, when no observed boundary-layer height is available:

$$u_*(z) = \sqrt{u_{*,s}^2 \left(1 - \frac{\alpha_0 f_c z}{u_{*,s}}\right)} \quad (3.13)$$

where $u_*(z)$ is the friction velocity measured at height z , $u_{*,s}$ is the friction velocity at the surface, $\alpha_0 = \frac{v_g}{u_{*,s}}$ is the ratio of geostrophic wind v_g and $u_{*,s}$ (taken as $\alpha_0 = 12$), f_c the Coriolis parameter ($1.46 \cdot 10^{-4} \sin(\phi)$, with ϕ latitude).

A direct comparison of this equation with measured friction velocities can not be made with the Rødsand data set, since a sonic anemometer is only available at one height. However, friction velocities derived from cup anemometer measurements of wind speed variances at the three heights 10 m, 30 m and 50 m can be compared. The difference between friction velocities derived from cup anemometer variances at 10 m and 50 m height versus stability parameter is shown in Figure 3.6, the difference between 10 m and 30 m is shown in Figure 3.7. A height dependence of the friction velocity is observed, which is independent of stability for the near-neutral stability range used. The mean difference over the height difference of 40.1 m is 0.036 m/s (i.e. 0.0009 m/s per meter), over the height difference of 19.6 m it is 0.021 m/s (0.0011 m/s per meter). The mean decrease of friction velocity with height of 0.00071 m/s per meter height difference from equation (13) is consistent with the data for both height differences. The average measured value has been used to derive the friction velocity at the surface from friction velocities derived at different heights from sonic and cup anemometer measurements.

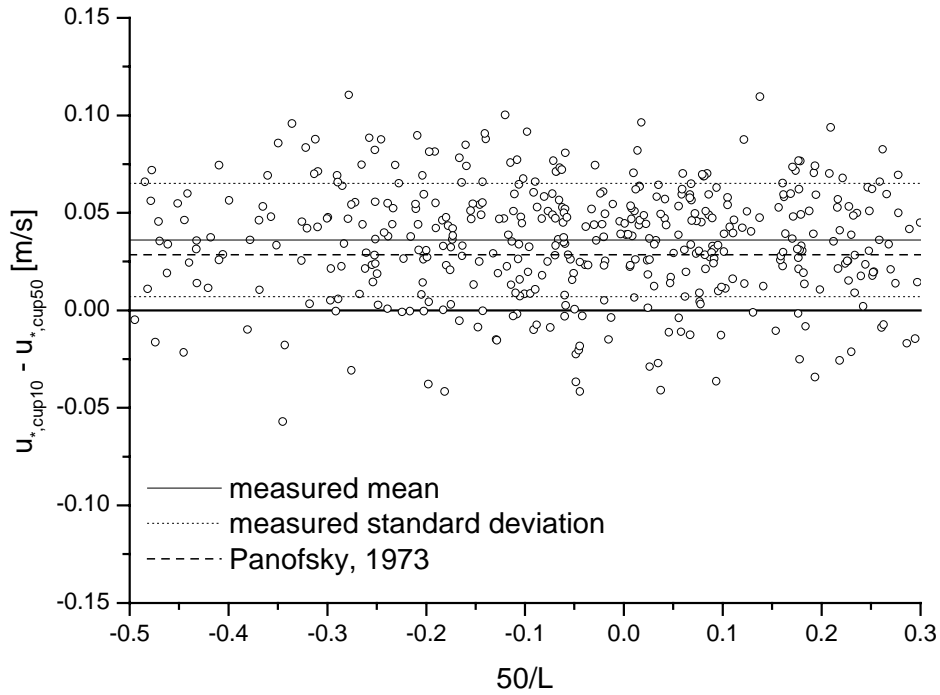


Figure 3.6: Difference between friction velocities derived from cup anemometer standard deviations at 10 m and 50 m height versus stability parameter; horizontal lines show the mean difference (0.036 m/s), its standard deviation (0.029 m/s) and the mean result of eq. (3.13)

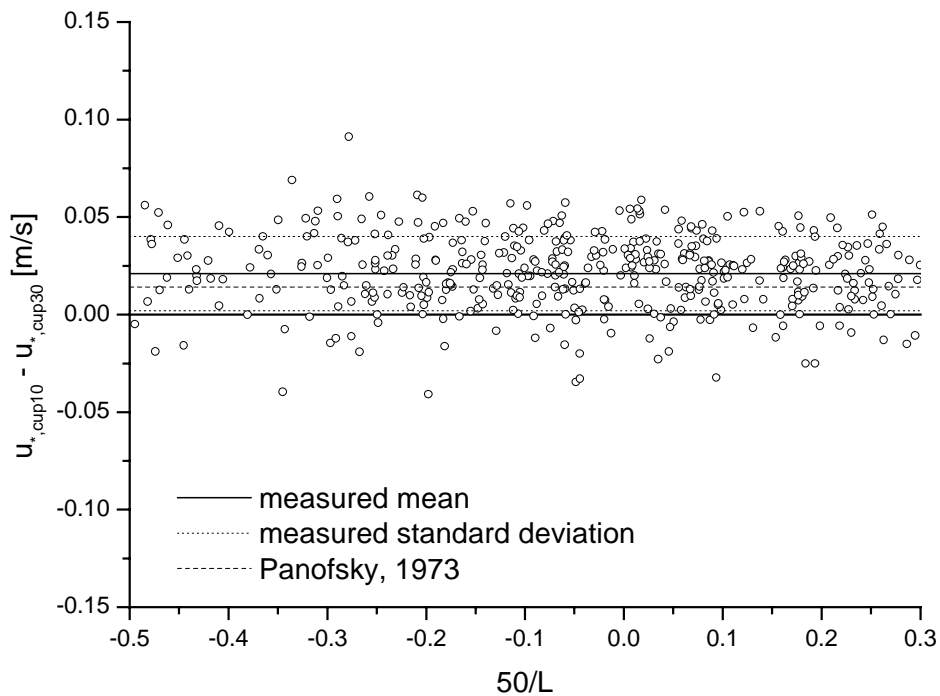


Figure 3.7: Difference between friction velocities derived from cup anemometer variances at 10 m and 30 m height versus stability parameter; horizontal lines show the mean difference (0.021 m/s), its standard deviation (0.019 m/s) and the mean result of eq. (3.13)

3.2.4.2 Correction of wind speeds for flow distortion of the measurement mast

At the Rødsand measurement mast, all cup anemometers as well as the sonic anemometer are mounted on booms pointing in the same direction of about 265°. Flow distortion from the measurement mast and the mounting of the instruments leads to measurement errors. They are obviously very large for situations with direct mast shade and such records (wind directions 85° +/- 35°) were omitted.

For other wind directions, a linear correction model was used, which was developed by Højstrup (1999) from measurements at a similar mast at the Vindeby site. In order to investigate the effects of flow distortion from the tower at the Vindeby site, anemometers were mounted at opposite sides of the mast at three different levels for a period of seven months. A triangular lattice measurement mast was used with a tower side length of 1.21 m and a boom length (measured from the nearest corner of the tower) of 2.51 m at 7 m height, leading to a boom length to tower side ratio of about 2. At 20 m and 38 m height it was about 2.5 and 4, respectively, with a tower side length of 0.95 m and 0.60 m and a boom length of 2.40 m and 2.32 m, respectively. The boom directions were 50° and 230°.

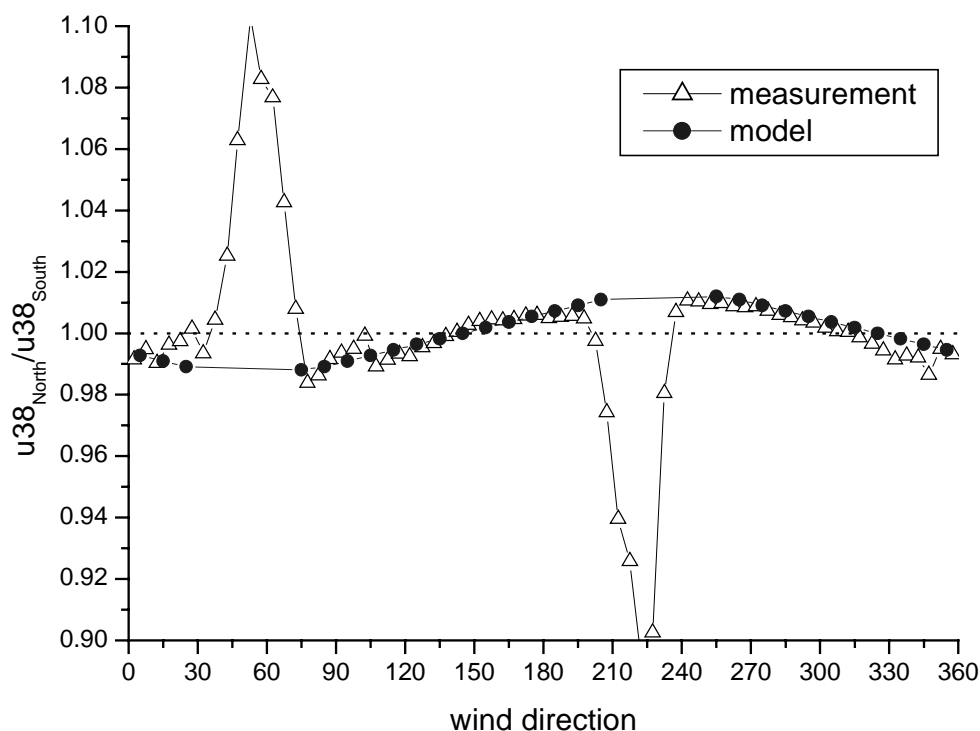


Figure 3.8: Triangles: Binned ratios of wind speed measurements at 38m . Circles: Model results assuming flow distortion linear away from tower wake influence (see also Figure 3.9); data are from the Vindeby measurement program

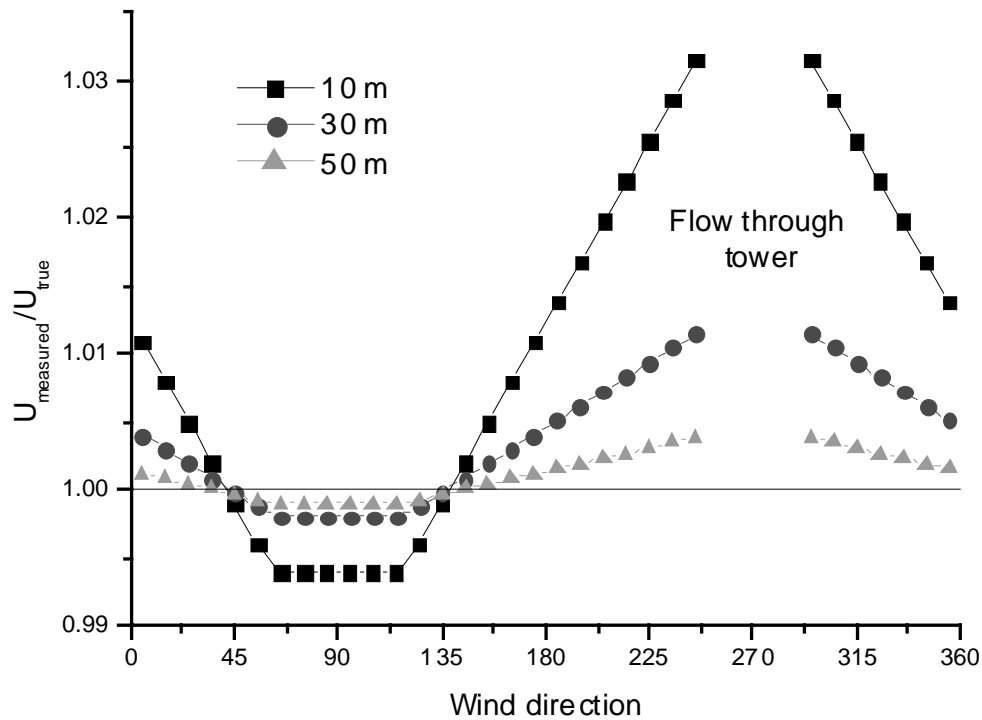


Figure 3.9: Correction for tower flow distortion of wind speed at Rødsand as a function of wind direction with the model by Højstrup (1999). Note that the correction is positive on average, and that the correction diminishes for increasing boom length to tower side ratio

Taking the ratio of wind speeds on opposite sides of the tower, averaging in direction bins, a similar picture for all three heights (see Figure 3.8 where only the highest height is shown) can be seen. Also in Figure 3.8 the result of a simple model (Højstrup, 1999) is shown, assuming that the tower induced flow distortion is linear in wind direction, away from the sectors directly influenced by the wake of the tower. From Figure 3.8 it is noted that the simple linear model works well outside of the sectors where one of the anemometers are in the wake of the mast and the other anemometer. For the three heights at Rødsand, correction factors of 1.033/0.994 (maximum increase and decrease), 1.012/0.998 and 1.004/0.999 for the three heights 10 m, 30 m and 50 m, respectively, are used for all wind speeds. The factors for 50 m height are also used for the sonic anemometer mean wind speed and friction velocity. These are illustrated in Figure 3.9 for all three heights.

Flow distortion of the wind speed standard deviation is assumed to be similar to that of the mean wind speed and the same correction factors are used for a simple correction. This approach is compared with measurements at Vindeby in Figure 3.10. Ratios of wind speed standard deviations of the two anemometers are shown, similar to Figure 3.8. A reasonable agreement between model and measurement is found.

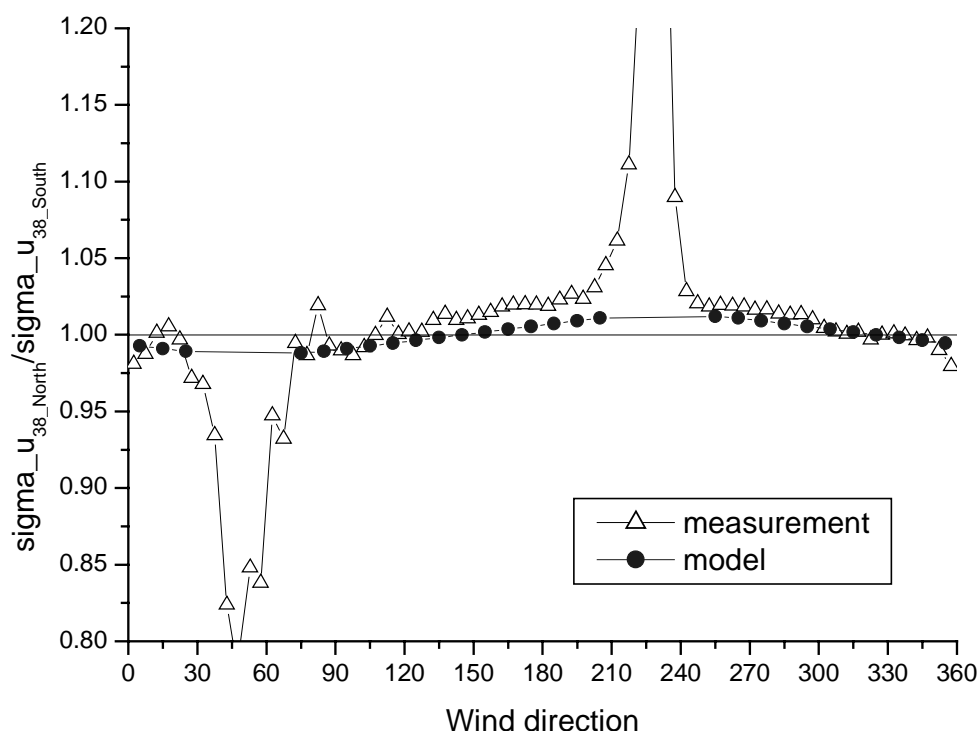


Figure 3.10: Triangles: Binned ratios of measurements of wind speed standard deviations at 38m . Circles: Model results assuming flow distortion linear away from tower wake influence; data are from the Vindeby measurement program

3.2.4.3 Transformation of wind speeds to water following co-ordinates

For the interaction of wind with waves the relevant wind speed is the difference between air and water movement. Wind measurements made from fixed structures, like the measurement mast at Rødsand, therefore need to be corrected for the water current. At Rødsand, the water current is measured at a mean water depth of 2.4 m. Differences between the current at this depth and the surface current have been neglected and all mean wind speeds measured at the mast have been transformed to refer to the moving reference frame of the water surface.

At Rødsand currents are generally slow, usually below 0.4 m/s, and only in some occasions reach values of up to 0.65m/s. Differences in wind speed due to the transformation are for 93% of the records below 2% and for 99% below 5%.

3.2.5 Data selection

The first step in data selection is the rejection of data from nonstationary situations, i.e. where the ambient conditions change too much during the 30 minutes of the record under investigation. For the most important quantities the change in time is computed for a time period of 30 minutes before to 30 minutes after the averaging period of the record. Time periods with large gradients are rejected. This was done for wave phase speed, 10 m wind speed, friction velocity and wind direction. Gradients of not more than 20% per hour were allowed for wave phase speed and wind speed, 30% for friction velocity and 40° for wind direction. Due to this selection, 83% of all measured records were rejected.

The second step is to reject measurements where the derived measured quantities can not be calculated. This is the case if the measurement height of the sonic anemometer of about 45 m is above the surface layer. This can lead to friction velocity measurements, which can not be transformed to the surface value. As a simple approximation, the height of the surface layer can be estimated as 10% of the boundary layer height z_h , which is estimated by Tennekes (1982) as:

$$z_h = 0.25 \frac{u_{*s}}{f_c} \quad (3.14)$$

Using this expression it is found that the surface layer might be shallower than 45 m if u_* is smaller than about 0.2 m/s. Such measurements have been rejected.

The third step is to select only measurements, where the conditions required by the theory under investigation are fulfilled. A simple power law relationship between sea surface roughness and wave age can not be expected to be existent for situations where other physical quantities play an important role, which are not represented in the power law. This is the case for situations 1. with non-neutral atmospheric stability, 2. with shallow water effects influencing the wave field (apart from the influence of depth on c_p), 3. with a wave field that is not in local equilibrium with the wind and 4. with flow that is not aerodynamically rough.

The condition of neutral atmospheric stratification is satisfied by correcting the measured wind speed for the influence of stability as described earlier. In addition, this correction is limited to a maximum of 3% correction in u_{10n} and data with larger deviations from neutral stability are omitted. This leads to limits of $-0.5 < z/L < +0.3$ (with $z=50m$).

The effect of water depth on the Charnock parameter is to some extent included in the wave age dependency since the wave phase speed c_p is changing with water depth. However, for even shallower water other effects like enhanced whitecapping will become important and are expected to have an influence on the Charnock parameter, which can not be described by wave age alone. To avoid such cases, data with wave phase speed c_p (derived from the measurement) less than 90% of the corresponding values for deep water waves are rejected.

The condition of locally generated wind waves is satisfied by selecting cases where the wave spectrum is single peaked. Furthermore, cases with a bandwidth close to that of the fitted JONSWAP spectrum are chosen. Records with a bandwidth of more than 0.25 are rejected (see Figure 3.4).

For aerodynamically smooth flow the functional relation between Charnock parameter and inverse wave age is expected to break down since the Charnock parameter may become dependent on the flow roughness Reynolds number. Therefore the analysis has to be confined to wave ages where smooth flow has no influence. In section 3.5.2 two approaches to ensure this are discussed. After Donelan (1990) the flow is rough if $u_* > 0.1m/s$, which is automatically fulfilled because of the selection for a minimum surface layer height (see above). The Toba et al. (1990) criterion of $R > R_{cr} = 2.3$ leads to a limit of inverse wave age of 0.05 for the Rødsand data (see discussion in section 3.5.2). Rather than selecting data for this limit, it is indicated in the appropriate plots and data with inverse wave age below it should be treated with caution.

401 records (7% of the total number of records) are left in the final data set.

3.3 Observed trend in sea roughness

3.3.1 Trend of sea roughness with wave age

Figure 3.11 gives an overview over the data. The Charnock parameter is plotted versus inverse wave age for all half-hourly records.

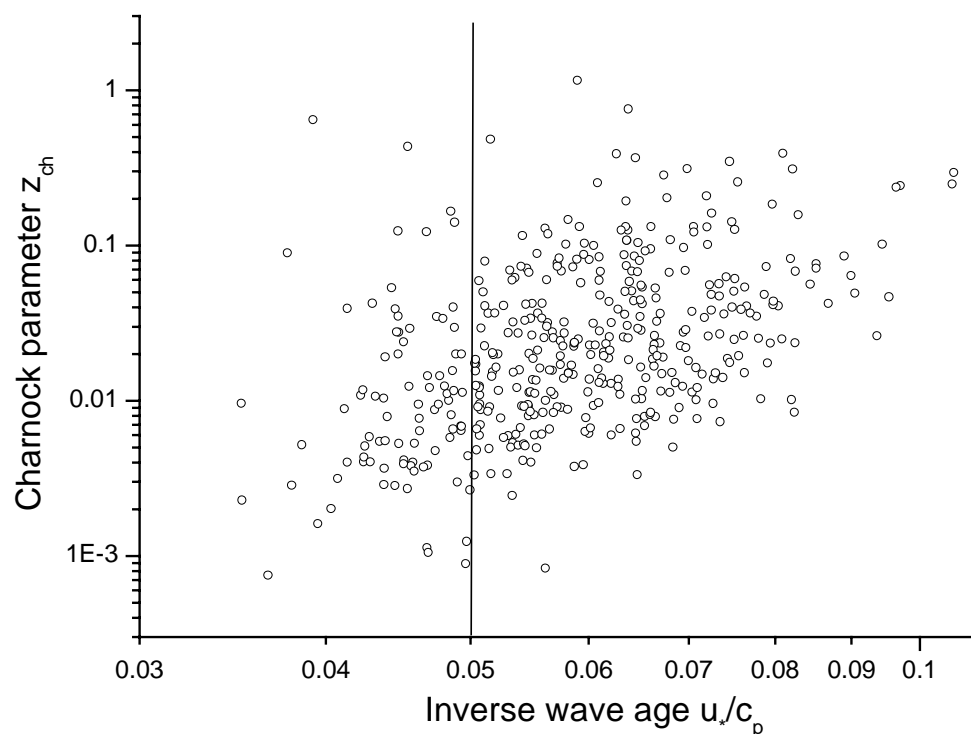


Figure 3.11: Charnock parameter versus inverse wave age from Rødsand data

A bin-averaging method is used for trend investigation. First the data are sorted for the value of the inverse wave age in bins. The bin width is 0.01. Afterwards averages of u_{10n} , u_* and u_*/c_p are calculated for the records in each bin. The bin values of z_{ch} are derived from the averaged parameters for each bin (see section 3.5 for a discussion of the bin-averaging method). The standard errors of u_{10n} and u_* have been used to estimate a standard error of the bin value of z_{ch} . Figure 3.12 shows a comparison of the bin values with the wave age dependent relation for the Charnock parameter from JHVL98. Having in mind the measurement uncertainties, the agreement is good. However, from the error bars it can be seen that the scatter in the data is too large to allow a quantification of the parameters in a power law. This can only be done by using a data set with larger wave age variation as shown in section 3.3.4.

Only one bin value is available for inverse wave ages below the flow roughness limit of 0.05, e.g. in the range where the trend might be influenced by smooth flow after the Toba et al., (1990) criterion. The value does not show a significant deviation from the observed general trend.

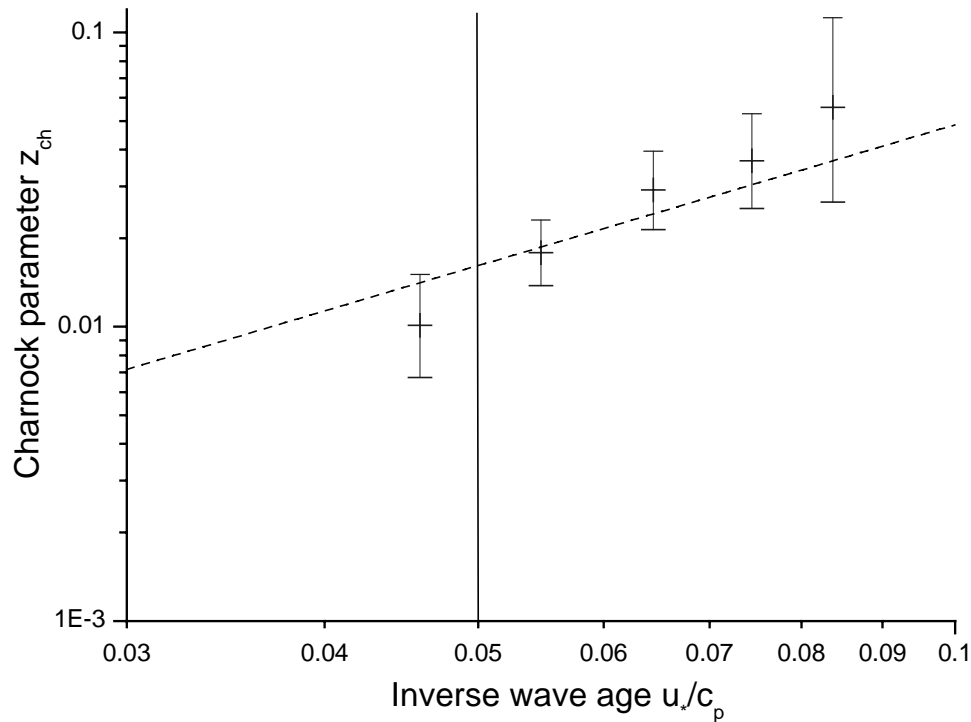


Figure 3.12: Charnock parameter versus inverse wave age from Rødsand data; bin values with respect to wave age are shown with their standard errors in comparison with the empirical fit of JHVL98

3.3.2 Trend obtained from cup anemometer measurements

With a sonic anemometer the wind stress can be measured with the well-established eddy-correlation method. Omnidirectional sonic anemometers as the one used at Rødsand are, however, susceptible to flow distortion errors especially in the vertical wind speed component and therefore in the friction velocity. Flow distortion errors are by their nature wind direction dependent. A concern is therefore that they coincide with a wind direction dependent variation of wave age values due to different fetch lengths. This could distort or even cause the observed trend of sea surface roughness with wave age.

To rule out this threat, the friction velocity has also been derived by an alternative indirect method from cup anemometer measurements (see section 3.2.3.1). This method is expected to be less accurate than the direct eddy-correlation method, but has the advantage of ruling out wind direction dependent flow distortion errors.

Data have been analysed as before, only with the friction velocity derived from the cup anemometer at 10 m height instead of that of the sonic anemometer. No selection has been made for low friction velocities, since the measurement height of 10 m can be expected to be always in the surface layer. The resulting data are shown in Figure 3.13 as Charnock parameter versus inverse wave age. The data have been bin-averaged as described in section 3.3.1. Figure 3.14 shows the result in comparison with the result obtained from the sonic anemometer and the relation proposed by JHVL98. The result from the analysis of the cup anemometer data supports the trend found from the sonic anemometer.

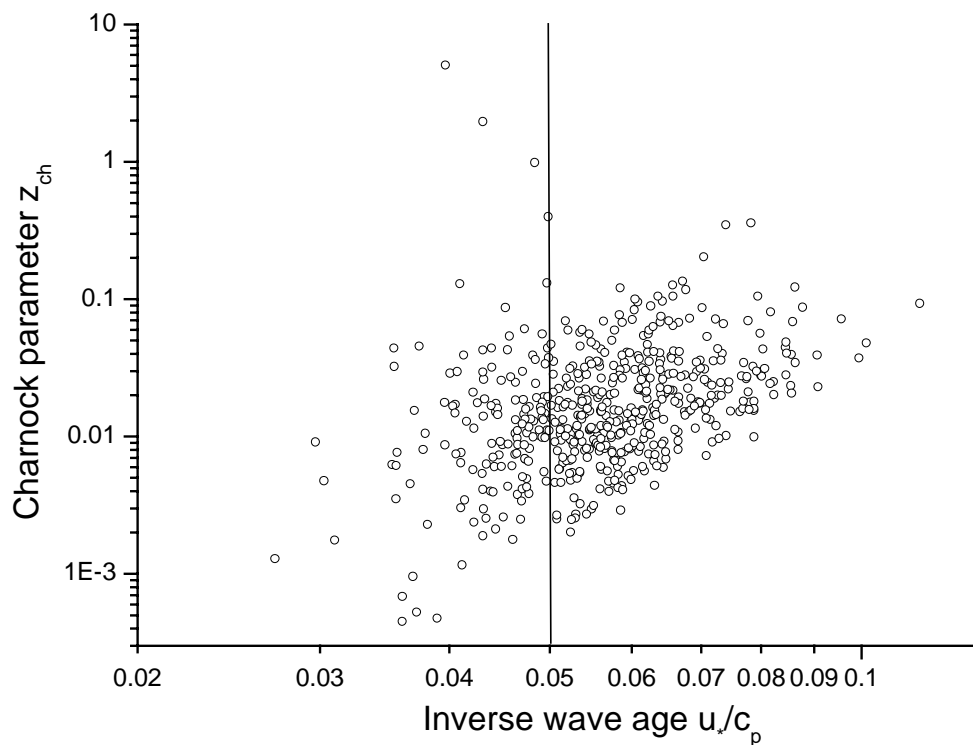


Figure 3.13: Charnock parameter versus inverse wave age from Rødsand data with friction velocity derived from cup anemometer measurement

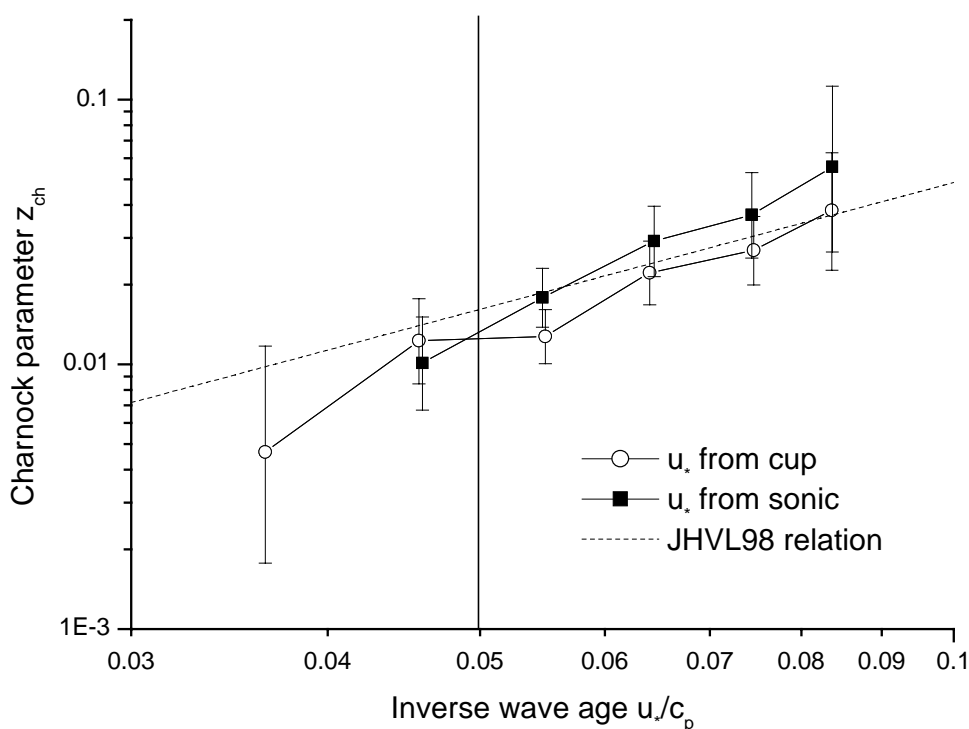


Figure 3.14: Charnock parameter versus inverse wave age from Rødsand data with friction velocity derived from cup and sonic anemometer measurements; bin values with respect to wave age are shown with their standard errors in comparison with the empirical fit of JHVL98

3.3.3 Trend obtained for different fetch lengths

The measurement location experiences fetches in a wide range from 10 km to more than 100 km (see Figure 3.1). To test a possible dependence of the relation between Charnock parameter and inverse wave age, four wind direction sectors with approximately uniform fetches have been selected (Table 3.2).

Table 3.2: Selected wind direction sectors with approximately uniform fetch

Direction [°]	Name	Fetch [km]	number of records
200-230	Lübecker Bucht	60-90	102
240-260	Fehmarn	30-40	49
270-290	Femerbelt	>100	77
300-350	Lolland	10-20	50

This requires the selection of the data for narrow wind direction sectors. The wind direction dependent flow distortion error of the sonic anemometer would in this case distort the results, since the Charnock parameter is very sensitive to a bias in friction velocity (an error of 8% in friction velocity causes a doubling of the Charnock parameter). Therefore the friction velocity derived from the cup anemometer has been used (see section 3.2.3.1). The data have been analysed as described in section 3.3.2.

The bin values of the Charnock parameter are plotted against inverse wave age for each wind direction sector (see Figure 3.15). The trend of increasing Charnock parameter with inverse wave age is generally confirmed, although with larger variations. These are caused by the low number of measurement data available in each wind direction sector (see Table 3.2). A systematic variation of the relation with fetch length is not visible, i.e. a dependence of the coefficients of the power law relation between Charnock parameter and inverse wave age on fetch length can not be found.

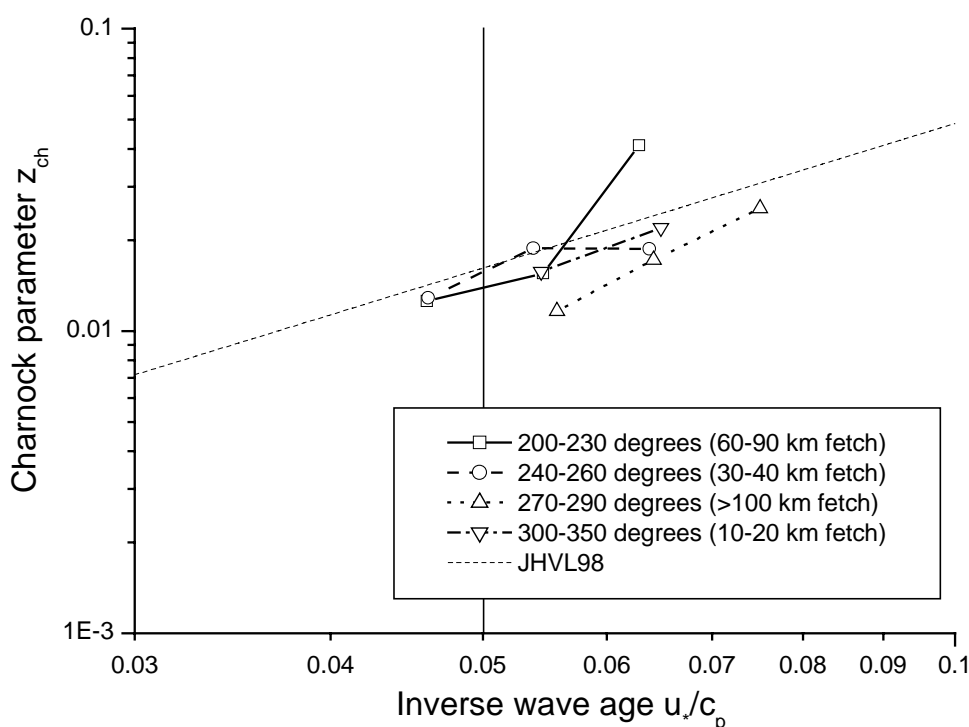


Figure 3.15: Charnock parameter versus inverse wave age from Rødsand measurement bin averaged with respect to wave age; data from four wind direction sectors with different fetches are shown together with the empirical fit of JHVL98

3.3.4 Trend obtained for an aggregated data set

The range of inverse wave age available at one measurement site is relatively small (in the Rødsand data set typically $0.04 < u^*/c_p < 0.09$). This, together with the considerable scatter in the data, makes the determination of parameters of a power law relation unreliable. Following JHVL98, measurement data from different locations and with a wide range of wave age values have therefore been combined in an aggregated data set. Data compiled in Donelan et al. (1993) have been used.

For each data set the median values of Charnock parameter and inverse wave age have been plotted (Figure 3.16). The median has been used as an approximation to the bin values from averaged measured quantities, since the measured quantities were not available individually. It can be seen that the result for the Rødsand measurement is close to the trend line proposed by JHVL98.

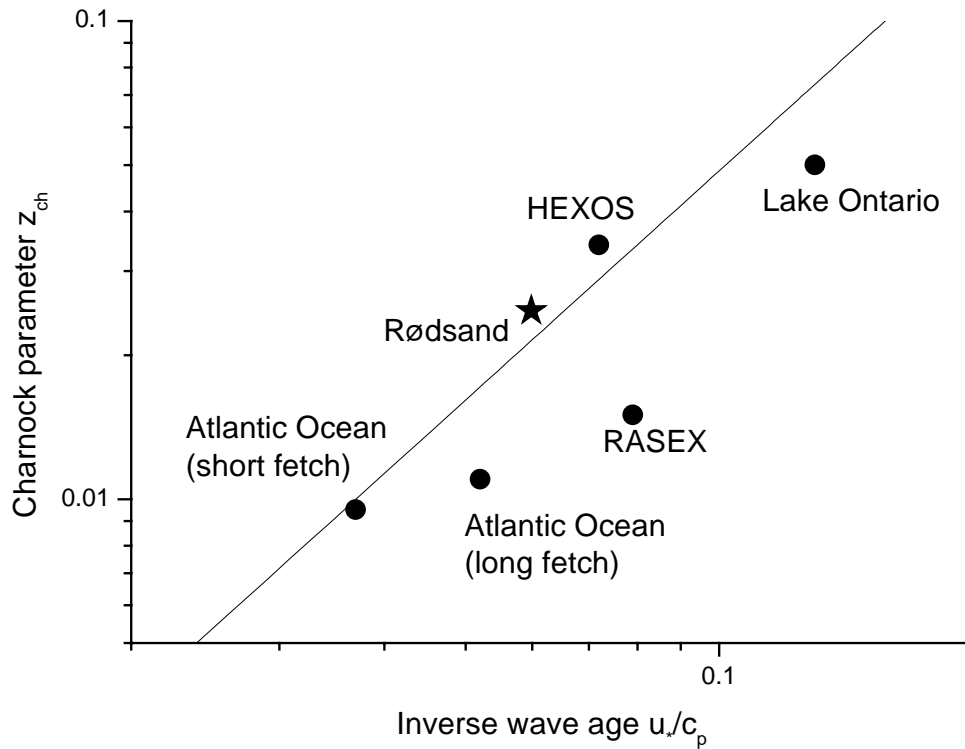


Figure 3.16: Scatter plot of averaged Charnock parameter versus inverse wave age for several data sets and comparison with the empirical fit of JHVL98

A comparison with other proposed trend lines in the literature (Toba et al. (1990), Drennan et al. (2000), Maat et al. (1991), Monbaliu (1994), Smith et al. (1992)) is made in Figure 3.17. It can be seen that a wide range of coefficients has been found for the power law relation $z_{ch}=A(u^*/c_p)^B$ (see Table 3.3). Some possible reasons for these differences are discussed in the following chapter.

Table 3.3: Parameter values proposed for the power law relation $z_{ch}=A(u^*/c_p)^B$ in the literature

	A	B
Toba et al., 1990	0.02	-0.5
Maat et al., 1991	0.8	1
Smith et al., 1992	0.48	1
Monbaliu, 1994	2.87	1.69
JHVL98	1.89	1.59
Drennan et al., 2000	1.7	1.7

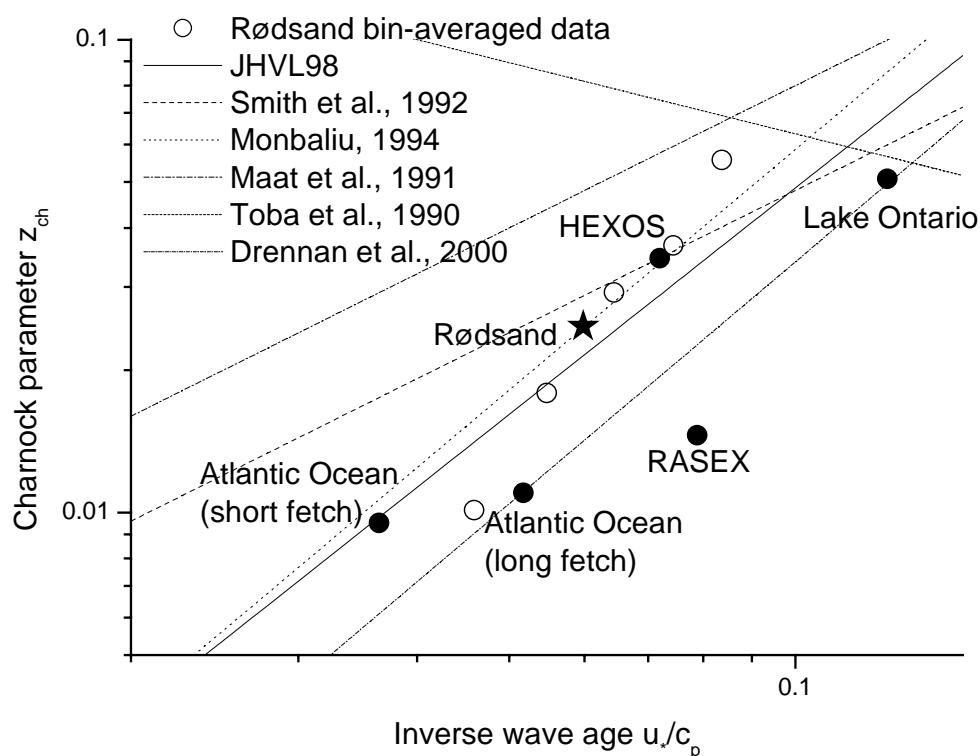


Figure 3.17: Comparison of averaged Charnock parameter versus inverse wave age for several data sets with proposed empirical relations

3.4 Influence of self-correlation

In Hicks (1981) a numerical method is described to investigate the functional relationship introduced by self-correlation. A functional relation is derived from an artificial random ‘data’ set of unrelated values for the input parameters to the analysis. The functional relationship found will solely be a result of the correlation introduced in the analysis. Here the question is if the introduction of a quantity describing the wave field, namely the wave phase speed as the only wave parameter in the relation, leads to a relation between Charnock parameter and wave age, which has physical meaning and is not a mere result of self-correlation.

For this purpose an artificial ‘data set’ has been produced, where the measured values of wave phase speeds are exchanged by random numbers. Instead of an uniformly distributed probability of the values as proposed by Hicks (1981), the probability distribution is chosen to follow those of the measured data set (Figure 3.18c). This is done by randomly redistributing the measured data of wave phase speed within the data set. To increase the data volume and improve ‘randomness’ the measured data set has been repeated several times. For friction velocity and neutral 10 m wind speed the actual measurement values are used without change. Figure 3.18a and b show their probability distributions in the Rødsand data set.

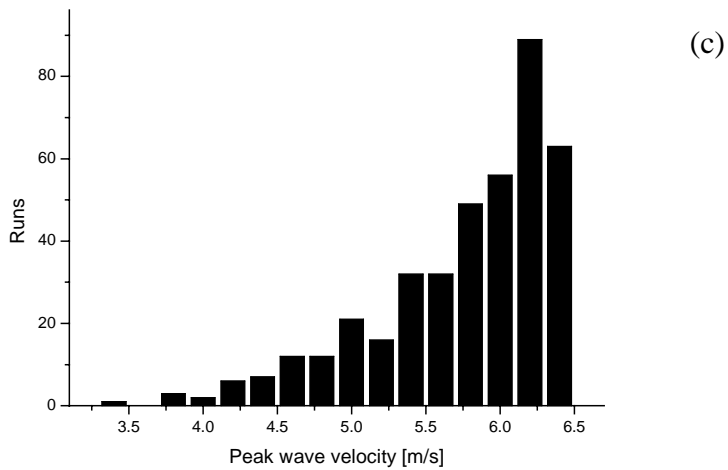
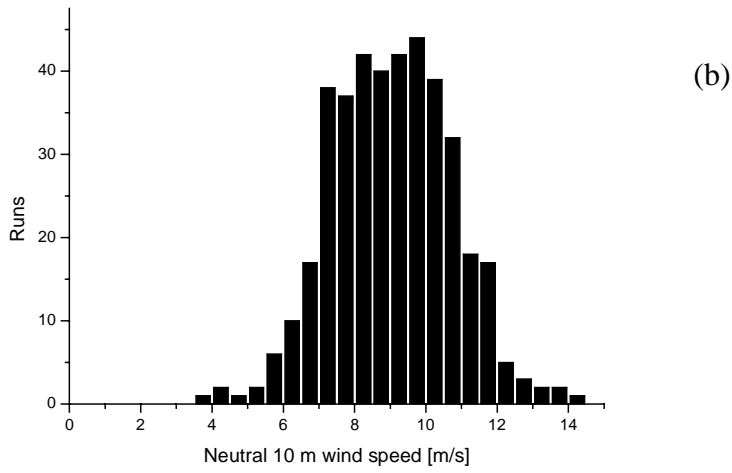
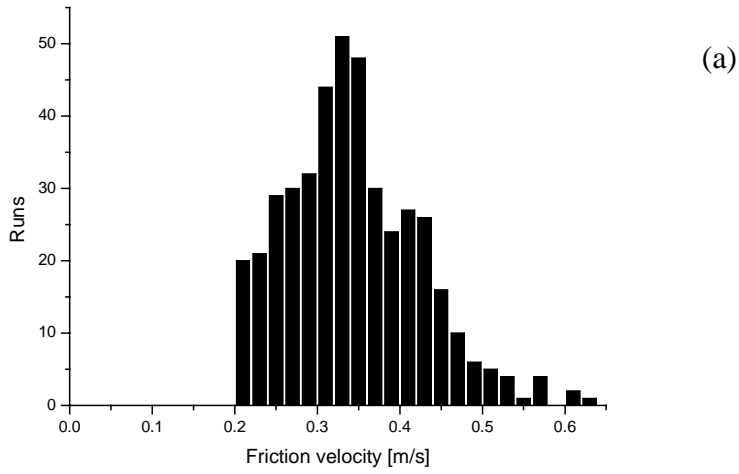


Figure 3.18: Probability distributions of u_* , u_{10m} , and c_p in the measured Rødsand data

Figure 3.19 shows the Charnock parameter versus inverse wave age for the random ‘data’. This can be compared with the measured data from Rødsand shown in Figure 3.11. Clearly the data points from the random data show larger spreading. However, a trend of increasing Charnock parameter for increasing inverse wave age can be found in both figures. This is clearly an undesired influence of the common scaling variable u_* .

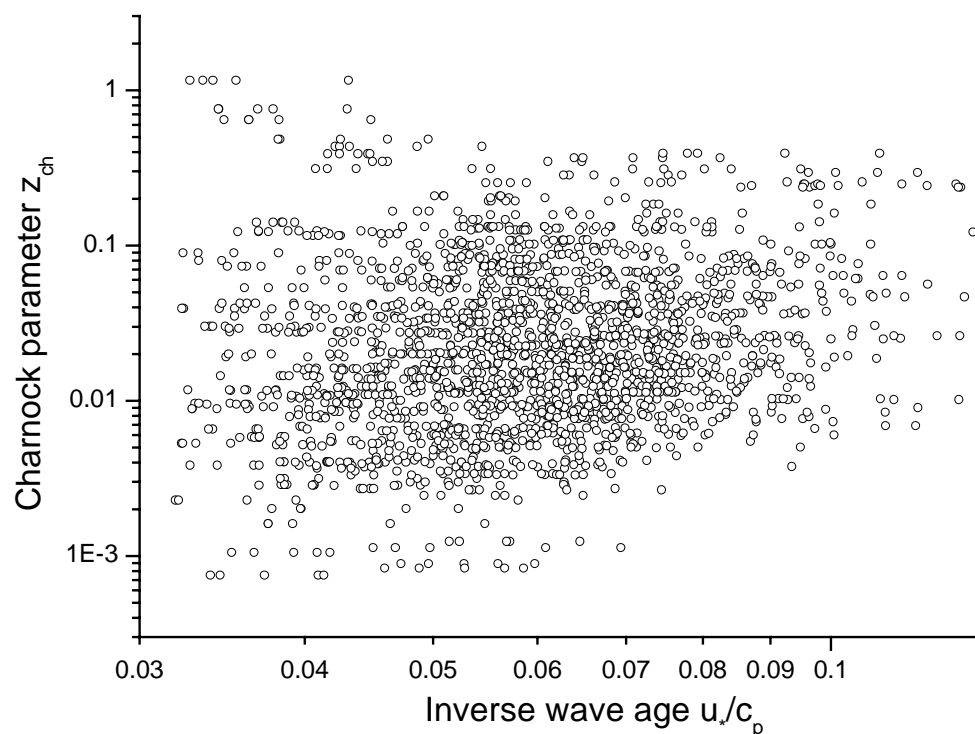


Figure 3.19: Charnock parameter versus wave age from simulated random ‘data’

The random ‘data’ have subsequently been analysed in the same way as the real data (see previous chapter): The ‘data’ have been sorted according to wave age bins, the input quantities u_{10m} , u_* and c_p have been averaged for each bin and the bin values of the derived quantities z_{ch} and wave age have been found from these averaged values. Figure 3.20 shows the resulting bin values of the random ‘data’ in comparison with those of the measured data and the trend line from JHVL98. It is obvious that both trend lines increase for increasing inverse wave age. The trend line of the random data set is the result of self-correlation of the friction velocity u_* . The difference between the two trends is the result of the physical dependency of the Charnock parameter on the wave phase speed c_p . Both trends appear to be different with the one of the random data showing a smaller slope. However, uncertainties in the measured data, as illustrated by the error bars, are too large to allow the difference in trends to be conclusive, i.e. not even the existence of a physical dependency between Charnock constant and wave age can be deduced from this data set due to self-correlation. This confirms the conclusion of JHVL98, that a trend which is not severely influenced by self-correlation can only be found when an aggregated data set is used. The range of wave age values has to be large enough to allow a statistically significant separation between the observed trend line and the trend line obtained without wave information.

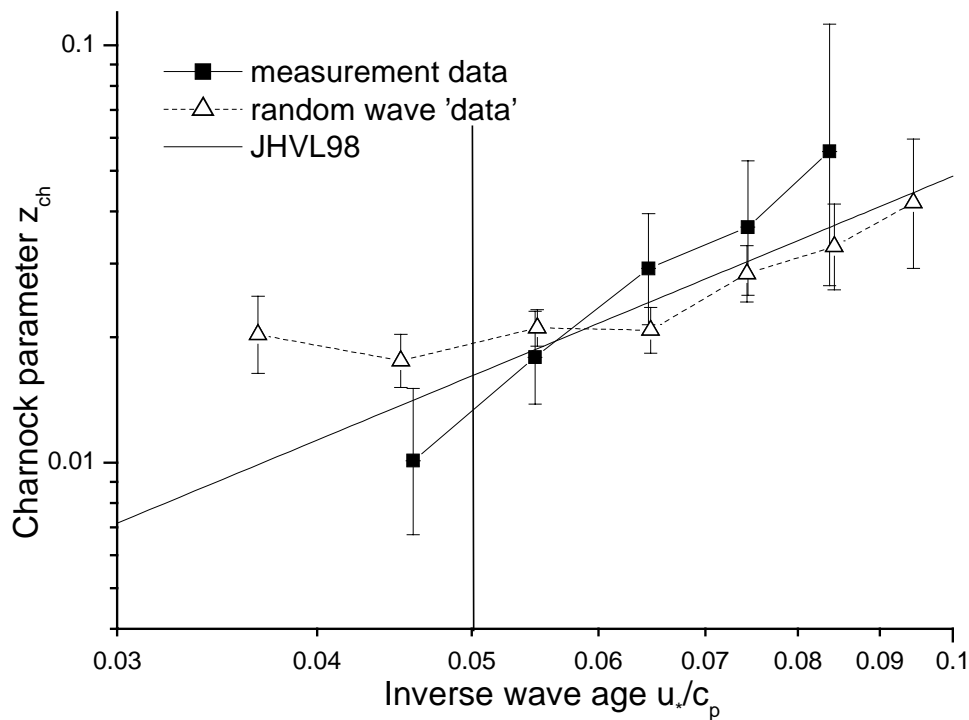


Figure 3.20: Wave age bin values of Charnock parameter versus inverse wave age from the Rødsand measurement and the simulated random 'data'; also shown is the JHVL98 relation

Ideally, the self-correlation should be investigated for the aggregated data set used in section 3.3.4. The measured quantities of these data sets were not available. Instead, a smaller sub-set of the Rødsand data are used to investigate the effect of different data sets on self-correlation. For this only data with a nearly constant neutral wind speed u_{10n} of 8-10m/s have been selected. The analysis of the data as well as the compilation and analysis of a simulated random 'data' set has been repeated and compared with the result of all data (Figure 3.21). The steepness of the relation between Charnock parameter and inverse wave age is larger for the data with a nearly constant wind speed. Also, the difference between the trends of the real and the random data is smaller for the data set with the narrow wind speed range. This shows that for this data subset the relation is almost entirely due to self-correlation of u_* .

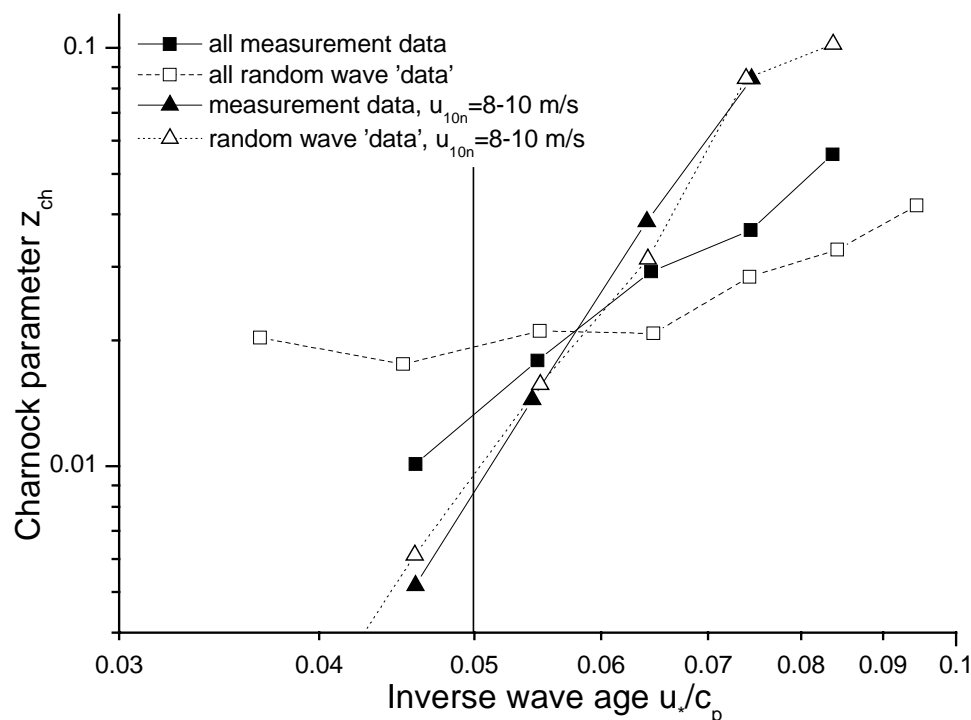


Figure 3.21: Comparison of wave age dependency of Charnock parameter for all data and a data subset with neutral wind speed 8-10 m/s; shown are results from the Rødsand measurement and simulated random 'data' sets

3.5 Discussion of analysis method

3.5.1 Bin-averaging

For the dependence of the Charnock parameter on inverse wave age a power law relation is assumed. The coefficients of the relation have to be found empirically by a fit to measured data. A problem arises if the data show a large statistical spreading and one of the scaling groups does not follow a normal probability distribution.

Data of measured Charnock parameters have a large spreading, mainly due to the sampling variability in the u_* measurement. Also, the Charnock parameter depends on physical quantities of u_* and u_{10n} in a highly non-linear way (see equation 7). Therefore it can not be simply averaged and a fit based on a rms-error of z_{ch} does not seem suitable. A simple example: Assuming 3 records with u_{10n} of 10 m/s and u_* of 0.2, 0.3 and 0.4 m/s the z_{ch} values are calculated to 0.000005, 0.001 and 0.03. The average of the z_{ch} values is 0.01. If instead the physical measured quantities are averaged and z_{ch} is calculated from the average u_{10n} and u_* values, the average z_{ch} is 0.001, i.e. one magnitude smaller.

To avoid these problems, a bin-averaging method is used instead of a direct fit or an averaging of z_{ch} . The procedure generally consists of two steps: First the data are sorted for the value of one parameter (sorting parameter) in bins. Afterwards one or several parameters are averaged over all records in each bin (averaged parameters) and derived quantities are calculated from these (bin values). In the resulting bin values the large statistical spreading has vanished and a linear fit can be made to determine the coefficients of the power law relation. For the determination of a power

law relation between Charnock parameter and inverse wave age, the inverse wave age is used as sorting parameter. The averaged parameters are the measured quantities u_* , u_{10n} and c_p . The Charnock parameter is then calculated from these averaged values for each bin. As an estimate of the measurement uncertainty, standard errors of z_{ch} are calculated from the standard errors of the averaged quantities.

Figure 3.22 shows the difference between the fits of a power law relation to the measured Charnock parameters and the bin values. The large difference is obvious. Also shown is the result of a fit to the logarithm of the measured Charnock parameter $\log_{10}(z_{ch})$. It can be seen that this is a good approximation to the bin-averaging method.

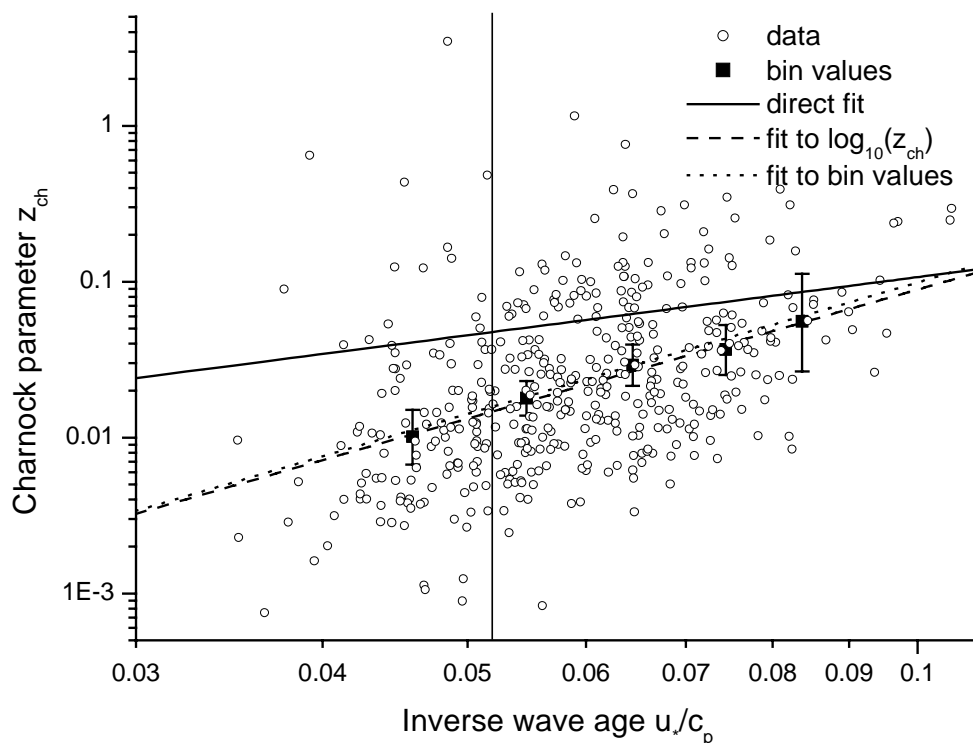


Figure 3.22: Comparison of methods to fit a power law relation between Charnock parameter and inverse wave age to measured data

In the previous chapter it was found that the trend of the Charnock parameter with inverse wave age is influenced or even determined by the self-correlation due to the variability in u_* , depending on the range of the u_* and c_p values in the data set. Since this self-correlation is part of the relation found from the measured data, it will also differ for different data sets. This partly explains the differences found from different data sets for the coefficients of the power law relation. The effect of different data sets on the relation found is shown again in Figure 3.23 for three different wind speed intervals. The data have been sorted according to wind speed and inverse wave age in a two-dimensional bin averaging. The small squares show the bin values of Charnock parameter versus inverse wave age for a certain wind speed and inverse wave age interval. As it was already found in Figure 3.21, the relation is steeper for a narrow wind speed interval due to the dominating influence of self-correlation in u_* .

Figure 3.23 also shows how the choice of the sorting parameter can influence the result of the trend investigation. The large squares are the bin values for the three wind speed intervals without sorting for inverse wave age. The different sorting

parameter, in this case wind speed, leads to a wrong apparent trend of Charnock parameter with inverse wave age.

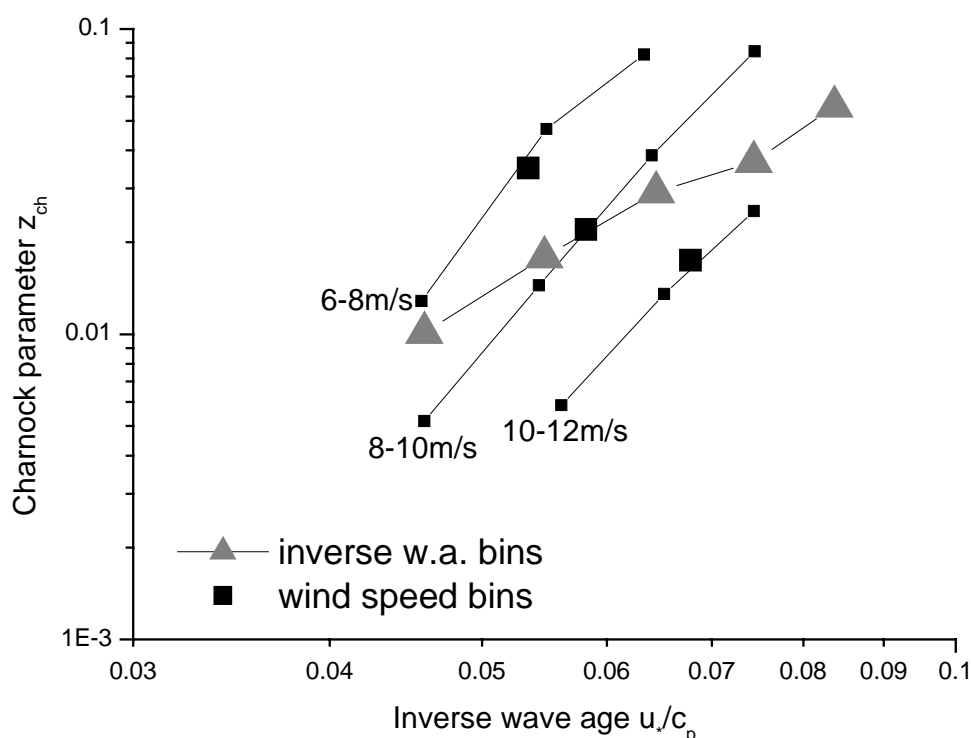


Figure 3.23: Charnock parameter versus wave age from Rødsand measurement; bin values from bin averaging with respect to inverse wave age (large triangles) and with respect to neutral wind speed at 10 m height (large squares) are shown as well as bin values after the data were sorted and bin averaged both in wind speed and inverse wave age bins (small squares)

3.5.2 Rough flow condition

One of the conditions for the dependence of sea surface roughness on wave age alone is that the air flow must be rough turbulent (see JHVL98). If this condition is not satisfied, it can be expected that the sea surface roughness would also depend on the Reynolds roughness number of the flow.

JHVL98 follow Toba et al. (1990) in defining a limiting roughness Reynolds number $R_{cr} = u_* z_0 / \nu$ (with ν = kinematic viscosity) for fully rough flow of 2.3. Since the value is important for the selection of data an attempt is made to reconstruct the origin in the literature. Toba et al. (1990) quote Schlichting (1979), who defines aerodynamically fully rough flow by:

$$\frac{u_* k_s}{\nu} > 70 \quad (3.15)$$

here k_s is the sand grain size used in experiments in rough pipes by Nikuradse (1933). For other flows this is related to the roughness parameter k by the empirically found formula by Schlichting (1936):

$$5.75 \log \left(\frac{k_s}{k} \right) = 8.5 - B \quad (3.16)$$

Concerning the flow of natural winds over the surface of the earth, Schlichting reports findings from Paeschke (1937), who found $B=5$ when the physical height of the vegetation is used as roughness parameter k . This leads to the relation $k_s=4k$ between Nikuradse's sand grain size k_s and the roughness parameter k . The logarithmic profile used by Schlichting:

$$\frac{u}{u_*} = 2.5 \ln \left(\frac{z}{k_s} \right) + B \quad (3.17)$$

can be used to relate his roughness parameter k to the surface roughness length z_0 . Inserting the result, $k=7.4 z_0$, and $k_s=4k$ in equation 3.17 leads to the limiting roughness Reynolds number used by JHVL98 and Toba et al. (1990):

$$R_{cr} = \frac{u_* z_0}{\nu} = 2.3 \quad (3.18)$$

Kitaigorodskii (1970) takes a similar approach also based on the measurements of Nikuradse (1933) and finds a similar limiting value of 3.0. The many assumptions about the similar behaviour of flow through pipes and in the atmosphere and about the similar effect of sand, vegetation and waves suggest that these values should be used with caution.

In the following it is shown that the application of the roughness Reynolds number as roughness criterion in a data set with large scatter can lead to a misleading impression about the overall trend in a z_{ch} versus u_*/c_p plot depending on the effective fetch of the site. This is caused by the large scatter of the measured sea surface roughness, which enters into the selection criterion as part of the flow roughness.

The rough flow condition can be written in terms of the Charnock parameter as:

$$z_{ch} > R_{cr} g \nu u_*^{-3} \quad (3.19)$$

where $R_{cr} = z_0 u_* / \nu$ is the critical flow roughness for rough turbulent flow. For growing wind-waves in fetch limited cases in deep water, Kahma and Calhoun (1994) obtained the following relationship:

$$\frac{u_*}{c_p} = 3.08 (gX)^{-0.27} u_*^{0.54} \quad (3.20)$$

where X is the upstream fetch over water in m. Equations 3.19 and 3.20 can be combined to give:

$$z_{ch} > 520.4 R_{cr} g \nu (gX)^{-1.5} \left(\frac{u_*}{c_p} \right)^{-5.56} \quad (3.21)$$

Equation 3.21 is the roughness flow condition expressed in terms of the dimensionless sea roughness (Charnock parameter), inverse wave age and fetch. On a z_{ch} versus u_*/c_p plot, this condition filters out all data points below the line given by Equation 3.21. The number of data points filtered out depends on the effective fetch at the site. This is illustrated in Figure 3.24 ($R_{cr}=2.3$, $g=9.81\text{m/s}^2$, $\nu=1.461 \times 10^{-5} \text{ m}^2/\text{s}$), which shows the limiting line of equation 3.21 for different fetch lengths. It can be seen that for typical ranges of z_{ch} and u_*/c_p and short to moderate fetch lengths ($<50\text{km}$) a large amount of data is filtered out, while a relatively small amount of data is filtered out for the longest fetch lengths ($>500\text{km}$).

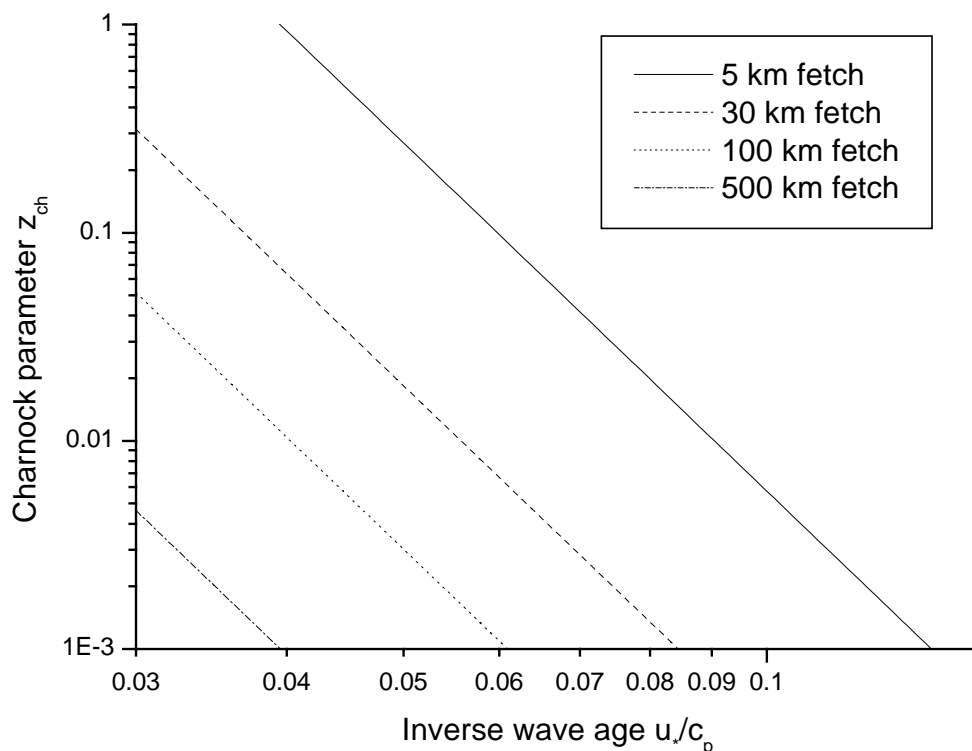


Figure 3.24: Sensitivity of the roughness flow criterion of JHVL98 with fetch on a plot of Charnock parameter versus inverse wave age ($R_{cr}=2.3$); based on equation 3.21

Figure 3.25 shows the Rødsand data segregated according to the flow roughness number. A trend of increasing Charnock parameter with inverse wave age can be seen, although with a large scatter in the data. Figure 3.25 also shows the calculated Reynolds criterion line using equation 3.21. It is observed that this corresponds closely to the data when an effective fetch of 30 km is used for the site. For this particular case, the average effective fetch was obtained using equation 3.20 and the measured values of c_p and u_* . Note that the effective fetch is not the same as the physical fetch, since the former also includes the influence of wind duration and water depth, since equation 3.20 is only valid for deep water and waves that are not duration limited.

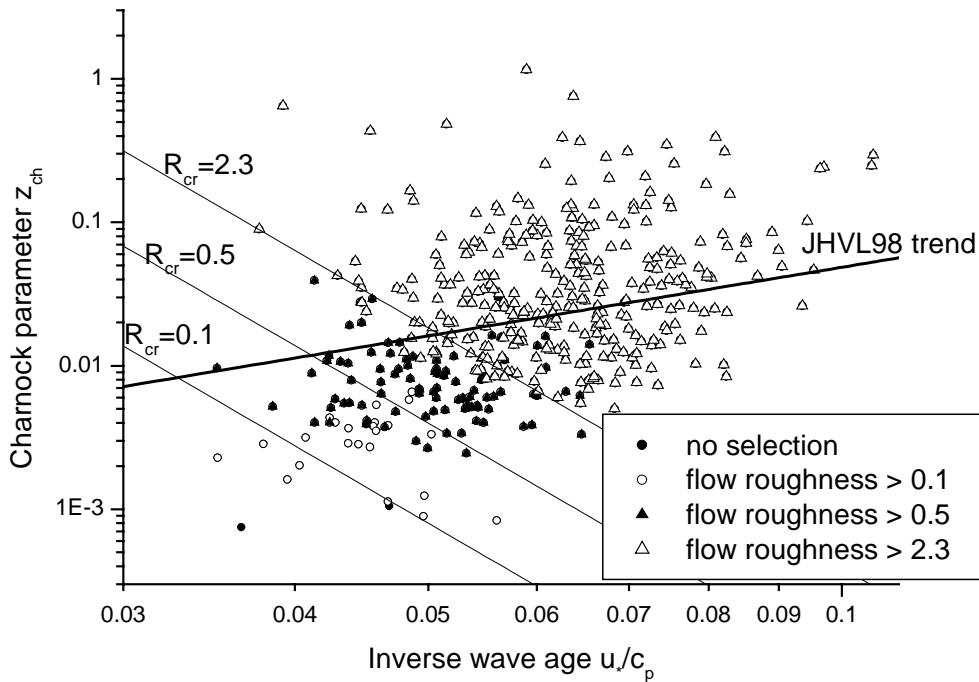


Figure 3.25: Charnock parameter versus inverse wave age from Rødsand data segregated according to flow roughness; also shown are the limiting lines of equation 3.21 for an effective fetch of 30 km and a R_{cr} of 2.3, 0.5 and 0.1

Applying this condition as a selection criterion to the data before bin averaging leads to problems. This is demonstrated in Figure 3.26, where the influence of the choice of flow roughness limit on the relation of Charnock parameter with wave age is shown. The data have been selected for different choices of the flow roughness limit and thereafter bin averaged. It can be seen that the relation between Charnock parameter and inverse wave age at small inverse wave ages changes drastically for different flow roughness criteria. This shows that for short to moderate fetch lengths, the scatter above the roughness criterion line can present itself as a trend of decreasing z_{ch} with increasing inverse wave age, i.e. can lead to a misleading impression about the overall trend in a z_{ch} versus u^*/c_p plot. This is probably the cause of the similar apparent trend in the RASEX data as reported by JHVL98. It can also be seen that the obtained trend – apart from the mentioned distortion - does not depend on the value used for the selection criterion for the flow roughness.

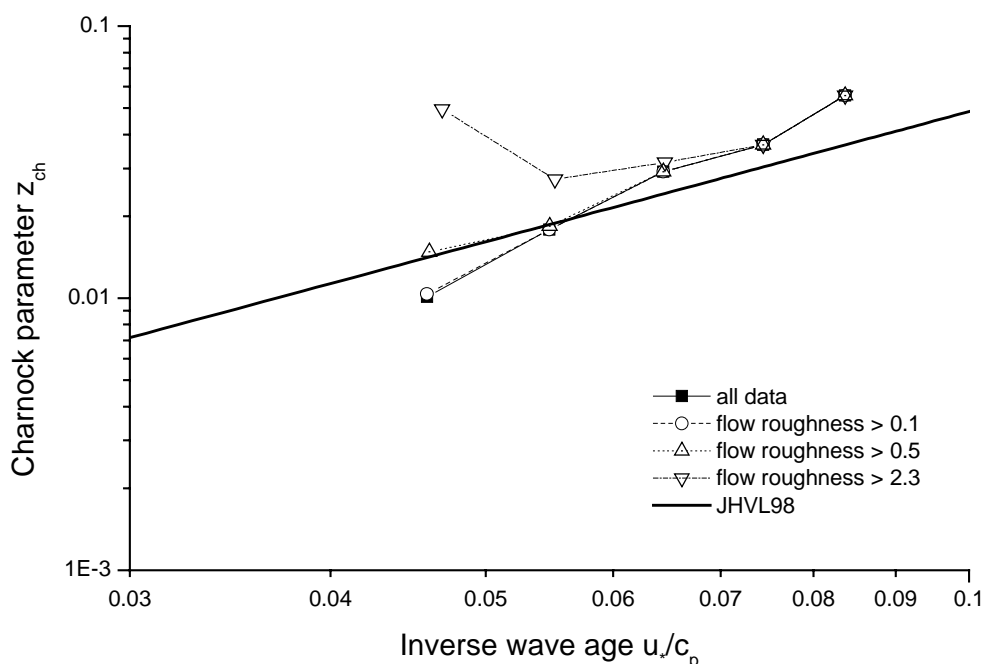


Figure 3.26: Charnock parameter versus inverse wave age for different flow roughness selection criteria

If it is assumed that the relation between z_{ch} and u_*/c_p is real and the scatter in the data around it is due to measurement variability, the criterion for flow roughness should be applied to the physical relation rather than the scattered data including measurement variability. In Figure 3.25 it can be seen that the limiting line for the roughness Reynolds number for an effective fetch of 30 km and $R_{cr}=2.3$ crosses the JHVL98 trend line at an inverse wave age of about 0.05. This criterion should therefore be used by rejecting data with lower inverse wave ages. In this way the distortion of the result due to application of a selection criterion to a scattered data set is avoided.

An approach different from that used by Toba et al. (1990) and Kitaigorodskii (1970) is proposed by Donelan (1990), who summarises open ocean experiments from Smith (1980) and Large and Pond (1981). He distinguishes only between smooth and rough flow and used the friction velocity as criterion for flow roughness:

$$z_0 = 0.11 \frac{V}{u_*} \quad \text{for } u_* < 2(\nu g)^{1/3} = 0.1 \frac{m}{s} \quad (\text{smooth flow}) \quad (3.22)$$

$$z_0 = 0.014 \frac{u_*^2}{g} \quad \text{for } u_* > 2(\nu g)^{1/3} = 0.1 \frac{m}{s} \quad (\text{rough flow}) \quad (3.23)$$

The limit for u_* is the value where the sea surface roughness for smooth and rough flow are equal. For the Rødsand data this criterion is automatically fulfilled since data with $u_* < 0.2$ m/s have been rejected already to ensure that the sonic anemometer is in the surface layer (see section 3.2.5).

3.6 Conclusion

New simultaneously measured wind and wave data from the field measurement program at Rødsand in the Danish Baltic Sea are presented. These data have been

used to test the wave age dependence of the Charnock parameter (or dimensionless sea surface roughness). A general trend of increasing sea roughness with inverse wave age is obtained which agrees with the trend found in JHVL98 and similar parameterisations.

By analysing a simulated data set of randomly generated wave 'data' it was shown that self-correlation severely influences the observed relation between Charnock parameter and wave age. Uncertainties in the measured data are too large to allow the difference in trends between real and simulated random 'data' to be conclusive. This means that with the Rødsand data set alone, not even the existence of a physical dependency between Charnock parameter and wave age can be proven. This is in agreement with the conclusion of JHVL98, that a trend, which is not severely influenced by self-correlation, can only be found with an aggregated data set where the range of wave age values is large enough to allow a statistically significant separation between the observed trend line and the trend line obtained without wave information.

By using a small sub-set of the Rødsand data it was shown that for a data set with narrower ranges of c_p and u_* the trend lines of real and random 'data' move closer together. We believe that for a data set with a very large range of wave age values the influences of self-correlation and physical dependency can be separated. Further research is needed here.

From this investigation it becomes clear that the dependence of the Charnock parameter on wave age is less pronounced than what could be expected without taking into account the influence of self-correlation. We therefore expect that, even if the physical nature of the trend can be shown, the improvement of the Charnock relation with a wave age dependent Charnock parameter is limited. Future research should consider also alternative approaches for the parameterisation of the Charnock parameter, e.g. with wave height or wave steepness.

In the literature, different coefficients for the power law between Charnock parameter and wave age have been found for different data sets. Such differences can be expected since for different data sets – and hence different ranges of the quantities u_* and c_p – different self-correlation relations follow, which lead to different coefficients in the power law relation.

Additionally, it is shown that the roughness Reynolds number criterion often applied to select data with rough turbulent flow can lead to a misleading impression about the trend in the data, since the sea surface roughness is present in both the selection rule and in the quantity under investigation. This is believed to be the cause of the apparent trend of a decrease in Charnock parameter with inverse wave age in the RASEX data as reported by JHVL98. The importance of this distortion varies with the effective fetch length at the site. It is mainly important for short to medium fetch lengths. Two alternative methods to ensure aerodynamically rough flow are discussed, which do not distort the relation. Instead of applying the roughness Reynolds number criterion to the (scattered) data it can be applied to the relationship found. This leads to a limiting inverse wave age, which in the case of the Rødsand data is $u_*/c_p > 0.05$. A different criterion for rough flow is the one by Donelan (1990), who finds a limit of $u_* > 0.1$ m/s for rough flow, by equalling the sea surface roughness estimated for rough and smooth flow.

A misleading trend can also be caused by the methods to obtain the parameterisation from the data. Investigation of the bin-averaging method showed that the choice of the sorting parameter in the bin-averaging analysis can lead to an inversion of the observed trend of Charnock parameter with wave age.

To sum up, we conclude that the Charnock parameter increases with inverse wave age. This increase can be described by a power law relation. Different coefficients for this relation found in the literature can probably be explained by self-correlation effects and differences in data selection and analysis. While the existence of the trend seems clear, the significance of it is not. We find that the importance – if not existence – of the physical dependency is questioned by self-correlation effects, i.e. that the relation is severely influenced or even determined by self-correlation effects. We believe that the physical dependency can only be proven for a large data set with a very wide range of wave age values. Self-correlation effects limit the usefulness of the relation for improving the Charnock relation for sea surface roughness by including wave age.

Acknowledgements

The research was funded by the Danish Technical Research Council (STVF) as part of the project “Wind-wave interaction in coastal and shallow areas”. We gratefully acknowledge the financial support of the Rødsand measurement program by the following: European Union, JOULE program (JOU2-CT93-0325), Office of naval research (N00014-93-1-0360) and ELKRAFT. The work of one of the authors (B. Lange) was partly funded by the European Commission through a Marie Curie Research Training Grant. Many thanks to Rebecca Barthelmie from Risø for managing the Rødsand field experiment since 1998. The technical support team at Risø and Mr Kobbarnagel of Sydfalster-El are acknowledged for their contribution to the data collection. The authors wish to thank the two anonymous reviewers for their important and useful comments, which led to a substantial improvement of the paper.

References

- Charnock, H., 1955: Wind stress over a water surface. *Quart. J. Roy. Meteor. Soc.*, **81**, 639-640.
- Donelan, M., 1990: Air-sea interaction. *Ocean Engineering Science Volume 9 Part A. The Sea*, B. Le Méhauté and D.M. Hanes, Eds., 239-292.
- Donelan, M.A., F.W. Dobson, S.D. Smith and R.J. Anderson, 1993: On the dependence of sea surface roughness on wave development. *J. Phys. Oceanogr.*, **23**, 2143-2149.
- Drennan, W. M., H. C. Graber, D. Hauser and C. Quentin, 2000: On the wave age dependence of wind stress over pure wind seas. submitted to *Journal of Geophysical Research*
- Garratt, J.R., 1992: *The atmospheric boundary layer*. Cambridge University Press, 316pp.
- Geernaert, G.L., K.B. Katsaros and K. Richter, 1986: Variation of the drag coefficient and its dependence on sea state. *J. Geophys. Res.*, **91**, 7667-7679.

- Hasselmann, K., T. P. Barnett, E. Bouws, H. Carlson, D. E. Cartwright, K. Enke, J. A. Ewing, H. Gienapp, D. E. Hasselmann, P. Kruseman, A. Meerburg, P. Müller, D. J. Olbers, K. Richter, W. Sell and H. Walden, 1973: Measurements of Wind-Wave Growth and Swell Decay during the Joint North Sea Wave Project (JONSWAP). *Dtsch. Hydrogr. Z. Suppl.*, A 12, No.8
- Hicks, B.B., 1978: Some limitations of dimensional analysis and power laws. *Bound.-Layer Meteor.*, **14**, 567-569.
- Hicks, B.B., 1981: An examination of turbulence statistics in the surface boundary layer. *Bound.-Layer Meteor.*, **21**, 389-402.
- Hsu, S.A., 1974: A dynamic roughness equation and its application to wind stress determination at the air-sea interface. *J. Phys. Oceanogr.*, **4**, 116-120.
- Højstrup, J., 1999: Vertical Extrapolation of Offshore Windprofiles. *Wind energy for the next millennium*. Proceedings. 1999 European wind energy conference (EWEC '99), Nice (FR). Petersen, E.L.; Hjuler Jensen, P.; Rave, K.; Helm, P.; Ehmann, H., Eds., 1220-1223.
- Johnson, H.K., J. Højstrup, H.J. Vested, S.E. Larsen, 1998: On the dependence of sea surface roughness on wind waves. *J. Phys. Oceanogr.*, **28**, 1702-1716.
- Kahma, K.K. and C.J. Calhoun, 1994: Growth curve observations. *Dynamics and Modelling of Ocean Waves*, G.J. Komen, L. Cavaleri, M. Donelan, K. Hasselmann, S. Hasselmann, P.A.E.M. Janssen, Cambridge University Press, 174-182.
- Kitaigorodskii, S.A., 1970: *The physics of air-sea interaction*. Translated from Russian by A. Baruch, Israel Program for Scientific Translations, Jerusalem, 237pp.
- Lange, B., R.J. Barthelmie and J. Højstrup, 2001: *Description of the Rødsand field measurement*. Report Risø-R-1268. Risø National Laboratory, DK-4000 Roskilde, Denmark, 59pp. (available at www.risoe.dk)
- Large, W.G. and S. Pond, 1981: Open ocean momentum flux measurements in moderate to strong winds. *J. Phys. Oceanogr.*, **11**, 464-482.
- Maat, N., C. Kraan and W. A. Oost, 1991: The roughness of wind waves. *Boundary-Layer Meteorology*, **54**, 89-103.
- Monbaliu, J., 1994: On the use of the Donelan wave spectral parameter as a measure for the roughness of wind waves. *Boundary-Layer Meteorol.*, **67**, 277-291.
- Mortensen, N.G. and J. Højstrup, 1995: The solent sonic – response and associated errors. *Proceedings of the 9th AMS symposium on meteorological observations and instrumentation*, March 27-31, 1995, Charlotte, N.C., pp.501-506; AMS, Boston, Massachusetts
- Nikuradse, J., 1933.: Strömungsgesetze in rauhen Röhren. *Forsch. Arb. Ing.-Wes.* No. 361.
- Paeschke, W., 1937: Experimentelle Untersuchungen zum Rauheits- und Stabilitätsproblem in der bodennahen Luftschicht, Dissertation, Universität Göttingen.
- Schlichting, H., 1936: Experimentelle Untersuchungen zum Rauheitsproblem. *Ing.-Arch.*, **7**, 1-34

- Schlichting, H., 1979: *Boundary-Layer Theory*. Seventh edition. McGraw-Hill, New York, 817 pp.
- Schotanus, P., F. T. M. Nieuwstadt and H. A. R. De Bruin, 1983: Temperature measurement with a sonic anemometer and its application to heat and moisture fluxes. *Bound.-Layer Meteor.*, **26**, 81-93.
- Smith, S.D., 1980: Wind stress and heat flux over the open ocean in gale force winds. *J. Phys. Oceanogr.*, **10**, 709-726.
- Smith, S.D., R.J. Anderson, W.A. Oost, C. Kraan, N. Maat, J. DeCosmo, K.B. Katsaros, K.L. Davidson, K. Bumke, L. Hasse, and H.M. Chadwick, 1992: Sea surface wind stress and drag coefficients: The HEXOS results. *Bound.-Layer Meteor.*, **60**, 109-142.
- Stull, R. B., 1988: *An introduction to boundary layer meteorology*. Kluwer Academic Publishers, 666pp.
- Taylor, P.K., M.J. Yelland, 2001: The dependence of sea surface roughness on the height and steepness of the waves. *J. Phys. Oceanogr.*, **31**, 572-590.
- Tennekes, H., 1982: Similarity relations, scaling laws and spectral dynamics. *Atmospheric turbulence and air pollution modelling*, F.T.M. Nieuwstadt and H. van Dop, Eds., Reidel, pp.37-68.
- Toba, Y., N. Iida, H. Kawamura, N. Ebuchi and I.S.F. Jones, 1990: Wave dependence on sea-surface wind stress, *J. Phys. Oceanogr.*, **20**, 705-721.
- Wyngaard, J. C., 1973: On surface-layer turbulence. *Workshop on Micrometeorology*. D. A. Haugen, Ed., American Meteorological Society, Boston, pp. 101-149.

4 The influence of thermal effects on the wind speed profile of the coastal marine boundary layer⁸

Abstract

The wind speed profile in a coastal marine environment is investigated with data from the measurement program Rødsand, where meteorological data are collected with a 50 m high mast in the Danish Baltic Sea, about 11 km from the coast. When compared with the standard Monin-Obukhov theory the measured wind speed increase between 10 m and 50 m height is found to be systematically larger than predicted for stable and partly for near-neutral conditions. The data indicate that the deviation is smaller for short (10-20 km) distances to the coast than for larger (>30 km) distances.

The theory by Csanady (1974) offers a qualitative explanation for these findings: When warm air is advected over colder water, a capping inversion might develop. The air below is constantly cooled by the water and gradually develops into a well-mixed layer with near-neutral stratification. Typical examples as well as scatter plots of the data are consistent with this explanation. The deviation of measured and predicted wind speed profiles is shown to be correlated with the height and strength of the inversion layer as estimated with Csanady's theory.

4.1 Introduction

Monin-Obukhov theory, although developed from measurements over land, has been found to be generally applicable over the open sea (see e.g. Edson and Fairall (1998)). In homogenous and stationary flow conditions, it predicts a log-linear profile of the vertical wind speed in the atmospheric surface layer:

$$u(z) = \frac{u_*}{\kappa} \left[\ln \left(\frac{z}{z_0} \right) - \Psi_m \left(\frac{z}{L} \right) \right] \quad (4.1)$$

The wind speed u at height z is determined by friction velocity u_* , aerodynamic roughness length z_0 and Monin-Obukhov length L . κ denotes the von Karman constant, taken as 0.4, and Ψ_m is a universal stability function. Thus, if the wind speed is known at one height, the vertical wind speed profile is determined by two parameters: the surface roughness z_0 and the Monin-Obukhov length L .

In coastal waters, when wind is blowing from land over the sea, the coastline constitutes a pronounced change in roughness and heat transfer. They pose a strong inhomogeneity to the flow, which may limit the applicability of Monin-Obukhov theory. Stimulated by measurements of large wind stress over Lake Ontario, Csanady (1974) described the processes governing the flow regime under the condition of warm air advection over colder water. He developed a theory of a well-mixed layer with a capping inversion for this condition. His theory is for equilibrium conditions only, and therefore does not describe the development of the flow regime in space and

⁸ This chapter has also been submitted for publication to *Boundary-Layer Meteorology* as: Lange B, Larsen S, Højstrup J, Barthelmie R.: The influence of thermal effects on the wind speed profile of the coastal marine boundary layer.

time. From measurements in the Swedish Baltic Sea, Smedman et al. (1997) develop a theoretical explanation of the flow regime over coastal waters under conditions of warm air advection, which also describes the evolution of the mixed layer. They use the travel time of the air over the water surface as additional parameter.

In this study we use data from the meteorological monitoring program at Rødsand in the Danish Baltic Sea to investigate the applicability of Monin-Obukhov theory to predict the wind speed profile at this site. Aim of this paper is to show that:

1. the vertical wind speed profile over coastal waters can deviate substantially from Monin-Obukhov prediction
2. this deviation is systematic for frequently occurring conditions and has an effect on the wind climatology
3. the flow regime leading to this deviation can qualitatively be understood with the theory by Csanady (1974)

The structure of the paper is as follows: In the next section the measurements and data analysis are presented. Section 4.3 compares the measured wind speed increase with height with Monin-Obukhov prediction and investigates different ways to derive the necessary parameters L and z_0 . A qualitative explanation for the deviations found there is offered in section 4.4. Conclusions are drawn in the last section.

4.2 The Rødsand field measurement program

4.2.1 Site

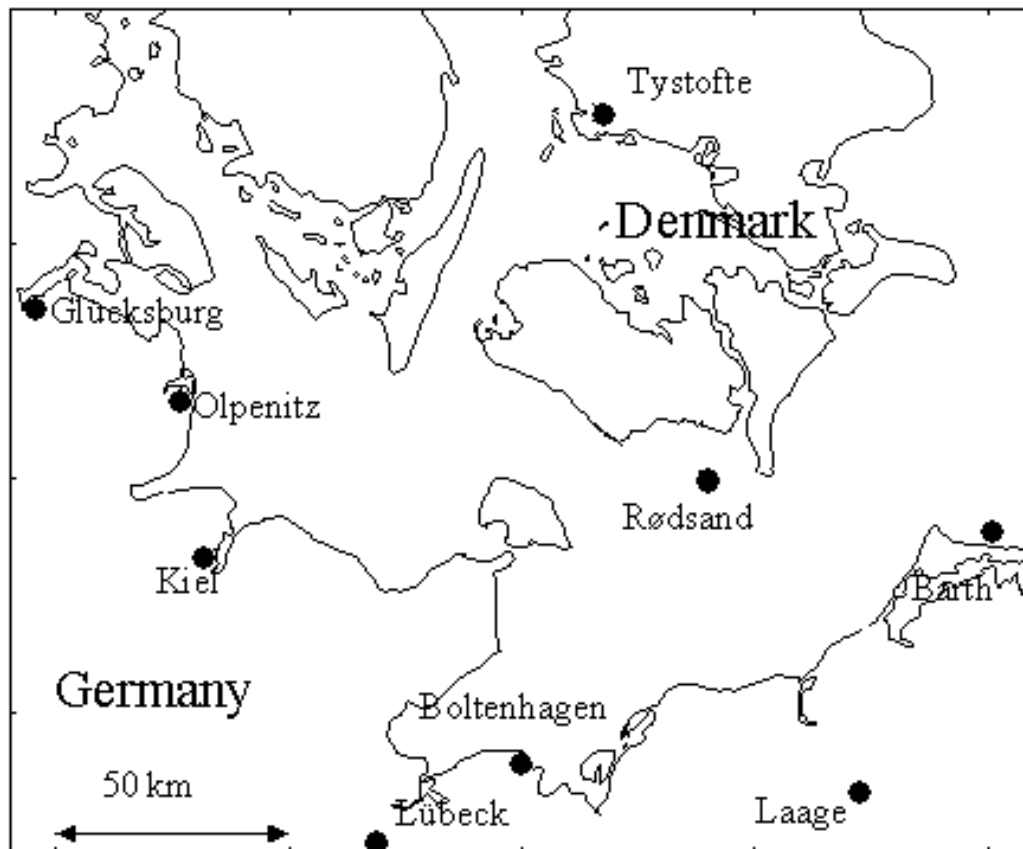


Figure 4.1: Map of the measurement stations

A 50 m high meteorological measurement mast has been established at Rødsand in October 1996 as part of a Danish study of wind conditions for proposed offshore wind farms. The mast is situated about 11 km south of the island Lolland in Denmark (11.74596°E, 54.54075°N) (see Figure 4.1). The mast is located in 7.7 m mean water depth with an upstream fetch (distance to coast) of 30 to more than 100 km for wind directions from SE to WNW (120°N to 290°N). In the NW to N sector (300°N to 350°N) the fetch is 10 to 20 km. The present study uses data from March 1998 to January 2000, when wave and current measurements were performed simultaneously.

4.2.2 Instrumentation and Measurements

The instrumentation of the measurement mast is listed in Table 4.1. About 8500 half-hourly records with simultaneous wind and wave measurements have been recorded. A detailed description of the instrumentation and data can be found in Lange et al. (2001).

Table 4.1: Instrumentation of the Rødsand measurement

	height above mean sea level	instrument	sampling rate
Wind speed	50.3 m	cup anemometer	5 Hz
	29.8 m	cup anemometer	5 Hz
	10.2 m	cup anemometer	5 Hz
Wind direction	29.7 m	wind vane	5 Hz
3 axis wind speed and temperature	46.6 m (42.3 m from 12.5.99)	ultrasonic anemometer	20 Hz
Air temperature	10.0 m	Pt 100	30 min mean
Temperature difference	49.8 m – 10.0 m	Pt 500	30 min mean
Sea temperature	about –2m	Pt 100	30 min mean
Sea level		DHI AWR201 acoustic wave recorder	8 Hz
Sea current		GMI current meter	8 Hz

Cup anemometers and wind vane

Mean wind speeds and variances are derived from cup anemometers located at three heights (see Table 4.1). Calibrated instruments of the type Risø P2546a are used. The calibration accuracy is estimated to be +/- 1%. Data are corrected for flow distortion errors due to the mast and the booms with a method developed by Højstrup (1999). Records from situations of direct mast shade have been omitted. The overall uncertainty of the wind speed measurement with cup anemometers is estimated to be +/- 2% and additionally +/- 0.1 ms⁻¹.

A wind vane of the type Risø Aa 3590 is used. The uncertainty of the instrument itself is negligible, but adjustment of the orientation of the instrument is difficult in the field and the absolute accuracy is estimated to be about +/-5°.

Sonic anemometer

The sonic anemometer is of the type Gill F2360a and is mounted at 46.6m height (at 42.3m height from 12/May/99) above mean sea level. It measures wind speed in three components (x,y,z) and air temperature with a resolution of 20 Hz.

Co-variances are calculated from the sonic anemometer measurements with linear trends removed before the calculation. Friction velocity is calculated with the eddy-correlation method as:

$$u_* = \left(\overline{u'w'^2} + \overline{v'w'^2} \right)^{0.25} \quad (4.2)$$

The mean wind speed has been corrected for flow distortion due to mast and booms. Additionally, sonic anemometers experience an array flow distortion, since transducers and struts of the instrument distort the wind flow in the measurement volume. For the horizontal wind speed component flow distortions are corrected with a sensor specific calibration. This is not the case for the vertical wind component. The estimated accuracy is about +/-5% for the horizontal wind speed component and +/-10% for the friction velocity.

Additionally a statistical uncertainty due to the sampling variability has to be considered. Using the approximation of Wyngaard (1973) derived from the Kansas data, the expected accuracy for the u_* measurements is about 10% for an eddy-correlation measurement at 45 m height with an averaging time of 30 minutes and a mean wind speed of 10 ms^{-1} .

Temperature sensors

For the air temperature measurement at 10 m height a PT100 sensor with radiation shield was used. The water temperature was also measured with a PT100 sensor about 2 m below mean sea level. For the temperature difference measurement two PT500 sensors were employed.

Wave and current measurement

Waves are measured by an acoustic wave recorder (AWR), which is a SONAR-type instrument positioned under water. The type is the HD-AWR201 from DHI Water and Environment, Denmark. Wave height and water depth are derived from the time series of water elevation measured by the AWR. The phase speed at peak frequency c_p is calculated using the measured water depth and the spectral peak frequency f_p , which is determined from the measured wave spectra.

The water current sensor is a two dimensional electromagnetic sensor measuring the horizontal water velocity, manufactured by GMI (Geophysical and Marine Instrumentation, Denmark). It is located 5.3 m above the sea bottom. The measurement accuracy of the sensor is estimated to be +/- 2%.

4.2.3 Data processing

Correction of the sonic anemometer measurements for elevation

As a first approximation it is usually assumed that the fluxes in the surface layer are independent of height, implying that the friction velocity and heat flux are constant. However, this assumption is not entirely correct and simple correction procedures have been applied to account for the small decrease of the fluxes with height.

Panofsky (1973) derives the following simplified expression for the height correction of the friction velocity from an analysis of the horizontal momentum equation at the surface and the top of the boundary layer:

$$u_*(z) = u_{*s} - 6f_c z \quad (4.3)$$

Here $u_*(z)$ is the friction velocity measured at height z , u_{*s} is the friction velocity at the surface and f_c the Coriolis parameter ($1.46 \cdot 10^{-4} \sin(\phi)$, with ϕ latitude). This leads to a correction of 0.03 ms^{-1} .

Lenschow et al. (1988) give an empirical relation for the decrease of the covariance of vertical wind speed and temperature, $\overline{w'T'}$, from its surface value $\overline{w'T'_s}$:

$$\overline{w'T'_s} = \begin{cases} \overline{w'T'}(z) \frac{1}{\left(1 - \frac{z}{z_i}\right)^{1.5}} & \text{for stable conditions} \\ \overline{w'T'}(z) \frac{1}{1 - 1.5 \frac{z}{z_i}} & \text{for unstable conditions} \end{cases} \quad (4.4)$$

where $z_i = 0.25u_{*s}/f_c$ is used to estimate the boundary layer height (Tennekes (1982)). This is only valid for near-neutral conditions, but is used here as a first order correction for all cases.

Transformation of wind speeds to water following co-ordinates

For a flow over a moving surface the relevant flow speed is the difference between flow and surface movement. When water currents are present, wind measurements made from fixed structures, like the measurement mast at Rødsand, therefore need to be transformed to the reference frame of the sea surface. At Rødsand, the water current is measured at a mean water depth of 2.4 m. Differences between the current at this depth and the surface current have been neglected and all mean wind speeds measured at the mast have been transformed to refer to the moving reference frame of the water surface. At Rødsand currents are generally weak, usually below 0.4 ms^{-1} , and differences in wind speed due to the transformation are therefore small (less than 3% wind speed difference for 95% of the records).

Data selection

Situations with fast temporal changes in flow conditions are not correctly described by Monin-Obukhov theory. Records with fast changes in atmospheric conditions have therefore been omitted for the analysis. For the important quantities the record under investigation was compared to the two previous and the following record and records with large changes were rejected (54% of the data). This was done for wind speed, wind direction and temperature measurements and for the derived stability parameters (see section 4.3.1.1). Differences of less than 20% were required for wind speed, 15° for wind direction, 0.5°C for air temperature and 0.2°C for water temperature. A maximum change of atmospheric stability of $10/L=0.1$ has been applied, where L is the Monin-Obukhov length determined from the three methods described in section 4.3.1.1.

For low wind speed cases the top of the atmospheric surface layer might be lower than the measurements at 50m and 45 m height. Using again the simple approximation for the height of the boundary layer, $z_i=0.25u_*/f_c$, and assuming that the height of the surface layer is about 10% of this, leads to a limiting value for u_* of about 0.2 ms^{-1} . Measurements with smaller u_* have been rejected (41% of the data). 1892 half-hourly records are used in the final database.

4.2.4 Air temperature measurements over land

The air temperature over land in the upwind direction from Rødsand has been estimated from measurements at synoptic stations of the German Weather Service (DWD) and the measurement station Tystofte in Denmark (operated by the Risø National Laboratory). Seven stations on mainland Germany close to the coast were selected, which cover wind blowing towards Rødsand from west, south and east (see Table 4.2 and Figure 4.1). The measurement station Tystofte is about 70 km inland (see Figure 4.1), but is assumed to give a fair approximation of the air temperature over land for a wind direction sector from 300° to 030° . Measurement height at all land stations is 2 m above ground level. From the German stations the measured temperatures of those stations with upwind direction closest to the measured wind direction at Rødsand have been linearly interpolated to estimate the upwind air temperature over land for Rødsand. For this the geostrophic wind direction determined from geostrophic drag law (see e.g. Garratt (1994)) has been used.

Table 4.2: Synoptic stations used for estimating the upwind air temperature over land

	latitude	longitude	height asl	direction from Rødsand
Glücksburg	54°49'	09°30'	27 m	281°
Olpenitz	54°40'	10°02'	4 m	279°
Kiel-Holtenau	54°22'	10°08'	27 m	256°
Lübeck-Blankensee	53°48'	10°42'	14 m	221°
Boltenhagen	54°00'	11°11'	15 m	210°
Laage	53°55'	12°17'	40 m	150°
Barth	54°20'	12°43'	7 m	112°

4.3 Prediction of wind speed profiles with Monin-Obukhov theory

4.3.1 Influence of stability on the vertical wind speed profile

4.3.1.1 Derivation of the Monin-Obukhov length

Atmospheric stability is described in Monin-Obukhov theory with the Monin-Obukhov length scale L as stability parameter. Three different ways to derive this parameter are considered:

1. L has been derived directly from the sonic anemometer measurements of u_* and $\overline{w'T'}$ (Sonic method).
2. It has been derived via the Richardson number from the temperature and wind speed difference measurements at 10 m and 50 m (Gradient method).

3. It is estimated from the air and water temperature measurements and one wind speed measurement at 10 m height (Bulk method).

No humidity measurement is available at Rødsand. Therefore only an average humidity flux could be accounted for in the calculation of the stability parameters. Following Geernaert and Larsen (1993), a relative humidity of 100% and 70% has been assumed at the surface and at 10 m height, respectively. The measured water temperature has been used to transform these to absolute humidity. The humidity scale q_* and the vertical humidity profile have been calculated with a diabatic profile with standard humidity stability functions and a humidity roughness length of $z_{0q}=2.1 \cdot 10^{-4}$ m (see Geernaert and Larsen (1993)).

Sonic method

L is determined directly from sonic anemometer measurements of friction velocity and heat flux by:

$$L_{sonic} = -\frac{u_{*s}^3}{\kappa \frac{g}{T} \overline{w'T'_s}} \quad (4.5)$$

Here $\overline{w'T'_s}$ is the covariance of temperature and vertical wind speed fluctuations at the surface, u_{*s} the surface friction velocity, T the reference temperature, g the gravitational acceleration and κ the von Karman constant (taken as $\kappa=0.4$).

The sonic anemometer measures sound virtual temperatures, which differ from virtual temperatures by $0.1\overline{T} \overline{w'q'}$ (see Schotanus et al. (1983)):

$$\overline{w'T'_{sonic}} = \overline{w'T''} + 0.51\overline{T} \overline{w'q'} = \overline{w'\Theta'_v} - 0.1\overline{T} \overline{w'q'} = \overline{w'\Theta'_v} - 0.1\overline{T}u_*q_* \quad (4.6)$$

Here q is the absolute humidity and Θ_v the virtual potential temperature. The assumptions for the humidity stated above have been used for the estimation of q_* .

Gradient method

Temperature and wind speed difference measurements at 10 m and 50 m height are used to estimate the gradient Richardson number Ri_{Δ} :

$$Ri_{\Delta}(z') = \frac{\frac{g}{\overline{T}} \left(\frac{\Delta \overline{T}_v}{\Delta z} + \frac{g}{C_p} \right)}{\left(\frac{\Delta u}{\Delta z} \right)^2} \quad (4.7)$$

Here $\Delta T/\Delta z$ is the virtual temperature difference ΔT_v at a vertical height difference Δz . Equally, $\Delta u/\Delta z$ is the wind speed difference Δu at the vertical height difference Δz . C_p is the specific heat of air at constant pressure. Humidity at the two heights has been estimated as described above. The height z' at which this Ri number is valid can be estimated as $z'=(z_1-z_2)/\ln(z_1/z_2)$ (see Larsen (1993)). The gradient Richardson number is converted to L by means of the following relation based on the Kansas results (Businger et al., 1971, Högström, 1988):

$$L_{Gradient} = \begin{cases} \left(\frac{z'}{Ri} \right) & Ri < 0 \\ \frac{z'(1-5Ri)}{Ri} & 0 < Ri < 0.2 \end{cases} \quad (4.8)$$

Bulk method

Air and sea temperature measurements together with the wind speed at 10 m height are used. An approximation method proposed by (Grachev and Fairall, 1997) has been used. Humidity has been accounted for by calculating the virtual temperatures with the assumptions stated above.

For the bulk method the sea surface temperature is required. This is not measured at Rødsand and therefore had to be replaced by the water temperature measured at a depth of about 2 m. This leads to a small but systematic overprediction of the temperature difference between the surface and 10 m height and consequently to an overprediction of the stability parameter $|10/L|$, i.e. the calculated values of $10/L$ are too high for stable and too low for unstable conditions.

4.3.1.2 Comparison of predicted and measured wind speed profile

The wind speed ratio between 50 m and 10 m height is predicted using Monin-Obukhov theory. From the diabatic wind profile (see eq. 4.1) the wind speed ratio is calculated as:

$$\frac{u(z_2)}{u(z_1)} = \frac{\left[\ln\left(\frac{z_2}{z_0}\right) - \Psi_m\left(\frac{z_2}{L}\right) \right]}{\left[\ln\left(\frac{z_1}{z_0}\right) - \Psi_m\left(\frac{z_1}{L}\right) \right]} \quad (4.9)$$

Here z_0 is the aerodynamic roughness length and $\Psi_m(z/L)$ the integrated stability function, for which the Businger-Dyer formulation (Businger et al., 1971) is used. For the empirical parameters β and γ the values of the Kansas measurement reanalysed by Höglström (1988) for a von Karman constant of 0.4 are used ($\beta=4.8$ and $\gamma=19.3$).

$$\Psi_m = \begin{cases} 2 \ln\left(\frac{1+\Phi_m^2}{2}\right) - 2 \tan^{-1}(\Phi_m) + \frac{\pi}{2} & \text{with } \Phi_m = \left(1 - \gamma \frac{z}{L}\right)^{1/4} \text{ for } z/L < 0 \\ -\beta \frac{z}{L} & \text{for } z/L > 0 \end{cases} \quad (4.10)$$

The aerodynamic roughness length of the sea is estimated with the Charnock relation (Charnock, 1955):

$$z_0 = z_{ch} \frac{u_*^2}{g} \quad (4.11)$$

The Charnock parameter is taken as $z_{ch}=0.0185$ (Wu, 1980). The influence of different methods to estimate the sea surface roughness on the prediction of the vertical wind speed profile will be investigated and compared in section 4.3.2.

The theoretical dependency of the wind speed ratio $u(50)/u(10)$ on the stability parameter $10/L$ is compared with the Rødsand measurements in Figure 4.2 to Figure 4.4, where the measured ratios are plotted versus the three different Monin-Obukhov lengths derived from the measurements as described in the previous section.

In Figure 4.2 the sonic method is used to determine L . The measured wind speed ratios show large scatter when plotted versus L derived by the sonic method. This can at least partly be explained by the sampling variability of the friction velocity measurement (see section 4.2.2), which has a large impact on L since it is cubed in the calculation (see eq. 4.5). In comparison with the prediction of Monin-Obukhov theory the agreement is best for unstable conditions ($10/L < -0.05$). For near-neutral and stable situations systematic deviations are found. The wind speed ratio is generally higher than expected. This is especially obvious for conditions, which are close to neutral on the stable side. Here the measured ratios are systematically higher than expected from theory. Data with northerly wind directions (295° - 075°), where the distance to the coast (fetch) is smallest, are marked with grey squares in the figure. These data show a different behaviour and seem to agree better with the theory for stable conditions, though with a very large scatter.

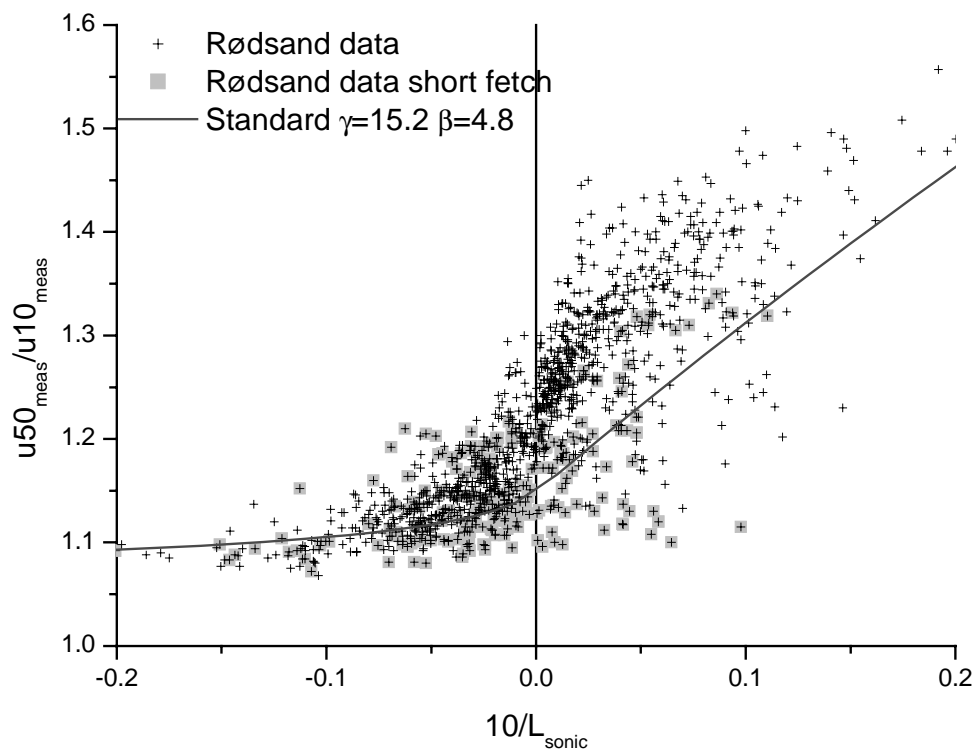


Figure 4.2: Ratios of wind speed at 50 and 10 m height at Rødsand versus the stability parameter $10/L$ with L derived from the sonic anemometer measurements; data with fetch $< 20\text{km}$ are marked; also shown is the prediction of Monin-Obukhov theory

The result for L derived with the gradient method is shown in Figure 4.3. The data show less scatter compared to the sonic method since no co-variances are used in the determination of L . Again a good agreement is found in the unstable region, while for

stable conditions the deviations are even more pronounced. The wind speed ratio is systematically higher than predicted by Monin-Obukhov theory and the deviation increases with increasing stability parameter $10/L$. The data from short fetches show again smaller ratios, which are, however, still higher than the theoretical prediction. The deviation from Monin-Obukhov prediction is larger than for the sonic method, which can be understood from the way in which L is calculated. In the determination of L with the gradient method the wind speed ratio between 10 m and 50 m height, which is predicted, is already included in the calculation of L . From eq. 4.7, 4.8 and 4.10 it can be seen that the diabatic term in the vertical wind profile is inversely proportional to the wind speed height ratio squared ($\Psi_m(z/L) \sim 1/\Delta u^2$) for stable stratification. Therefore any deviation between measured and predicted profile is amplified with this method.

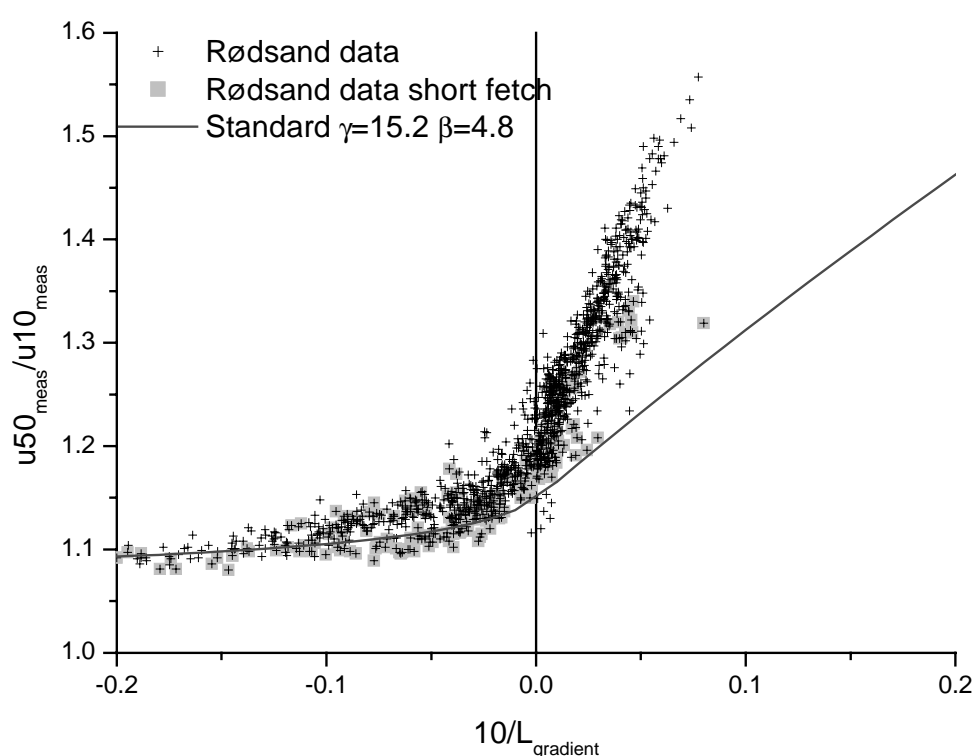


Figure 4.3: Ratios of wind speed at 50 and 10 m height at Rødsand versus the stability parameter $10/L$ with L derived from the wind and temperature difference measurements at 10 and 50 m height; data with fetch $<20\text{km}$ are marked; also shown is the prediction of Monin-Obukhov theory

For the bulk method the measured ratios versus $10/L$ are shown in Figure 4.4. Here again the scatter is smaller than for the sonic method. As for the other two methods, the agreement is good for unstable data and systematically higher ratios are found for stable conditions compared with theory. The deviations are smallest for the bulk method. Short fetch data show again on average smaller ratios and for the bulk method and a systematic deviation of these data from theoretical predictions can not be seen. The small magnitude of the deviation in the bulk method is due to the fact that only an absolute wind speed and not a wind speed difference enters in the calculation of L . In contrary to the gradient method a deviation of the measured from

the predicted profile will therefore only lead to a small relative difference in the calculation of L . Additionally, the systematic error caused by using the bulk water temperature instead of the sea surface temperature (see section 4.3.1.1) leads to an overprediction of $10/L$ on the stable side. This partly compensates the deviations between measured and predicted wind speed profile.

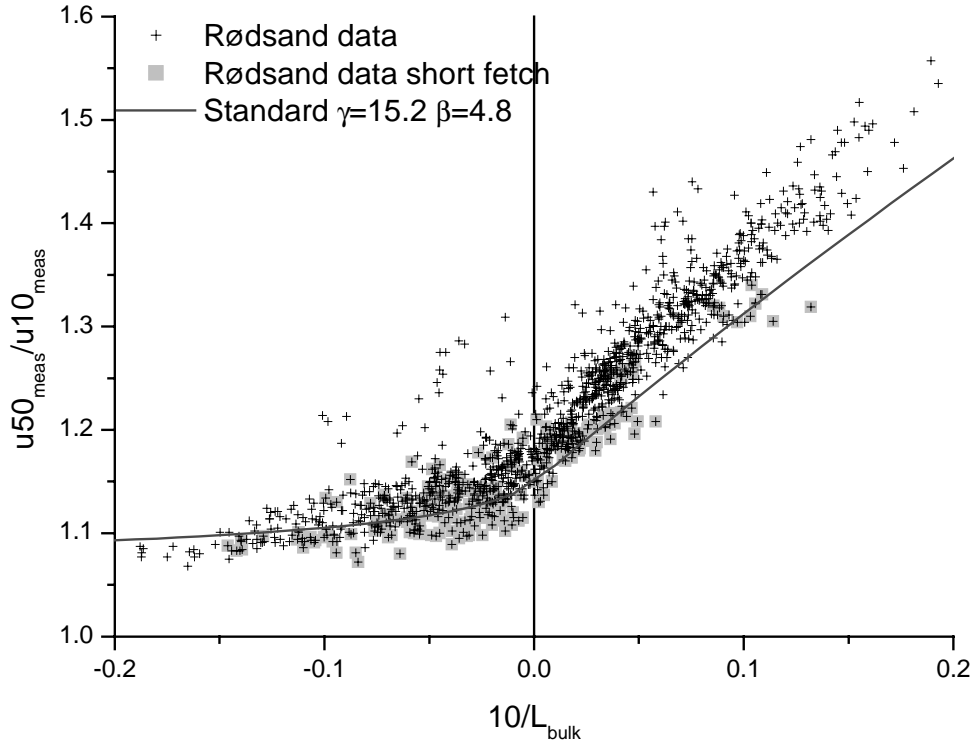


Figure 4.4: Ratios of wind speed at 50 and 10 m height at Rødsand versus the stability parameter $10/L$ with L derived from the bulk method (see text); data with fetch $<20\text{km}$ are marked; also shown is the prediction of Monin-Obukhov theory

The ratio $u50_{\text{meas}}/u50_{\text{pred}}$ between measured and predicted wind speed at 50 m height can be used as a measured for the deviation of the prediction, where the prediction is made from the measured wind speed at 10 m height with eq. 4.9:

$$\frac{u(50)_{\text{meas}}}{u(50)_{\text{pred}}} = \frac{u(50) \left[\ln\left(\frac{10}{z_0}\right) - \Psi_m\left(\frac{10}{L}\right) \right]}{u(10) \left[\ln\left(\frac{50}{z_0}\right) - \Psi_m\left(\frac{50}{L}\right) \right]} \quad (4.12)$$

The bin-averaged ratios $u50_{\text{meas}}/u50_{\text{pred}}$ for the three different methods to derive L are compared in Figure 4.5 together with their standard errors. Only bins with more than 20 records are shown. It can be seen that the deviations between measurement and Monin-Obukhov theory increase with increasing stability parameter $10/L$ for all methods to derive L , with the exception of the sonic method for stable conditions. Deviations are between 0% and 3% for unstable conditions and between 3% and 17% for stable conditions.

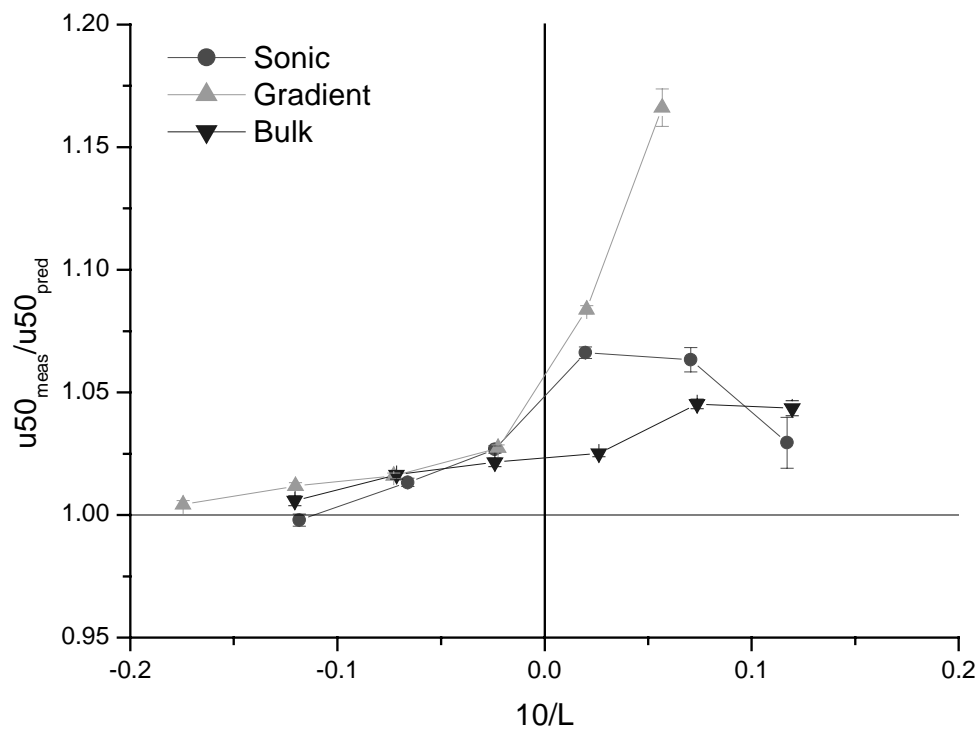


Figure 4.5: Bin-averaged ratio of measured and predicted 50 m wind speed versus stability parameter $10/L$ with L determined by the sonic, gradient and bulk methods

4.3.2 Influence of roughness on the vertical wind speed profile

4.3.2.1 Models to estimate the sea surface roughness

Compared to land surfaces the surface roughness of water is very low. Additionally, it is not constant, but depends on the wave field, which in turn is determined by the wind speed, distance to coast (fetch), etc. It is investigated how different models to describe the sea surface roughness influence the prediction of the wind profile (eq. 4.1). It is important to know if they can explain the ratios $u50_{\text{meas}}/u50_{\text{pred}}$ between the measured wind profile and the predictions of Monin-Obukhov theory. Three models for sea surface roughness z_0 are considered:

1. A constant z_0 is assumed.
2. The classical Charnock approach relating sea surface roughness to friction velocity is used.
3. An extension of the Charnock relation is considered, which takes into account the influence of fetch on the sea surface roughness by means of the wave age.

Constant roughness

The assumption of a constant sea surface roughness is often used in applications because of its simplicity, e.g. in the wind resource estimation program WASP (Mortensen, 1993). A value of $z_0=0.2$ mm is assumed.

Charnock relation

The most common model taking into account the wave field by its dependence on friction velocity is the Charnock relation (Charnock, 1955) (see eq. 4.11). The Charnock parameter z_{ch} is assumed to be a constant. The standard value of $z_{ch}=0.0185$ has been used (Wu, 1980).

For comparison the Charnock parameter has also been determined from the measurement data. Because of the deviations found above only unstable data ($10/L_{sonic}<-0.05$) were used. A Charnock parameter of 0.03 was found, which is higher than the standard value, but still in the range of other experimental values found for limited fetch conditions (see Garratt, 1994).

Wave age dependent model

The Charnock relation works well for the open ocean, but for coastal areas it was found that the Charnock parameter is site specific, due to the influence of other physical variables like fetch on the wave field. An extension of the Charnock relation by a parameterisation of the Charnock parameter with wave age as additional parameter by (Johnson et al., 1998) is used:

$$z_{ch} = A \left(\frac{c_p}{u_*} \right)^B \quad (4.13)$$

Here c_p/u_* is the wave age, the ratio of the velocity of the peak wave component c_p and the friction velocity u_* . The values for the empirical constants A and B are taken from Johnson et al. (1998): A=1.89; B=-1.59.

4.3.2.2 Comparison of predicted and measured wind speed gradients

The three z_0 models have been used to predict the wind speed at 50 m height from the 10m wind speed. The ratio $u_{50_{meas}}/u_{50_{pred}}$ is shown in Figure 4.6 for the bulk method as example. The difference of the results with the different z_0 models is much smaller than the difference between the different methods to derive L. They can therefore not be the reason for the deviations found. For near-neutral conditions the wave age model yields slightly smaller and the constant z_0 slightly larger deviations compared to the Charnock model.

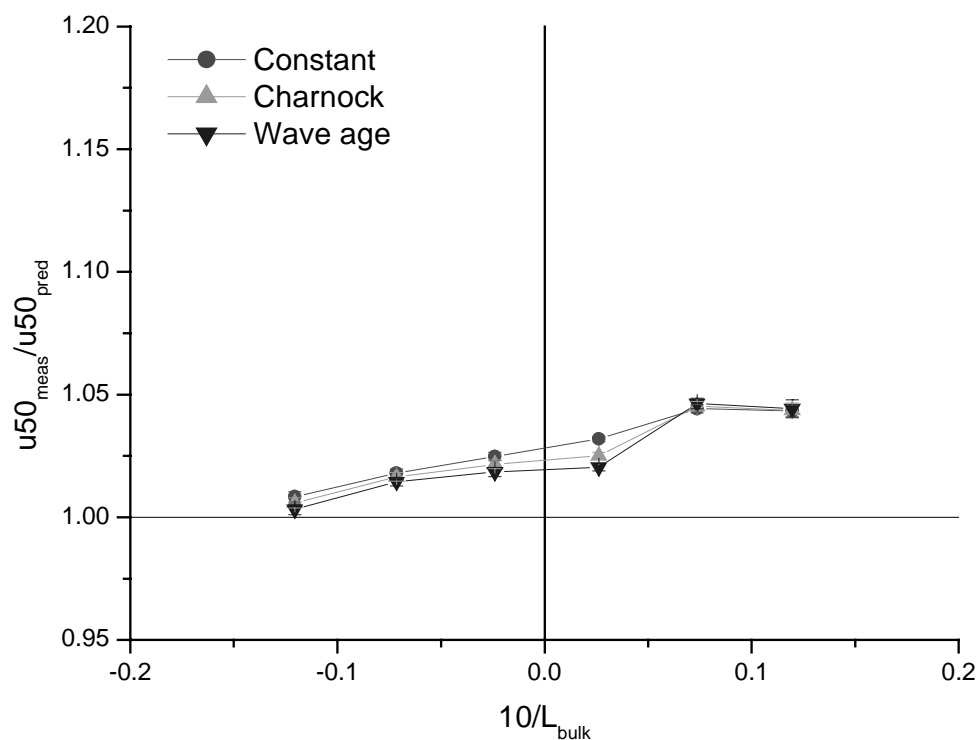


Figure 4.6: Bin-averaged ratio of measured and predicted 50 m wind speed versus stability parameter $10/L$ with L determined by the bulk method; three different methods to estimate the sea surface roughness have been used in the predictions: Constant sea surface roughness, Charnock relation and a wave age dependent extension of the Charnock relation

4.3.3 Average deviations

The extrapolation of the wind speed from 10m to 50m has been tested. The ratio between measured and estimated 50 m wind speed has been built with all models and its bias and rms-error calculated. It is given in the left two columns of Table 4.3. From the models to derive L the bias and rms-error are lowest for the bulk method. For the sea surface roughness the constant value, shows the smallest deviation both with respect to bias and rms-error.

The data were also divided into cases with stable and unstable atmospheric conditions (see Table 4.3). The Monin-Obukov-length L used for the selection was determined with the sonic method. It can be seen that the bias is very different between both conditions. The rms-errors are about the same when L is determined with the sonic method, but different for the other two methods. The comparison shows clearly the large deviations from theory in the stable regime.

Table 4.3: Comparison of different methods to predict the wind speed at 50 m height from the 10m wind; Bias and standard deviation of modelled time series compared to the measured one are shown for all data and separately for stable and unstable conditions

	all data		stable data		unstable d.	
	bias [%]	rms [%]	bias [%]	rms [%]	bias [%]	rms [%]
L from Sonic method						
Constant	4.6	4.8	6.4	5.4	2.5	2.9
Charnock	4.3	4.9	6.3	5.4	2.1	2.9
Wave age	4.1	5.0	6.2	5.6	1.8	3.0
L from Gradient method						
Constant	5.9	4.8	9.1	4.3	2.4	2.0
Charnock	5.7	5.0	9.0	4.7	2.0	2.0
Wave age	5.5	5.3	8.9	5.0	1.7	2.1
L from Bulk method						
Constant	3.0	2.7	4.2	2.8	1.7	1.8
Charnock	2.7	3.0	4.0	3.2	1.3	1.8
Wave age	2.5	3.3	3.9	3.7	0.9	2.0

4.4 The inhomogeneous flow regime in the coastal zone

4.4.1 Qualitative description of the flow regime

The measurement station Rødsand is surrounded by land in distances between 10 and 100 km and thus the air in the boundary layer will always be advected from land. Due to the large differences in heat capacity and conduction between land and water the air over land will often be warmer than the sea surface temperature. Especially at daytime, when the land is heated by the sun, and in early spring, when the water temperature is still low from winter, warm air is advected over the colder sea to the measurement station. Large temperature differences between the advected air and the sea surface can occur. At Rødsand temperature differences of up to 9°C were measured.

The flow regime which develops in this situation has been described by several authors (see e.g. Csanady (1974), Garratt (1987), Garratt and Ryan (1989), Melas (1989), Tjernström and Smedman (1993), Smedman et al. (1997)). We follow the explanation given by Csanady (1974) and Smedman et al. (1997): When warm air is blown over the cold sea, an internal boundary layer will develop at the shoreline due to the roughness and heat flux change. In the case of warm air advection over cold sea this is a stable internal boundary layer (SIBL), since the air close to the sea surface will be cooled. The SIBL is characterised by low turbulence and therefore small fluxes and slow growth. The warm air is cooled from below while the sea surface temperature will remain almost constant in this process due to the large heat capacity of water. Eventually, the air close to the sea surface will have the same temperature as the water and the atmospheric stability will be close to neutral at low heights. Above the internal boundary layer the air still has the temperature of the air over land and

near the top of the SIBL an inversion lid has developed with strongly stable stratification separating these two regions. Thus, while the stability in the mixed layer is close to neutral, the elevated stable layer influences the wind speed profile and leads to a larger wind speed gradient than expected for an ordinary near neutral condition.

Due to the small fluxes through the inversion lid this flow regime is a quasi-equilibrium state and can survive for large distances before eventually the heat flow through the inversion evens out the difference in potential temperatures. Eventually the neutral boundary layer is recovered, which is known from open ocean observations (see e.g. Edson and Fairall (1998)).

4.4.2 Qualitative comparison with Rødsand data

Two example cases have been selected, where large deviations of the measured and predicted wind speed ratio at 10 and 50 m height prevailed for a longer time period. Their time series are plotted in Figure 4.7 and Figure 4.8.

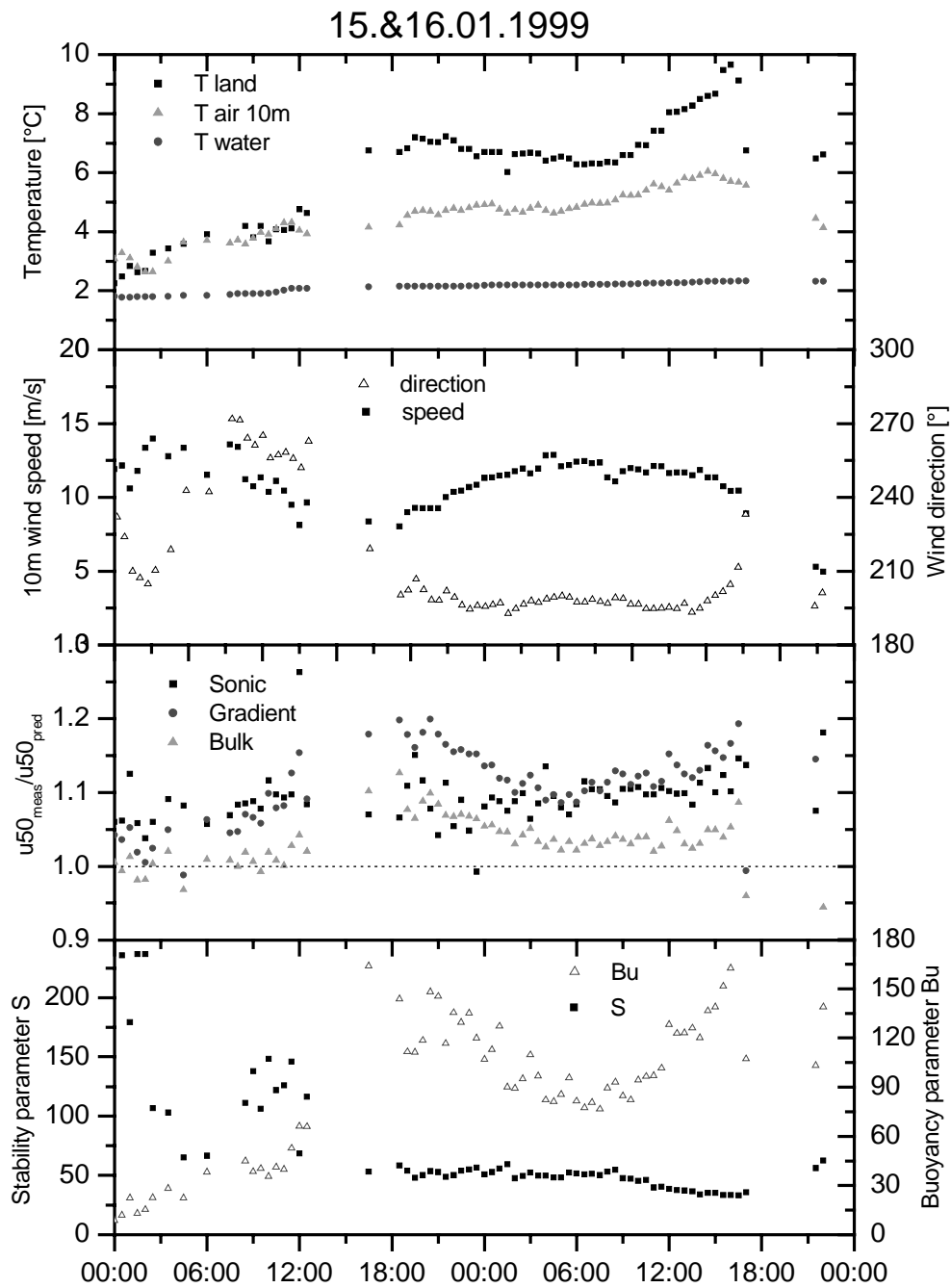


Figure 4.7: Time series of measurements at Rødsand for 15. and 16.1.1999; shown are air temperatures at 10m height and over upwind land (see section 4.2.4) and water temperature (uppermost panel); wind speed at 10 m height and wind direction (second panel); ratio of measured and predicted wind speed at 50 m height with three methods to determine L (sonic, gradient and bulk)(third panel); stability parameter S and buoyancy parameter Bu (lowest panel)

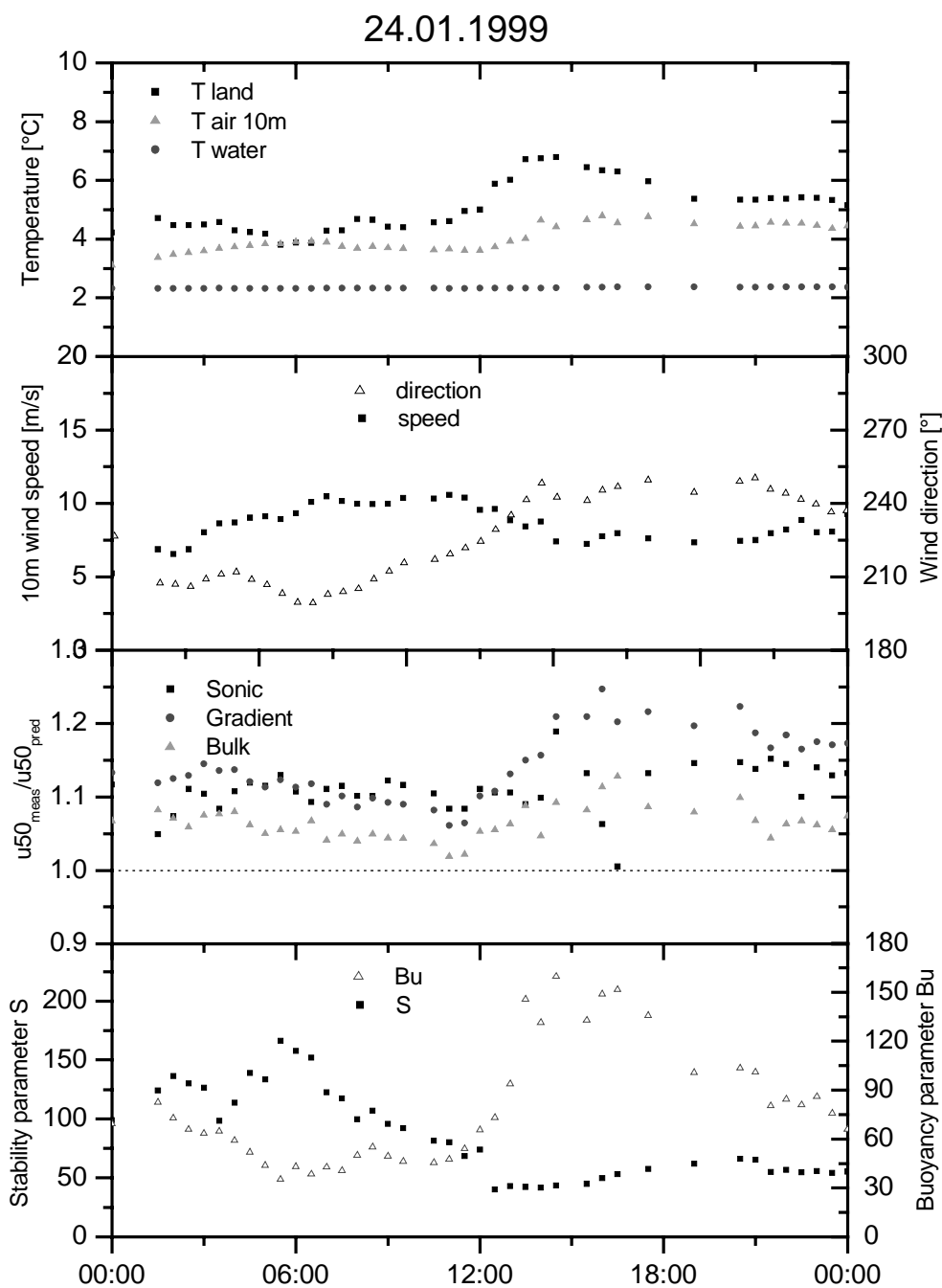


Figure 4.8: As above, but for 24.1.1999

Figure 4.7 shows a time series of 48 hours, 15. and 16. January 1999. In the uppermost graph air and water temperatures at Rødsand are shown along with the air temperature over the upwind land. Temperature differences between air over land and water range from about 1 to 7°C. The air temperature measured at Rødsand is very close to the land air temperature at the beginning of the period, but does not follow the large increase during daytime. A temperature difference of about 3°C between air

temperature over land and at Rødsand is reached in the afternoons of both days. The wind direction (see second graph) varies between 200° and 270° until 18:00 on the first day and stays almost constant at about 190° from then until almost the end of the time period. Wind speed at 10 m height (see second graph) is also more variable during the first period with values between 8 and 14 ms^{-1} . On the second day it slowly increases from 8 to 13 ms^{-1} and slightly decreases at the end of the measurement period to about 11 ms^{-1} . The third graph shows the ratio $u_{50_{\text{meas}}}/u_{50_{\text{pred}}}$ between measured and predicted 50 m wind speed, where the three different methods to derive L have been used: sonic, gradient and bulk. The Charnock relation has been used for the sea surface roughness. Large deviations between measured and predicted 50 m wind speed can be seen, up to about 20% for the gradient, 15% for the sonic and 10% for the bulk method. The variation of this ratio $u_{50_{\text{meas}}}/u_{50_{\text{pred}}}$ shows some correlation with the air temperature over land when the bulk or gradient methods are used for the prediction. When the sonic measurement is used to derive L and predict the 50 m wind speed the scatter in the ratio $u_{50_{\text{meas}}}/u_{50_{\text{pred}}}$ is larger and a pattern following the air temperature over land can not be seen. The lowest graph will be discussed in section 4.4.3.

Figure 4.8 shows a time series of one day (24.1.1999), where the temperature difference between air over land and sea varies between 2 and 5°C and the air temperature over sea is 0 - 3°C lower than that over land. Wind direction varies between 200° and 250° at wind speeds of 7 - 11 ms^{-1} . Ratios $u_{50_{\text{meas}}}/u_{50_{\text{pred}}}$ are similar to those in the first example with higher ratios in the afternoon, where also the air temperature over land is highest.

If the explanation given above (section 4.4.1) is responsible for the deviations of the wind speed profile from Monin-Obukhov theory, the data with large deviations should stem from situations where warm air is blown over a colder sea, i.e. where the air temperature over land is higher than the water temperature. This behaviour can be seen in the two examples.

To test if this is a typical behaviour the deviation of measured and predicted wind speed at 50 m height is plotted versus the difference between air temperature over land and sea temperature. The result is shown in Figure 4.9, with the gradient method used to determine L and the Charnock relation for z_0 as an example. It can be generalised that for the vast majority of the data with large deviations the air temperature measured over land is larger than the sea temperature.

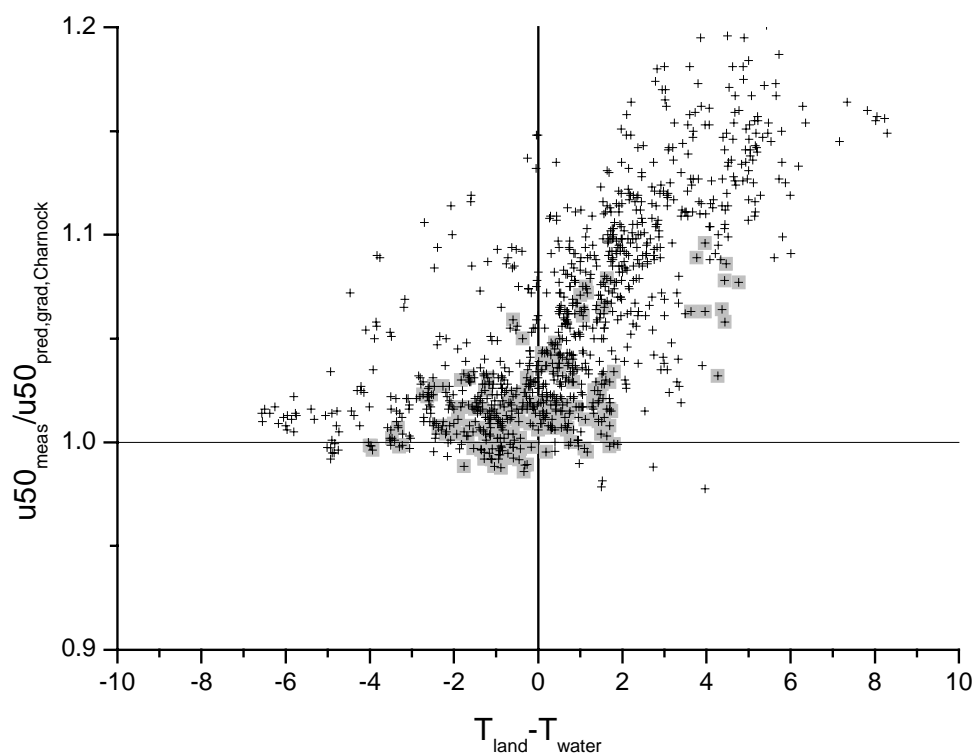


Figure 4.9: Scatter plot of ratio of measured and predicted (gradient method for L , Charnock equation for z_0) wind speed at 50 m height versus temperature difference between air temperature over the upwind land area and the water temperature at Rødsand

4.4.3 Comparison of the Rødsand data with theoretical approaches

Csanady (1974) developed a theory for a mixed layer flow with capping inversion. He proposes the so-called buoyancy parameter Bu to predict if such a flow regime will develop:

$$Bu = \frac{b}{fv_g} = g \frac{\Delta\rho}{\rho} \frac{1}{fv_g} \quad (4.14)$$

Here g is the gravitational acceleration, b is the buoyant acceleration ($b=g\Delta\rho/\rho$), ρ the air density, $\Delta\rho$ the air density difference between surface and geostrophic level at constant pressure, f the Coriolis parameter and v_g the geostrophic wind speed.

Since only mast data up to 50 m height are available at Rødsand, the geostrophic wind speed and the air density at geostrophic level have to be estimated. The geostrophic wind speed is estimated from the geostrophic drag law (see e.g. Garratt (1994)), with z_0 estimated with the Charnock relation (see section 4.3.2.1). For the calculation of the air density difference it is assumed that the air at this height is advected from land without temperature change. This is consistent with Csanady's model since the capping inversion only allows a very small heat flux. The potential temperature at geostrophic level is then equal to the potential temperature over land. It is additionally

assumed that the temperature stratification over land is neutral. Then the potential temperature measured over land at 2 m height can be used as an estimation of the potential temperature over sea at geostrophic height.

Csanady (1974) found that an inversion lid is likely to develop if $Bu > 30$. The deviation of measured and predicted 50 m wind speed is shown versus the buoyancy parameter Bu in Figure 4.10. The gradient method has been chosen here to determine L since it shows the largest ratios $u50_{meas}/u50_{pred}$. The roughness z_0 is estimated with the Charnock relation. The scaling with Bu leads to a clearly reduced scatter when compared to Figure 4.9, where only the temperature difference between land and sea is used. Three regions can be distinguished in Figure 4.10: For negative Bu , i.e. cold air over warmer water, generally small deviations are found. For Bu larger than 30, i.e. warm air over cold water, where an inversion lid should exist, large deviations are found that increase with growing Bu . For intermediate Bu between 0 and 30, i.e. warm air over cold water, but according to Csanady (1974) without inversion lid, a wide range of deviations is found: Two clusters can be distinguished, one with deviations similar to those of negative Bu and one with deviations of an extension of the trend line of large and increasing $Bu > 30$. In the intermediate region both regimes seem to overlap. Data with short fetch (marked with grey squares) show a tendency of smaller deviations. However, these might be outside the applicability of this equilibrium theory. Some conflicting observations occur, probably because the assumption of a neutral stratification over land will inevitably be wrong in some cases.

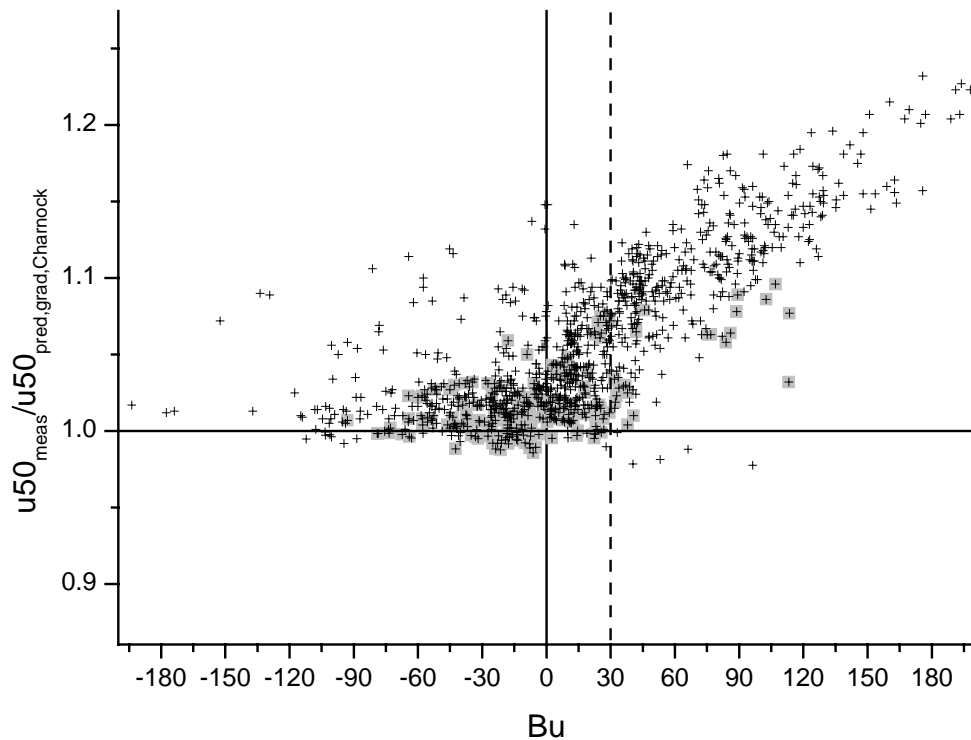


Figure 4.10: Scatter plot of ratio of measured and predicted (gradient method for L , Charnock equation for z_0) wind speed at 50 m height versus buoyancy parameter Bu

Smedman et al. (1997) argue that not only the temperature difference, but also the travel time of the warmer air above the cold water will determine the development of

a mixed layer. They propose a bulk stability parameter S to distinguish between an ordinary stable layer and a mixed layer with capping inversion:

$$S = \sqrt{tf} \frac{\Theta}{\Delta\Theta} \quad (4.15)$$

where $t=X/v_g$ is the travel time (with X =distance to upwind coast and v_g =geostrophic wind speed), f Coriolis parameter, Θ reference temperature, $\Delta\Theta$ temperature difference between air over land and sea. They find that for ordinary stable profiles $S < 75$, while for profiles with near neutral stratification and inversion lid $S > 75$.

The Smedman et al. (1997) formulation can be interpreted as an extension of Csanady's theory to conditions with limited fetch. The bulk stability parameter S is connected to Csanady's buoyancy parameter Bu by:

$$S = \frac{g}{\sqrt{f}} \frac{\sqrt{X}}{\sqrt{v_g^3}} \frac{1}{Bu} \quad (4.16)$$

This shows that S and Bu are inversely proportional and have a very different dependency on wind speed.

The deviation of measured and predicted 50 m wind speed is shown versus the bulk stability parameter S in Figure 4.11. For negative S , i.e. warm air over cold water, deviations are usually small. For positive S , large deviations can be seen, which decrease with increasing S .

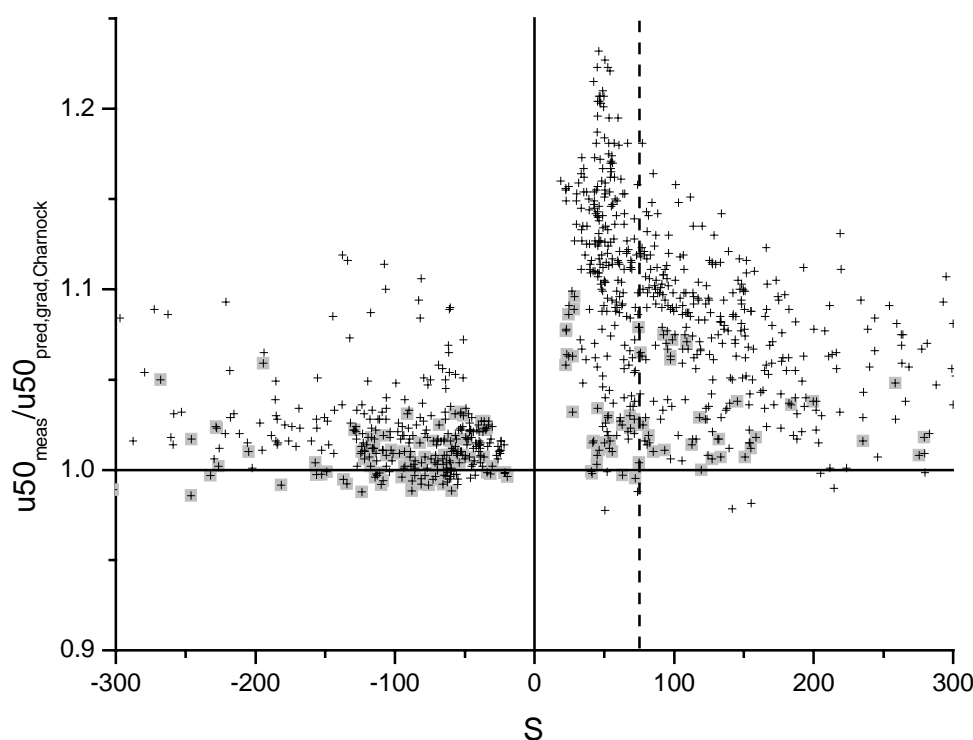


Figure 4.11: Scatter plot of ratio of measured and predicted (gradient method for L , Charnock equation for z_0) wind speed at 50 m height versus bulk stability parameter S

For a theory including the development of the flow with increasing fetch, it could be expected that the deviations measured for different fetches collapse when plotted

versus S . This is not the case. The data with short fetch show clearly smaller deviations than the data with longer fetch for the same S .

The buoyancy parameter Bu and the bulk stability parameter S are also shown in the example cases (see Figure 4.7 and Figure 4.8). Also here high Bu and low S values can be seen for the time periods with large deviations.

The buoyancy parameter Bu or the bulk stability parameter S aim to determine if a mixed layer with inversion lid can develop in a certain situation. The influence of such a flow regime on the wind speed profile can be expected to depend on the depth of this mixed layer. If the inversion is very high it will probably have little influence on the wind speed profile up to 50 m height, while a low inversion height can be expected to have a large impact. Csanady (1974) proposes the following expression for the depth of the mixed layer h in equilibrium conditions:

$$h = A \frac{1}{g} \frac{\rho}{\Delta\rho} u_*^2 \quad (4.17)$$

He estimates the empirical parameter A to 500. Tjernström and Smedman (1993) found a reasonable agreement of the height of the inversion predicted with eq. 4.17 with that estimated from airborne measurements over the Baltic Sea.

The ratio $u_{50_{\text{meas}}}/u_{50_{\text{pred}}}$ is shown versus the mixed layer depth h in Figure 4.12 (in logarithmic scale). The gradient method has been used to determine L and the Charnock equation for the estimation of z_0 . A clear correlation can be seen with large ratios for low inversion heights of a few 100m, decreasing rapidly with increasing inversion height.

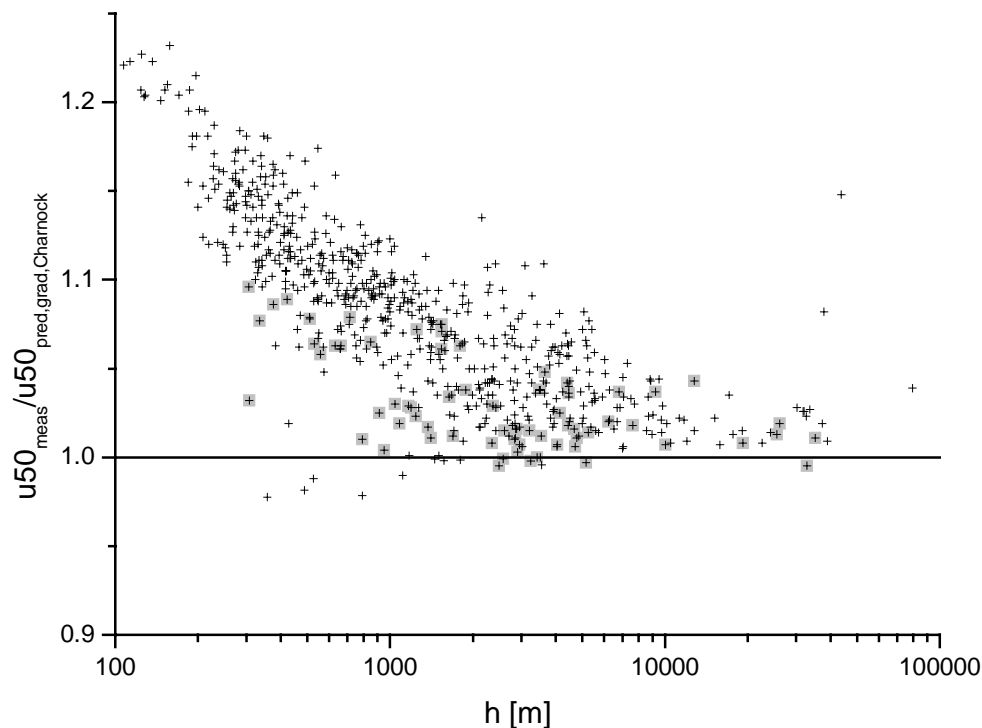


Figure 4.12: Scatter plot of ratio of measured and predicted (gradient method for L , Charnock equation for z_0) wind speed at 50 m height versus mixed layer depth h after Csanady (1974)

It has to be kept in mind that the estimated inversion height h is for equilibrium conditions only, i.e. when the mixed layer and capping inversion already are developed. Therefore the theory can not be used for small fetches. This limitation might be the reason that the deviation of the measured wind speed profile and the Monin-Obukhov prediction found for small fetches (<20km, grey squares) is smaller than for long fetches (>30 km).

4.5 Conclusion

Data from the measurement program Rødsand have been used to investigate the wind speed profile in the coastal marine surface layer. The 50 m high meteorological mast is located 11 km from land and experiences fetches from 11 to more than 100 km. The measured wind speed ratio between 10 m and 50 m height is found to be systematically larger than expected with Monin-Obukhov theory for most data in near-neutral and for almost all data in stable conditions. The deviations are more pronounced for large fetch (>30km) than for fetches of 10-20km, in contrary to the intuitive expectation that the importance of coastal influences decreases for increasing fetch.

Different methods to derive the Monin-Obukhov length L and the sea surface roughness from the measurements have been compared.

The deviations between measured and predicted wind speed profile were found for all three methods used to derive L . They all predict a smaller wind speed increase from 10 m to 50 m than measured. The magnitude of the deviation differs for different methods to derive L since the methods are differently sensitive for deviations of the wind speed profile. Different methods to estimate the sea surface roughness have been tested. They only lead to small differences in the wind profiles and can therefore not be responsible for the deviations found between the measured and predicted wind speed increase from 10 m to 50 m.

A qualitative explanation for the failure of Monin-Obukhov theory for the coastal marine boundary layer in near-neutral and stable conditions is offered by Csanady (1974). He describes the flow regime for warm air advection over a colder sea. If certain conditions are fulfilled, an inversion lid with strongly stable stratification will develop at the top of the internal boundary layer with small turbulent transport. The heat flow through the inversion will therefore be small, while the air below the inversion is cooled continuously from the sea surface. It will eventually take the temperature of the sea and become a well-mixed layer with near-neutral stratification. In such a situation of strong height variation of atmospheric stability Monin-Obukhov theory must fail and the wind speed ratio between 10 m and 50 m height predicted for this near-neutral or weakly stable stratification is too small. With temperature data from land stations surrounding the Rødsand site it is shown that the deviations in the wind speed profile actually occur in conditions of warm air advection over a colder sea, as required by this theory. It can also be seen that measurements with short fetch (<20 km) show smaller deviations. This might indicate that for these fetches the inversion lid is still under development, which could be expected from the theory.

The conditions under which a flow regime of a mixed layer with capping inversion will occur, has been quantified by Csanady (1974) by the buoyancy parameter Bu for equilibrium conditions, i.e. when the inversion lid has been formed. A clear dependency of the deviation in the wind profile on the parameter Bu is found. The

data show largest deviations for $Bu > 30$, which is the limit estimated by Csanady for the formation of an inversion lid.

Smedman et al. (1997) extend the theory by taking into account the development of the flow with fetch. They propose a bulk stability parameter S to predict if an inversion develops. A clear dependency of the deviation on S is found, but the influence of fetch on the deviation measured at Rødsand is not captured.

The deviation between measured and predicted wind speed profile is expected to be influenced not only by the existence of an inversion lid, but also by its height. Csanady (1974) gives a relation to estimate the inversion height h . The comparison with the measurement data reveals a clear correlation between h and the deviation in the wind speed profile. Largest deviations are found for low inversion heights, while for large estimated inversion heights the deviations are small.

These findings strongly support the view that the deviations found in the measurements from standard Monin-Obukhov theory can be qualitatively explained with the existence of a flow regime consisting of a mixed layer with capping inversion as described by Csanady. We conclude that Monin-Obukhov theory can not be applied to the coastal marine boundary layer under conditions of warm air advection even for fetches larger than 30 km. Further research is needed to find an alternative model describing the fluxes and profiles in the coastal marine boundary layer under these conditions.

Since warm air advection occurs frequently in coastal waters, at least in the Baltic Sea, this effect has an important influence on the average vertical wind speed profile and therefore implications also for the wind climatology at such sites. Wind speeds at greater heights predicted from lower measurements with Monin-Obukhov theory e.g. will systematically be estimated too low. It is important to note that this effect is largest for quite large distances of several tens of kilometres to the upwind coast and not close to the coast, where one would usually expect influences of the coastal discontinuity to be largest.

Acknowledgements

The Rødsand measurement program was funded by the following: JOULE program of the European Union (JOU2-CT93-0325), Office of naval research (N00014-93-1-0360), Danish Energistyrelsen (UVE J.nr. 51171/96-0040) and ELKRAFT. The technical support team at Risø and Mr Kobbarnagel of Sydfalster-El are acknowledged for their contribution to the data collection. The air temperature data from the German synoptic stations were made available by the German Weather Service (DWD).

References

- Businger, J. A., Wyngaard, J. C., Izumi, Y., and Bradley, E. F.: 1971, 'Flux-profile relationships in the atmospheric surface layer' *J. Atmos. Sci.* 28, 181-189.
- Charnock, H.: 1955, 'Wind stress over a water surface' *Quart. J. Roy. Meteor. Soc.* 81, 639-640.
- Csanady, G. T.: 1974, 'Equilibrium theory of the planetary boundary layer with an inversion lid' *Boundary-Layer Meteorol.* 6, 63-79.

- Edson, J. B., and Fairall, C. W.: 1998, 'Similarity relationships in the marine atmospheric surface layer for terms in the TKE and scalar variance budgets' *J. Atmos. Sci.* 55, 2311-2328.
- Garratt, J. R.: 1987, 'The stably stratified internal boundary layer for steady and diurnally varying offshore flow', *Boundary-Layer Meteorol.* 38, 169-394.
- Garratt, J. R., and Ryan B. F.: 1989, 'The structure of the stably stratified internal boundary layer in offshore flow over the sea' *Boundary-Layer Meteorol.* 47, 17-40.
- Garratt, J. R.: 1994, *The atmospheric boundary layer*, Cambridge University Press, Cambridge, 316 pp.
- Geernaert, G., and Larsen, S.: 1993, 'On the role of humidity in estimating marine surface layer stratification and scaterometer cross section' *J. Geophys. Res.* 98(C1), 927-932.
- Grachev, A. A., and Fairall C. W.: 1997, 'Dependence of the Monin-Obukhov stability parameter on the bulk Richardson number over the Ocean' *J. Appl. Meteor.* 36, 406-414.
- Högström, U.: 1988, 'Nondimensional wind and temperature profiles' *Boundary-Layer Meteorol.* 42, 55-78.
- Højstrup, J.: 1999, 'Vertical Extrapolation of Offshore Wind Profiles' in E. L. Petersen, P. Hjuler Jensen, K. Rave, P. Helm, H. Ehmann (eds.), *Wind energy for the next millennium. Proceedings. 1999 European wind energy conference (EWEC '99)*, Nice, FR, March 1—5, 1999, James and James Science Publishers, London, U.K., pp. 1220-1223.
- Johnson, H. K., Højstrup, J., Vested H. J., and Larsen S. E.: 1998, 'On the Dependence of Sea Surface Roughness on Wind Waves' *J. Phys. Oceanogr.* 28, 1702-1716.
- Lange, B., Barthelmie R. J., and Højstrup J.: 2001, *Description of the Rødsand field measurement*, Report Risø-R-1268, Risø National Laboratory, 4000 Roskilde, DK, 60 pp.
- Larsen, S. E.: 1993, 'Observing and modelling the planetary boundary layer' in E. Raschke and D. Jacob (eds.), *Energy and water cycles in the climate system*, NATO ASI series I, volume 5, Springer-Verlag, Berlin, Heidelberg, pp. 365-418.
- Lenschow D. H., Li X. S. , Zhu C. J., and Stankov, B. B.: 1988, 'The stably stratified boundary layer over the Great Plains, I, Mean and turbulence structure' *Boundary-Layer Meteorol.* 42, 95-121.
- Melas, D.: 1989, 'The temperature structure in a stably stratified internal boundary layer over a cold sea' *Boundary-Layer Meteorol.* 48, 361-375.
- Mortensen, N. G., Landberg L., Troen, I., and Petersen, E. L.: 1993, *Wind Analysis and Application Program (WASP) - User's Guide*, Report Risø-I-666(EN) (v.2), Risø National Laboratory, 4000 Roskilde, DK, 133 pp.
- Panofsky, H. A.: 1973, 'Tower Micrometeorology', in D.A. Haugen (ed.), *Workshop on Micrometeorology*, American Meteorological Society, Boston, pp. 151-176.
- Schotanus, P.: 1983, 'Temperature measurement with a sonic anemometer and its application to heat and moisture fluxes' *Boundary-Layer Meteorol.* 26, 81-93.

Smedman, A.-S., Bergström, H. and Grisogono, B.: 1997, 'Evolution of stable internal boundary layers over a cold sea' *J. Geophys. Res.* 102(C1), 1091-1099.

Tennekes, H.: 1982, 'Similarity relations, scaling laws and spectral dynamics', in F. T. M. Nieuwstadt, and H. van Dop (eds.), *Atmospheric turbulence and air pollution modelling*, Reidel, Hingham, MA, pp.37-68.

Tjernström, M., and Smedman, A.-S.: 1993, 'The vertical turbulence structure of the coastal marine atmospheric boundary layer', *J. Geophys. Res.* 98(C3), 4809-4826.

Wu, J.: 1980, 'Wind stress Coefficients over Sea Surface near Neutral Conditions – A Revisit', *J. Phys. Oceanogr.* 10, 727-740.

Wyngaard, J. C.: 1973, 'On surface-layer turbulence', in D.A. Haugen (ed.), *Workshop on Micrometeorology*, American Meteorological Society, Boston, pp. 101-149.

5 Importance of thermal effects and sea surface roughness for offshore wind resource assessment

Abstract

The economic feasibility of offshore wind power utilisation depends on the favourable wind conditions offshore compared to sites on land, which have to compensate the additional cost. But not only the mean wind speed is different, also the whole flow regime, as can e.g. be seen in the vertical wind speed profile. The commonly used models to describe this profile have been developed mainly for land sites. Their applicability for wind power prediction at offshore sites is investigated using data from the measurement program Rødsand in the Danish Baltic Sea.

Monin-Obukhov theory is often used for the description of the wind speed profile. From a given wind speed at one height, the profile is predicted using the two parameters Monin-Obukhov length and sea surface roughness. Different methods to estimate these parameters are discussed and compared. Significant deviations to Monin-Obukhov theory are found for near-neutral and stable conditions, when warmer air is advected from land with a fetch of more than 30 km. The measured wind shear is larger than predicted.

As a test application, the wind speed measured at 10 m height is extrapolated to 50 m height and the power production of a wind turbine at this height is predicted with the different models. The predicted wind speed is compared to the measured one and the predicted power output to the one using the measured wind speed. To be able to quantify the importance of the deviations from Monin-Obukhov theory, a simple correction method to account for this effect has been developed and is tested in the same way.

The models for the estimation of the sea surface roughness were found to lead only to little differences. For the purpose of wind resource assessment even the assumption of a constant roughness was found to be sufficient. The different methods to derive the Monin-Obukhov length L were found to differ significantly for near-neutral and stable atmospheric stratification. Also here the simplest method using only bulk measurements was found to be sufficient.

For situations with near-neutral and stable atmospheric stratification and long (>30 km) fetch, the wind speed increase with height is larger than what is predicted from Monin-Obukhov theory for all methods to estimate L and z_0 . It is also found that this deviation occurs at wind speeds important for wind power utilisation, mainly at 5-9 ms^{-1} .

The power output estimation has also been compared with the method of the resource estimation program WAsP. For the Rødsand data set the prediction error of WAsP is about 4%. For the extrapolation with Monin-Obukhov theory with different L and z_0 estimations it is 5-9%. The simple wind profile correction method, which has been developed, leads to a clear improvement of the wind speed and power output predictions. When the correction is applied, the error reduces to 2-5%.

5.1 Introduction

It is expected that an important part of the future expansion of wind energy utilisation at least in Europe will come from offshore sites. The first large offshore wind farms are currently being built in several countries in Europe. The economic viability of such projects depends on the favourable wind conditions of offshore sites, since the higher energy yield has to compensate the additional installation and maintenance cost. A reliable prediction of the wind resource is therefore crucial. This requires the modelling of the vertical structure of the surface layer flow, especially the vertical wind speed profile. This is needed e.g. to be able to extrapolate wind speed measurements performed at lower heights to the planned hub height of a turbine. Also for turbine design the wind shear is an important design parameter, especially for the large rotor diameters planned for offshore sites.

The wind speed profile in the atmospheric surface layer is commonly described by Monin-Obukhov theory. In homogenous and stationary flow conditions, it predicts a log-linear profile:

$$u(z) = \frac{u_*}{\kappa} \left[\ln \left(\frac{z}{z_0} \right) - \Psi_m \left(\frac{z}{L} \right) \right] \quad (5.1)$$

The wind speed u at height z is determined by friction velocity u_* , aerodynamic roughness length z_0 and Monin-Obukhov length L . κ denotes the von Karman constant (taken as 0.4) and Ψ_m is a universal stability function. Thus, if the wind speed is known at one height, the vertical wind speed profile is determined by two parameters: the surface roughness z_0 and the Monin-Obukhov length L .

The surface roughness of the sea is low compared to land surfaces. This is the main reason for the high wind speeds offshore. However, the roughness is not constant with wind speed like for land surfaces, but depends on the wave field present, which in turn depends on wind speed, upstream fetch (distance to coast), water depth, etc. Different models have been proposed to describe these dependencies. Most commonly used is the Charnock model [5.1], which only depends on friction velocity. Numerous attempts have been made to improve this description by including more information about the wave field, e.g. by including wave age [5.2] or wave steepness [5.3] as additional parameters. These additional parameters require wave measurements, which are often not available for wind power applications. A fetch dependent model has therefore been developed, where the wave age has been replaced by utilising an empirical relation between wave age and fetch [5.4].

The Monin-Obukhov length L has to be derived from measurements at the site. Different methods are available using different kinds of input data: The calculation of L with the eddy-correlation method requires fast response measurements, e.g. by an ultrasonic anemometer. Wind speed and temperature gradient measurements at different heights can be used to derive L via the Richardson number [5.5]. The method with least experimental effort employs a wind speed measurement at one height, water and air temperatures to calculate the bulk Richardson number, which is then related to L [5.5].

Monin-Obukhov theory, although developed from measurements over land, has been found to be generally applicable over the open sea [5.6]. This has been questioned for sites where the flow is influenced by the vicinity of land. [5.7] and [5.8] showed that

the land-sea discontinuity influences the flow for distances of up to 100-200 kilometres. Offshore wind power plants will therefore always be subject to such influences.

In coastal waters, when wind is blowing from land over the sea, the coastline constitutes a pronounced change in roughness and heat transfer. These changes pose a strong inhomogeneity to the flow, which may limit the applicability of Monin-Obukhov theory. Stimulated by measurements of large wind stress over Lake Ontario, Csanady described the processes governing the flow regime under the condition of warm air advection over colder water [5.9]. He developed an equilibrium theory of a well-mixed layer with a capping inversion for this condition.

Monin-Obukhov theory is a key part of the European Wind Atlas method [5.10] and the wind resource estimation program WAsP [5.11], which is most commonly used for offshore wind potential studies (see e.g. [5.12]) and wind resource estimations from measurements (see e.g. [5.13]). Also other approaches, like the methodology used in the POWER project [5.14] is based on this theory.

Also mesoscale flow modelling is used for wind power studies. A comparison of the mesoscale model MIUU [5.15] and the WAsP program showed differences of up to 15% in mean wind speed [5.16]. However, such models are too computationally demanding to be used in wind power applications and a simpler model is needed to be able to estimate these effects.

A validation study with three offshore masts in Denmark revealed differences between measurements and WAsP model results, which correlated with fetch [5.17]. A combination of the simplified assumptions used in WAsP was believed to be responsible for the deviations.

In this study the impact of different methods and models for the extrapolation of wind speed measurements on the prediction of the wind turbine power production is re-investigated with data from the Rødsand measurement program in the Danish Baltic Sea, about 10 km off the coast. A simple ad hoc correction to the Monin-Obukhov wind speed profile is developed with the aim to investigate the importance deviations from the Monin-Obukhov profile of on wind resource estimations. The deviations occur when warmer air is flowing from land over a colder sea, creating an inhomogeneous wind flow.

Measured wind speeds at 10 m height are extrapolated to 50 m height with Monin-Obukhov theory with different methods to derive L and different models for the sea surface roughness. This has been repeated including the simple wind profile correction for inhomogeneous wind flow. The results are compared with the measured wind speed at 50 m height. By converting the wind speeds to power output of an example turbine the impact of the deviations in wind speed on the estimation of the power production is investigated.

The Rødsand measurement program is briefly introduced in the following section. In section 5.3 Monin-Obukhov theory is used to predict the wind speed profile with different methods for the derivation of L and models for estimating z_0 . The simple correction of the Monin-Obukhov profile for inhomogeneous wind flow in the coastal zone is developed in section 5.4. In section 5.5 the impact of the different methods, models and correction on the estimation of the power production of a wind turbine is investigated, before conclusions are drawn in the final section.

5.2 The Rødsand field measurement program

The field measurement program Rødsand has been established in 1996 as part of a Danish study of wind conditions for proposed offshore wind farms. A detailed description of the measurement, instrumentation and data can be found in [5.18] and [5.19].

The 50 m high meteorological mast is situated about 11 km south of the island Lolland in Denmark (11.74596°E, 54.54075°N) (see Figure 5.1). The instrumentation of the measurement mast is listed in Table 5.1. The mast is located in 7.7 m mean water depth with an upstream fetch of 30 to more than 100 km for wind directions from SE to WNW (120°N to 290°N). In the NW to N sector (300°N to 350°N) the fetch is 10 to 20 km.

All wind speed data are corrected for flow distortion errors due to the mast and the booms with a method developed by Højstrup [5.20]. Records from situations of direct mast shade have been omitted. Friction velocity is calculated from the data of the ultrasonic anemometer with the eddy-correlation method. Simple correction procedures have been applied to account for the small decrease of the fluxes with height (see [5.19]).

The air temperature over land in the upwind direction from Rødsand has been estimated from measurements at synoptic stations of the German Weather Service (DWD) and the measurement station Tystofte in Denmark (operated by the Risø National Laboratory) (see Table 5.2 and Figure 5.1). A more detailed description can be found in Lange et al. [5.19].

Not all instruments are available for long time measurements at Rødsand. Therefore two data sets are used:

- A data set with shorter measurement period, where also ultrasonic and wave measurements are available. This data set consists of about 4200 half-hourly records. This data set is used for all analysis except in section 5.5.2.
- A data set of two years measurement time (5/99 to 5/01), but without sonic and wave measurements, is used in section 5.5.2. The data set consists of 64000 records of 10-minutes averages (61% availability).

The data have only been selected for the availability of all measurements. For the purpose of wind resource estimations all available data have to be used. Therefore the data have not been selected for stationarity, although Monin-Obukhov theory is only valid for stationary flow conditions. A similar analysis with data selected for the applicability of the theory can be found in Lange et al. [5.19].

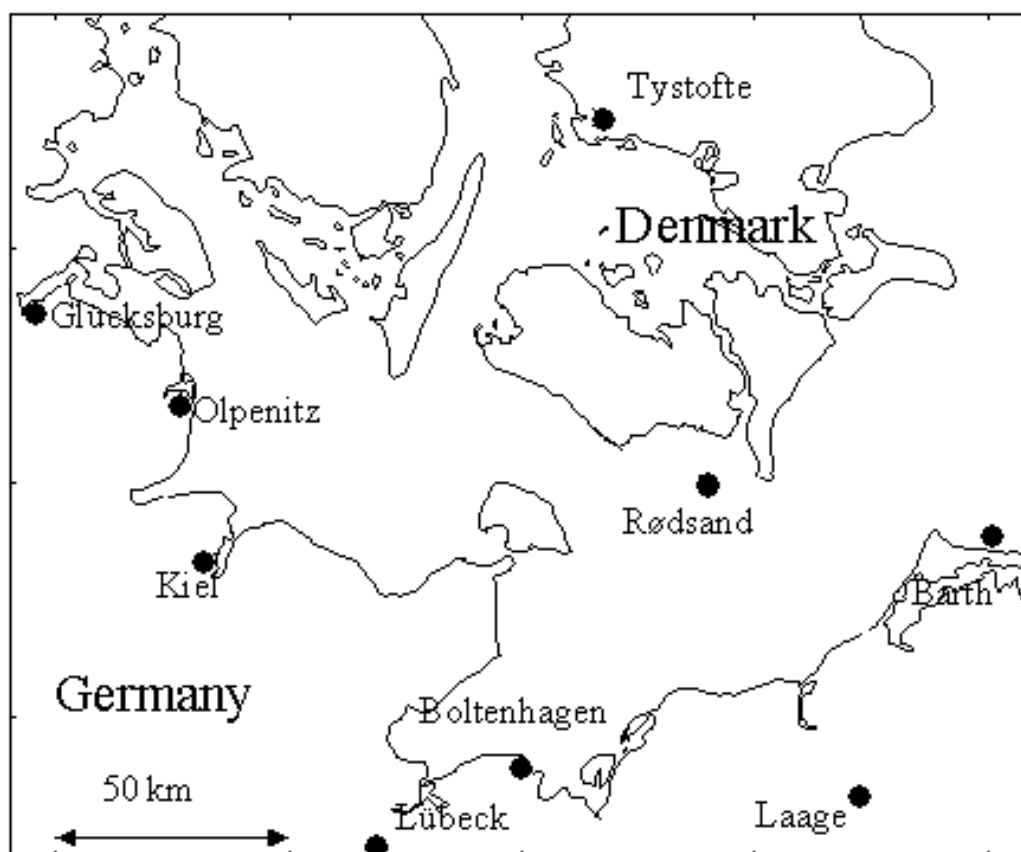


Figure 5.1: Map of the measurement stations

Table 5.1: Instrumentation of the Rødsand measurement

	height above mean sea level	instrument	sampling rate
Wind speed	50.3 m	cup anemometer	5 Hz
	29.8 m	cup anemometer	5 Hz
	10.2 m	cup anemometer	5 Hz
Wind direction	29.7 m	wind vane	5 Hz
3 axis wind speed and temperature	46.6 m (42.3 m from 12.5.99)	ultrasonic anemometer	20 Hz
Air temperature	10.0 m	Pt 100	30 min mean
Temperature difference	49.8 m – 10.0 m	Pt 500	30 min mean
Sea temperature	about –2m	Pt 100	30 min mean
Sea level		DHI AWR201 acoustic wave recorder	8 Hz
Sea current		GMI current meter	8 Hz

Table 5.2: Synoptic stations used for estimating the upwind air temperature over land

	latitude	longitude	height asl	direction from Rødsand
Glücksburg	54°49'	09°30'	27 m	281°
Olpenitz	54°40'	10°02'	4 m	279°
Kiel-Holtenau	54°22'	10°08'	27 m	256°
Lübeck-Blankensee	53°48'	10°42'	14 m	221°
Boltenhagen	54°00'	11°11'	15 m	210°
Laage	53°55'	12°17'	40 m	150°
Barth	54°20'	12°43'	7 m	112°

5.3 Extrapolation with Monin-Obukhov theory

5.3.1 Derivation of Monin-Obukhov length

Atmospheric stability is described in Monin-Obukhov theory with the Monin-Obukhov length scale L as stability parameter. Three different ways to derive this parameter are considered:

Sonic method

L is determined directly from sonic anemometer measurements of friction velocity and heat flux by:

$$L_{sonic} = -\frac{u_{*s}^3}{\kappa \frac{g}{T} \overline{w'T'_s}} \quad (5.2)$$

Here $\overline{w'T'_s}$ is the covariance of temperature and vertical wind speed fluctuations at the surface and u_{*s} the surface friction velocity, T the reference temperature, g the gravitational acceleration and κ the von Karman constant (taken as $\kappa=0.4$).

The sonic anemometer measures sound virtual temperatures, which differ from virtual temperatures by $0.1\overline{T} \overline{w'q'}$ [5.21]:

$$\overline{w'T'_{sonic}} = \overline{w'T'} + 0.51\overline{T} \overline{w'q'} = \overline{w'\Theta'_v} - 0.1\overline{T} \overline{w'q'} = \overline{w'\Theta'_v} - 0.1\overline{T}u_*q_* \quad (5.3)$$

Here q is the absolute humidity and Θ_v the virtual potential temperature. No humidity measurement is available at Rødsand. Therefore only an average humidity flux could be accounted for in the calculation of the stability parameters. Following Geernaert and Larsen [5.22], a relative humidity of 100% and 70% has been assumed at the surface and at 10 m height, respectively. The measured water temperature has been used to transform these to absolute humidity. The humidity scale q_* and the vertical humidity profile have been calculated with a diabatic profile with standard humidity stability functions and a humidity roughness length of $z_{0q}=2.1 \cdot 10^{-4}$ m [5.22].

Gradient method

Temperature and wind speed difference measurements at 10 m and 50 m height are used to estimate the gradient Richardson number Ri_Δ :

$$Ri_{\Delta}(z') = \frac{\frac{g}{T} \left(\frac{\Delta \bar{T}_v}{\Delta z} + \frac{g}{C_p} \right)}{\left(\frac{\Delta \bar{u}}{\Delta z} \right)^2} \quad (5.4)$$

Here $\Delta T_v/\Delta z$ is the virtual temperature difference ΔT_v at a vertical height difference Δz . Equally, $\Delta u/\Delta z$ is the wind speed difference Δu at the vertical height difference Δz . C_p is the specific heat of air at constant pressure. Humidity at the two heights has been estimated as described above. The height z' at which this Ri number is valid can be estimated as $z' = (z_1 - z_2) / \ln(z_1/z_2)$ [5.23]. The gradient Richardson number is converted to L by means of the following relation based on the Kansas results [5.24], [5.25]:

$$L_{Gradient} = \begin{cases} \left(\frac{z'}{Ri} \right) & Ri < 0 \\ \frac{z'(1 - 5Ri)}{Ri} & 0 < Ri < 0.2 \end{cases} \quad (5.5)$$

Bulk method

Air and sea temperature measurements together with the wind speed at 10 m height are used. An approximation method proposed by Grachev and Fairall [5.26] has been used. In the calculation of the virtual temperatures, humidity has been accounted for with the assumptions stated above.

For the bulk method the sea surface temperature is required. This is not measured at Rødsand and therefore had to be replaced by the water temperature measured at a depth of about 2 m. This leads to a small but systematic over-prediction of the temperature difference between the surface and 10 m height and consequently to an over-prediction of the stability parameter $|10/L|$, i.e. the calculated values of $10/L$ are slightly higher for stable and lower for unstable conditions.

5.3.2 Sea surface roughness

Compared to land surfaces the surface roughness of water is very low. Additionally, it is not constant, but depends on the wave field, which in turn is determined by the wind speed, distance to coast (fetch), etc. It is investigated how different models to describe the sea surface roughness influence the prediction of the wind profile (eq.). Four models for sea surface roughness z_0 are considered:

Constant roughness

The assumption of a constant sea surface roughness is often used in applications because of its simplicity, e.g. in the wind resource estimation program WAsP [5.11]. A value of $z_0 = 0.2$ mm is assumed.

Charnock relation

The most common model taking into account the wave field by its dependence on friction velocity u_* is the Charnock relation [5.1]:

$$z_0 = z_{ch} \frac{u_*^2}{g} \quad (5.6)$$

Here g is the gravitational acceleration and z_{ch} the empirical Charnock parameter. The standard value of $z_{ch}=0.0185$ has been used [5.27].

Wave age model

The Charnock relation works well for the open ocean, but for coastal areas it was found that the Charnock parameter is site specific, due to the influence of other physical variables like fetch on the wave field. Numerous attempts have been made to find an empirical relation for the sea surface roughness with an improved description of the wave field. No consensus on the most suitable scaling groups has emerged yet. Different relations have been tested with the Rødsand data [5.4] and an extension of the Charnock relation by a parameterisation of the Charnock parameter with wave age as additional parameter by Johnson et al. [5.2] is used:

$$z_{ch} = A \left(\frac{c_p}{u_*} \right)^B \quad (5.7)$$

Here c_p/u_* is the wave age, the ratio of the velocity of the peak wave component c_p and the friction velocity u_* . The values for the empirical constants A and B are taken from [5.2]: $A=1.89$; $B= -1.59$.

Fetch model

The wave age model requires measurements of the peak wave velocity, which is often not available for wind power applications. A fetch dependent model has therefore been developed, where the wave age has been replaced by utilising an empirical relation between wave age and fetch.

Kahma and Calkoen [5.28] found the following empirical relation between the dimensionless peak frequency and the dimensionless fetch:

$$\frac{u_*}{g} \omega_p = C \left(\frac{g}{u_*^2} x \right)^D \quad (5.8)$$

Here ω_p is the peak wave frequency and x the fetch in metres. The coefficients were found to be $C=3.08$ and $D= -0.27$.

The influence of fetch on wave parameters has been determined by field experiments with winds blowing approximately perpendicular to a straight coastline. To use these relations an effective fetch for a given direction, α has been defined as the integral over all direction from $\alpha= -90^\circ$ to $\alpha= +90^\circ$, weighted by a cosine squared term, normalised and divided by the fetch which would result from a straight coastline.

$$x_{eff}(\phi) = \frac{2 \int_{-\pi/2}^{\pi/2} x(\phi - \varphi) \cos^2(\phi - \varphi) d\varphi}{4 / \pi} \quad (5.9)$$

With the assumption of deep water conditions the left hand side of eq. (5.8) can be identified as the inverse wave age u_*/c_p using the dispersion relation. This relation can then be used to eliminate the wave age from eq. (5.7):

$$z_{ch} = AC^B \left(\frac{g}{u_*^2} x_{eff} \right)^{BD} \quad (5.10)$$

5.3.3 Comparison of predicted and measured wind speed profiles

The wind speed ratio between 10 m and 50 m height is predicted using Monin-Obukhov theory. From the diabatic wind profile (see eq.) the wind speed ratio is calculated as:

$$\frac{u(z_2)}{u(z_1)} = \frac{\left[\ln\left(\frac{z_2}{z_0}\right) - \Psi_m\left(\frac{z_2}{L}\right) \right]}{\left[\ln\left(\frac{z_1}{z_0}\right) - \Psi_m\left(\frac{z_1}{L}\right) \right]} \quad (5.11)$$

Here z_0 is the aerodynamic roughness length and $\Psi_m(z/L)$ the integrated stability function, for which the Businger-Dyer formulation [5.24] is used. For the empirical parameters β and γ the values of the Kansas measurement reanalysed by [5.25] for a von Karman constant of 0.4 are used ($\beta=4.8$ and $\gamma=19.3$).

$$\Psi_m = \begin{cases} 2 \ln\left(\frac{1 + \Phi_m^2}{2}\right) - 2 \tan^{-1}(\Phi_m) + \frac{\pi}{2} & \text{with } \Phi_m = \left(1 - \gamma \frac{z}{L}\right)^{1/4} \quad \text{for } z/L < 0 \\ -\beta \frac{z}{L} & \text{for } z/L > 0 \end{cases} \quad (5.12)$$

A deviation Δ is defined as the ratio between measured and predicted wind speed at 50 m height, where the prediction is made from the measured wind speed at 10 m height with eq. (5.11):

$$\frac{u(50)_{meas}}{u(50)_{pred}} = \frac{u(10) \left[\ln\left(\frac{10}{z_0}\right) - \Psi_m\left(\frac{10}{L}\right) \right]}{u(50) \left[\ln\left(\frac{50}{z_0}\right) - \Psi_m\left(\frac{50}{L}\right) \right]} \quad (5.13)$$

This ratio $u50_{meas}/u50_{pred}$ has been computed for the Rødsand data for all combinations of the three models to derive the Monin-Obukhov length L and the four models for the sea surface roughness.

Systematic deviations are found in all cases for data with stable stratification. As example, the ratio $u50_{meas}/u50_{pred}$ for the gradient method to derive L is shown in Figure 5.2 with the Charnock relation used to model the sea surface roughness. A good agreement is found in the unstable region ($10/L < -0.05$). For stable conditions the wind speed at 50 m height is systematically higher than predicted by Monin-Obukhov theory. The deviation increases with increasing stability parameter $10/L$.

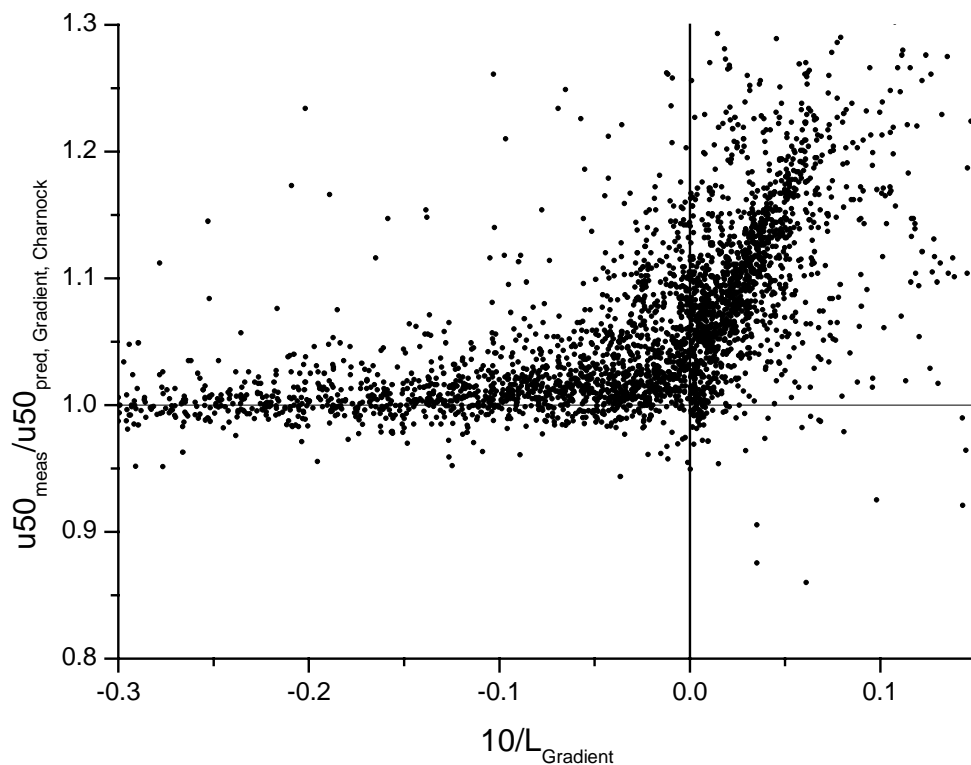


Figure 5.2: Ratio $u50_{meas}/u50_{pred}$ between measured and predicted 50 m wind speeds versus $10/L$; L derived with the gradient method and z_0 with the Charnock model

The large scatter, which is visible in Figure 5.2, is due to the fact, that the data have not been selected for stationary flow conditions. Data from periods with large changes in the atmospheric flow lead to large scatter. From [5.19] it can be seen that the scatter is considerably reduced if records with large gradients in wind speed, wind direction, temperatures etc. are excluded from the analysis.

For comparison of the different methods, the bin-averaged ratios $u50_{meas}/u50_{pred}$ for the three different methods to derive L are shown in Figure 5.3 together with their standard errors. Only bins with more than 20 records have been used. It can be seen that for all methods the agreement is good for unstable stratification. For near-neutral and stable stratification the wind speed at 50 m height is predicted too low with all methods. The deviations increase with increasing stability parameter $10/L$ for all methods, with the exception of the sonic method for stable conditions. Deviations are between -3% and 3% for unstable conditions and between 3% and 18% for stable conditions.

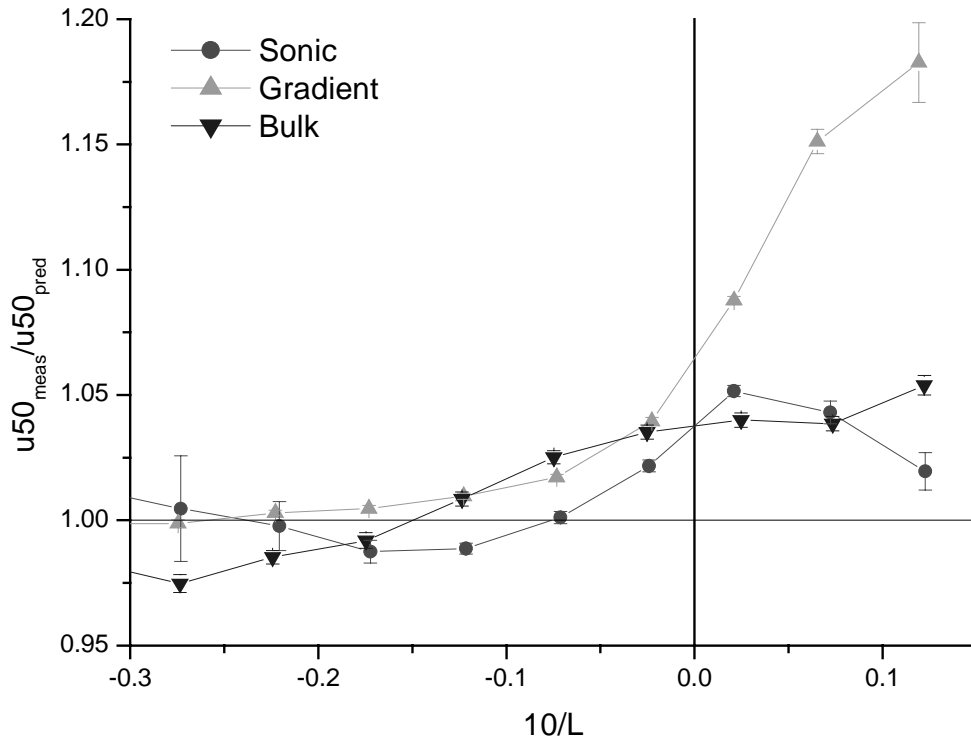


Figure 5.3: Bin-averaged ratio of measured and predicted 50 m wind speed versus stability parameter $10/L$ with L determined by the sonic, gradient and bulk methods and z_0 with Charnock model

The difference in the magnitude of the deviations can be understood from the way the Monin-Obukhov length is calculated in the different methods. In the determination of L with the gradient method the wind speed ratio between 10 m and 50 m height, which is predicted, is already included in the calculation of L . From eq. (5.4), (5.5) and (5.12) it can be seen that the diabatic term in the vertical wind profile is inversely proportional to the wind speed height ratio squared ($\Psi_m(z/L) \sim 1/\Delta u^2$) for stable stratification. Therefore any deviation between measured and predicted profile is amplified with this method. The small magnitude of the deviation in the bulk method is due to the fact that only absolute quantities are used instead of differences. In contrary to the gradient method a deviation of the measured from the predicted profile will therefore only lead to a small relative difference in the calculation of L . Additionally, the systematic error caused by using the bulk water temperature instead of the sea surface temperature leads to a small over-prediction of $10/L$ on the stable side. This partly compensates the deviations between measured and predicted wind speed profile.

To investigate if the deviations can be caused by inappropriate modelling of the sea surface roughness, the four different roughness models are compared in Figure 5.4. The bin-averaged ratios $u50_{\text{meas}}/u50_{\text{pred}}$ are plotted versus the stability parameter $10/L$. The bulk method has been used to derive L . It can be seen that the choice of model for the sea surface roughness does not have a large impact on the dependence of the deviations on the stability parameter z/L . Thus they can not be responsible for the deviations found.

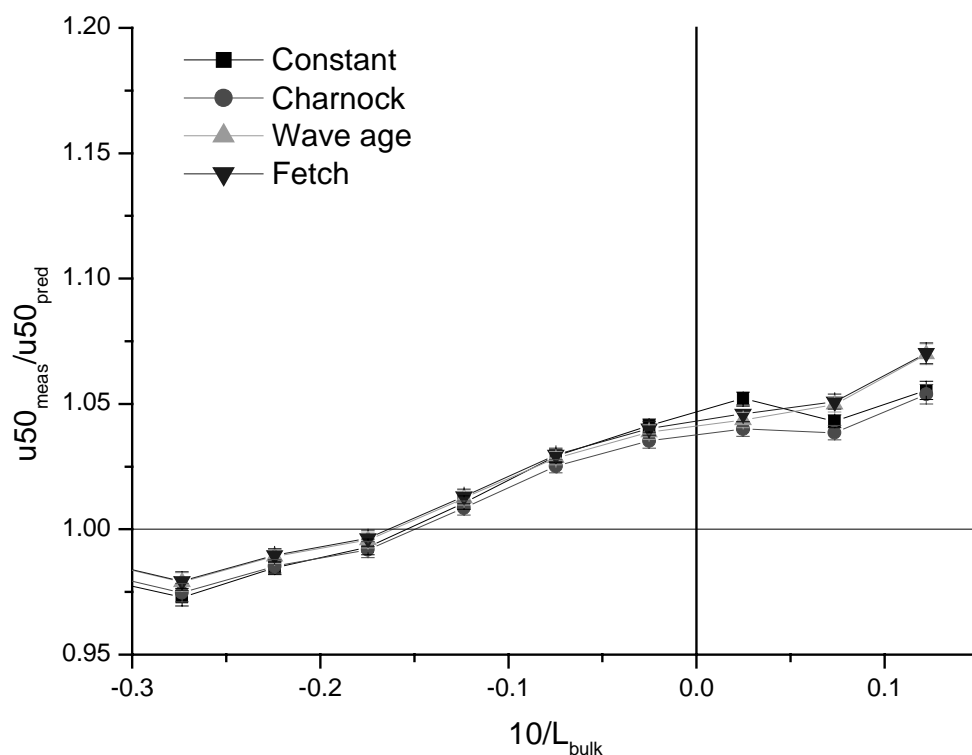


Figure 5.4: Bin-averaged ratio of measured and predicted 50 m wind speed versus stability parameter $10/L$ with L determined by the bulk method and z_0 modelled with four different models (see text)

Sea surface roughness mainly depends on wind speed (or friction velocity, which is related). Figure 5.5 shows the dependency of the bin-averaged deviation on wind speed at 10 m height for the four roughness models. The data are selected for unstable ($L < 0$) and stable ($L > 0$) stratification. For unstable stratification the deviations are small ($< 4\%$), while for stable data deviations of up to 25% are found. The constant roughness assumption leads to the smallest deviations up to a wind speed of about 8 m/s, but to the largest deviations for higher wind speeds. From the other models, the Charnock relation always shows the smallest deviation. The wave age and fetch models show only little difference and slightly larger deviations than the Charnock model.

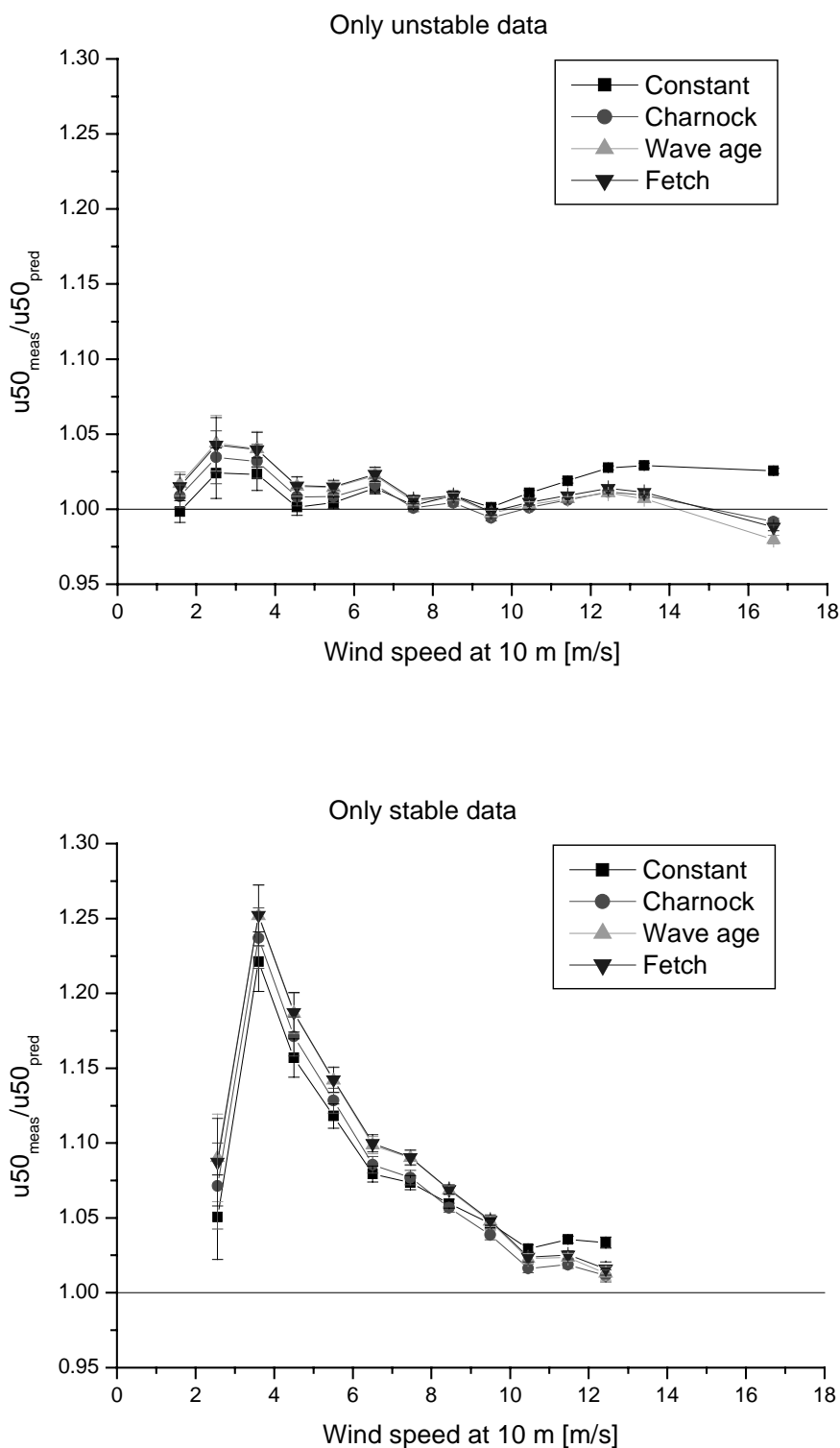


Figure 5.5: Bin-averaged ratio of measured and predicted 50 m wind speed versus wind speed at 10 m height with L determined by the bulk method and z_0 modelled with four different models (see text)

5.4 Correction of the Monin-Obukhov wind speed profile for coastal influence

5.4.1 Description of the flow regime

The measurement station Rødsand is surrounded by land in distances between 10 and 100 km and thus the air in the boundary layer will always be advected from land. Due to the large differences in heat capacity and conduction between land and water the air over land will often be warmer than the sea surface temperature. Especially at daytime, when the land is heated by the sun, and in early spring, when the water temperature is still low from winter, warm air is advected over the colder sea to the measurement station. Large temperature differences between the advected air and the sea surface can occur. At Rødsand temperature differences of up to 9°C were measured.

The flow regime that develops in this situation has been described by several authors. We follow the explanation given by Csanady [5.9] and Smedman et al. [5.29]: When warm air is blown over the cold sea, immediately a stable stratification develops as the air adjacent to the sea surface will be cooled. Simultaneously an internal boundary layer develops at the shoreline due to the roughness and heat flux change. In the case of warm air advection over cold sea this is a stable internal boundary layer (SIBL), characterised by low turbulence and therefore small fluxes and slow growth. The warm air is cooled from below while the sea surface temperature will remain almost constant in this process due to the large heat capacity of water. Eventually, the air close to the sea surface will have the same temperature as the water and the atmospheric stability will be close to neutral at low heights. Above the internal boundary layer the air still has the temperature of the air over land and near the top of the SIBL an inversion lid has developed with strongly stable stratification separating these two regions. Thus, while the stability in the mixed layer is close to neutral, the elevated stable layer influences the wind speed profile and leads to a larger wind speed gradient than expected for an ordinary near neutral condition.

Due to the small fluxes through the inversion lid this flow regime is a quasi-equilibrium state and can survive for large distances before eventually the heat flow through the inversion evens out the difference in potential temperatures. Eventually the neutral boundary layer is recovered, which is known from open ocean observations [5.6].

5.4.2 Prediction of the inversion height

A theory for a mixed layer flow with capping inversion has been developed by Csanady [5.9]. The so-called buoyancy parameter Bu is proposed to predict if such a flow regime will develop. He found that an inversion lid is likely to develop if $Bu > 30$. Bu is estimated from:

$$Bu = \frac{b}{fv_g} = g \frac{\Delta\rho}{\rho} \frac{1}{fv_g} \quad (5.14)$$

Here g is the gravitational acceleration, b is the buoyant acceleration ($b = g\Delta\rho/\rho$), ρ the air density, $\Delta\rho$ the air density difference between surface and geostrophic level at constant pressure, f the Coriolis parameter and v_g the geostrophic wind speed.

For the Rødsand measurement, the geostrophic wind speed and the air density at geostrophic level have been estimated from the measured data at the Rødsand mast and at the surrounding land stations. It has been assumed that the air at this height is advected from land without temperature change and that the temperature stratification over land is neutral (see [5.19]).

The buoyancy parameter Bu aims to determine if a mixed layer with inversion lid can develop in a certain situation. The influence of a flow regime with mixed layer and capping inversion on the wind speed profile can be expected to depend on the height of the inversion. If the inversion is very high it will probably have little influence on the wind speed profile up to 50 m height, while a low inversion height can be expected to have a large impact. Csanady proposes the following expression for the depth of the mixed layer h in equilibrium conditions [5.9]:

$$h = A \frac{1}{g} \frac{\rho}{\Delta\rho} u_*^2 \quad (5.15)$$

He estimates the empirical parameter A to 500. The inversion height estimated from airborne measurements over the Baltic Sea has been found to agree reasonably well with eq. (5.15)[5.30].

The bin averaged ratio $u_{50_{\text{meas}}}/u_{50_{\text{pred}}}$ for situations with long fetch (>30 km) is shown versus the inversion height h in Figure 5.6 (in logarithmic scale). The bulk method has been used to determine L and the Charnock equation for the estimation of z_0 . A correlation can be seen with large ratios for low inversion heights of below 100 m, decreasing rapidly with increasing inversion height and reaching a constant level at an inversion height of about 1000 m. This is in accord with the picture that an inversion height in the order of the boundary layer height will not lead to changes in the profile.

It has to be kept in mind that the estimated inversion height h is for equilibrium conditions only, i.e. when the mixed layer and capping inversion already are developed. Therefore the theory can not be used for small fetches. The correlation between h and the ratio $u_{50_{\text{meas}}}/u_{50_{\text{pred}}}$ has been found to hold for fetches larger than 30 km in [5.19].

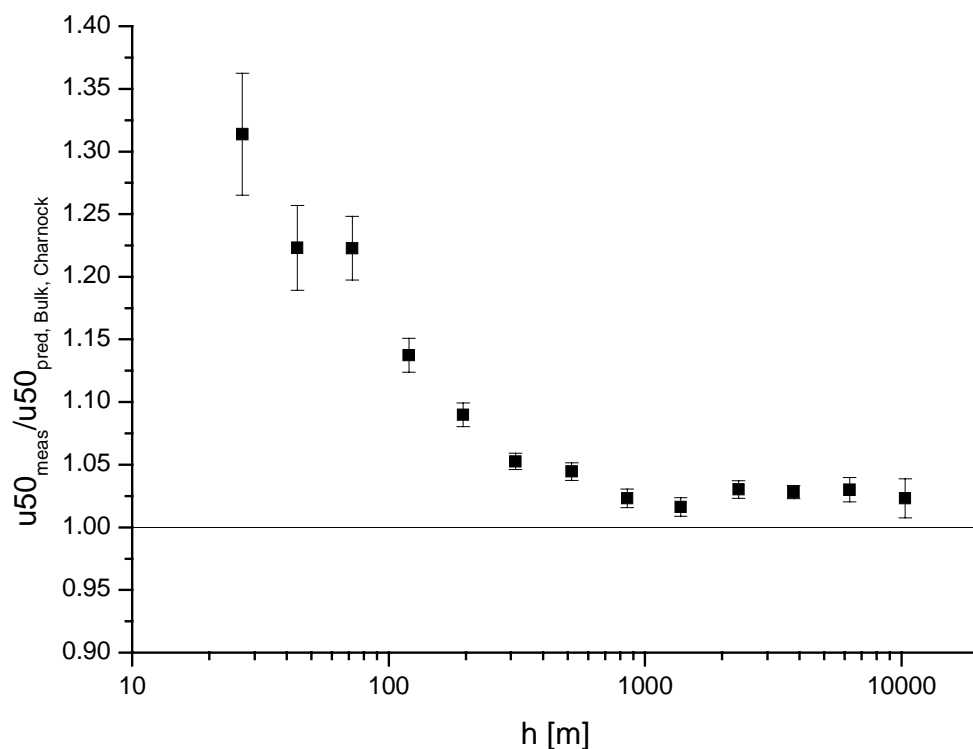


Figure 5.6: Ratio $u50_{meas}/u50_{pred}$ bin averaged for the estimated height of inversion layer h (from eq. (5.15))

5.4.3 Development of a simple correction method

The deviations due to thermal effects in coastal waters will lead to errors in wind resource prediction made with Monin-Obukhov theory. If e.g. the mean wind speed at hub height is estimated from measurements at a lower height, the wind resource will be estimated too low.

A micrometeorological model to take into account these effects is not available. Therefore a simple correction method is developed here to investigate the importance of this effect for wind resource estimations. In Figure 5.6 it is shown that the deviation decreases with increasing height of the inversion layer. It is assumed that the deviation increases linearly with height. The simplest correction method is therefore to add a linear correction term to the wind speed profile of Monin-Obukhov theory (see eq. 5.1), which is proportional to the measurement height z and inversely proportional to the estimated inversion height h :

$$u(z) = \frac{u_*}{\kappa} \left[\ln\left(\frac{z}{z_0}\right) - \Psi_m\left(\frac{z}{L}\right) + c \frac{z}{h} \right] \quad (5.16)$$

This correction is used for all records with fetch greater than 30 km and buoyancy parameter Bu greater than 30. From the Rødsand measurements the correction factor c is estimated to be about 4.

The effect of this correction on the ratio $u_{50_{\text{meas}}}/u_{50_{\text{pred}}}$ is shown in Figure 5.7 to Figure 5.8. In Figure 5.7 the ratio $u_{50_{\text{meas}}}/u_{50_{\text{pred}}}$ is bin averaged with respect to the stability parameter $10/L$ for different methods to derive L . This can be compared to Figure 5.3, where the same is shown without correction. It can be seen that the deviations on the stable side are reduced considerably for all three methods. Especially for the gradient method the deviation is greatly reduced since with this method the proposed wind speed profile with correction for thermal influences is used twice: in the calculation of L and in the prediction of the 50 m wind speed. For the sonic method also the deviation in the unstable regime decreases. This is due to the fact that some records with large deviations and $Bu > 30$ are erroneously regarded as unstable by the sonic method, probably due to the large measurement uncertainty and sampling variability of the friction velocity.

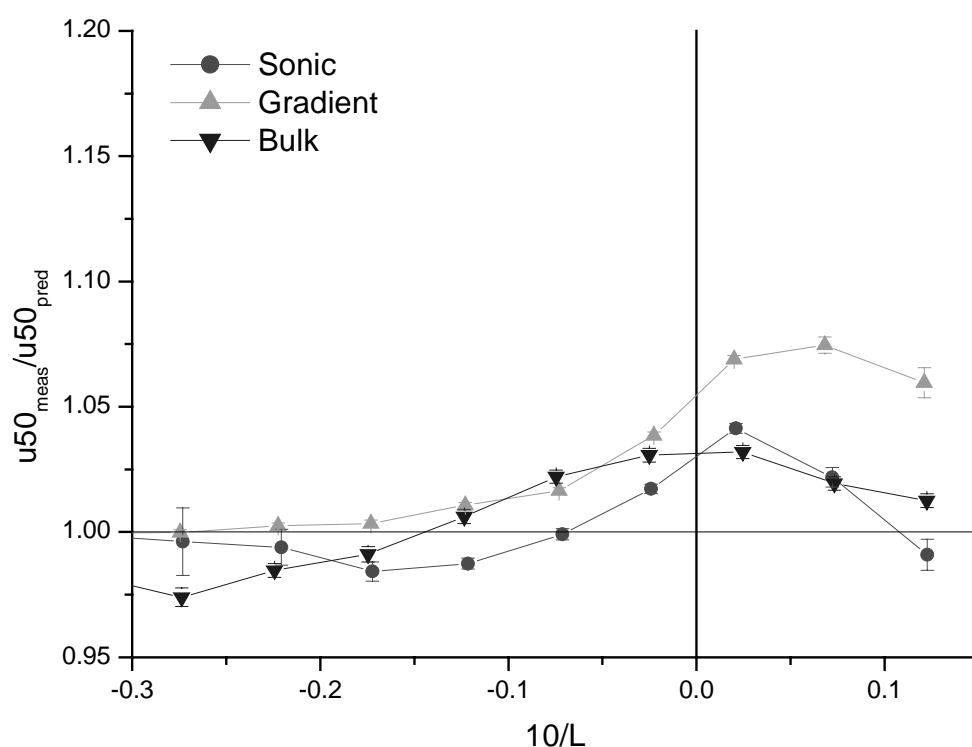


Figure 5.7: Bin-averaged ratio of measured and predicted 50 m wind speed versus stability parameter $10/L$ with L determined by the sonic, gradient and bulk methods and z_0 with Charnock model; the proposed correction method for thermal influences is used

Figure 5.8 shows the ratio $u_{50_{\text{meas}}}/u_{50_{\text{pred}}}$ versus wind speed as in Figure 5.5, but with the proposed wind profile correction. It can be seen that the reduction of the deviation is largest for small wind speeds. This is due to the fact that the inversion height after Csanady is proportional to the friction velocity squared (see eq. (5.15)). Since the correction is inversely proportional to h , it decreases with increasing wind speed. However, comparing Figure 5.8 with Figure 5.5 it should be noted that the correction is effective for wind speeds up to 12 ms^{-1} .

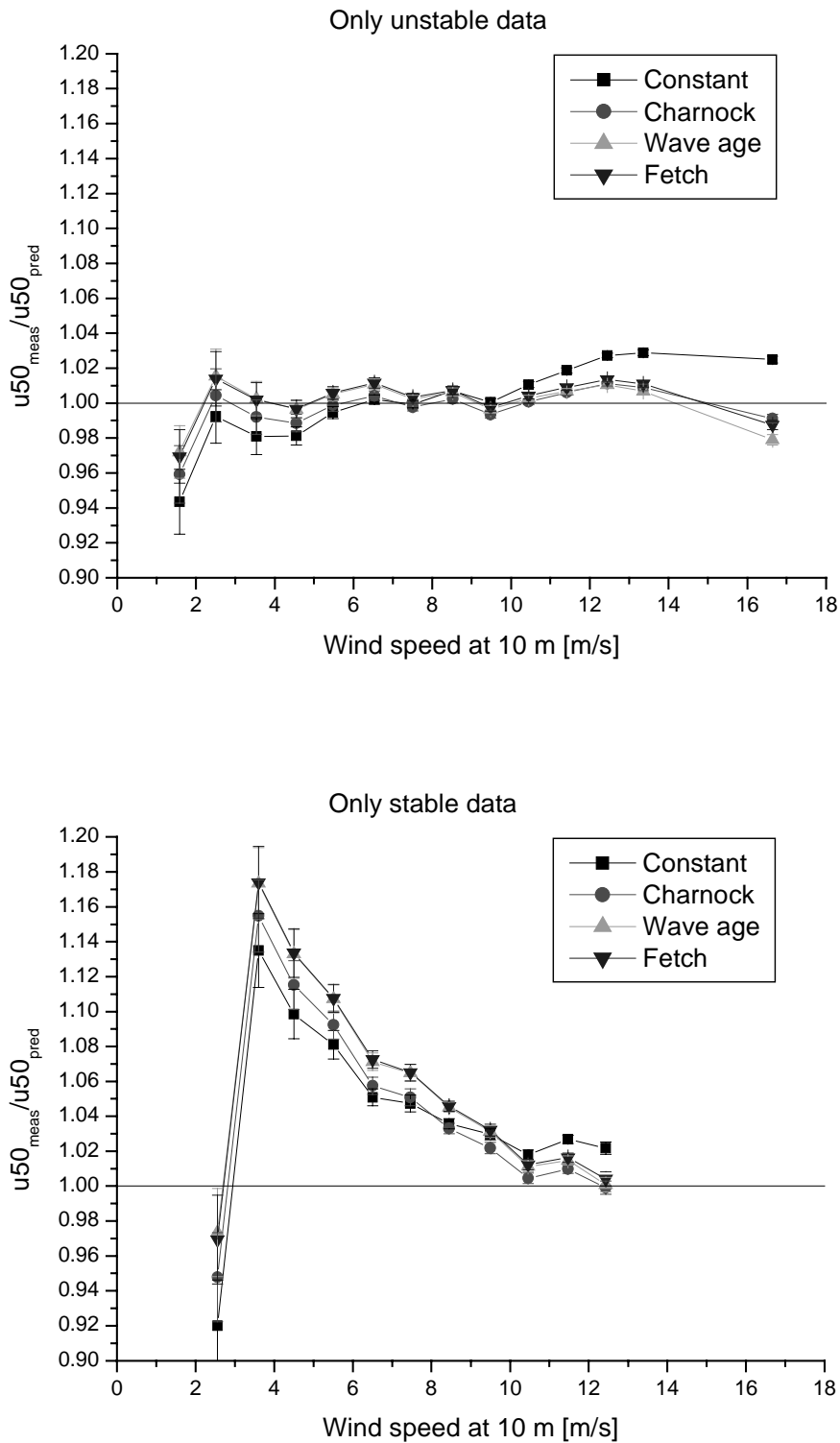


Figure 5.8: Bin-averaged ratio of measured and predicted 50 m wind speed versus wind speed at 10 m height with L determined by the bulk method and z_0 modelled with four different models (see text); the proposed correction method for thermal influences is used

5.5 Predictions of power production

So far, different methods to derive the stability parameter L , different models for the sea surface roughness and a simple wind profile correction for the influence of a thermally modified flow regime have been discussed. In the context of wind energy utilisation it is important to know, which impact these different approaches have for the prediction of the power output of an offshore wind turbine. It is not only important how large an effect like e.g. the fetch dependence of the sea surface roughness is, but also how frequent it occurs and at which wind speed.

This is investigated in an example application: the power production of an example wind turbine with hub height 50 m and 1 MW rated power output (see Figure 5.9 for the power curve) is estimated from the wind speed measurement at 10 m height using the different methods and models described in the previous sections. The estimated production is then compared with that obtained by using the measured wind speed at 50 m height. The background for this example is that often wind speed measurements are made at meteorological masts, which are lower than the hub height of the proposed turbines. These need to be extrapolated to hub height for the prediction of the power production.

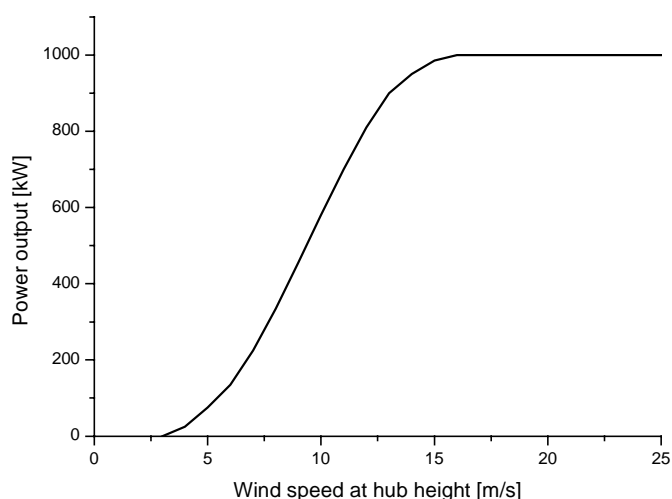


Figure 5.9: Power curve of the example wind turbine

5.5.1 Comparison of different methods

The measured wind speed at 10 m height is extrapolated to hub height and converted to power output with the power curve of the example turbine. For the extrapolation to hub height different methods are used for:

- derivation of the Monin-Obukhov length L : Sonic method, gradient method and bulk method (see section 5.3.1)
- modelling the sea surface roughness z_0 : constant roughness, Charnock relation, wave age model, fetch model (see section 5.3.2)
- simple wind profile correction for deviations from Monin-Obukhov theory for warm air advection from land (see section 5.4)

The resulting mean of the power output is compared to that derived from the measured wind speed at 50 m (hub height).

The mean power output for the data set derived from the measured wind speed at hub height (50 m) is 498 kW. This is compared to the power output estimated from the extrapolation of the wind speed from 10 m measurement height to hub height. The result is shown in Table 5.3. In Figure 5.10 the power output prediction error, defined as $(P_{\text{pred}} - P_{\text{meas}})/P_{\text{meas}}$, is shown for all extrapolation methods.

Table 5.3: Comparison of the impact of different methods to predict the wind speed at 50 m height from 10 m on the estimation of the power production of an example wind turbine; the mean power output derived from the wind measurement at 50 m height is 498 kW

	Mean power output without correction [kW]	Mean power output with correction [kW]
L from Sonic method		
Constant	471	483
Charnock	473	484
Wave age	467	478
Fetch	466	478
L from Gradient method		
Constant	456	473
Charnock	458	474
Wave age	453	468
Fetch	452	467
L from Bulk method		
Constant	469	481
Charnock	471	483
Wave age	465	476
Fetch	465	476

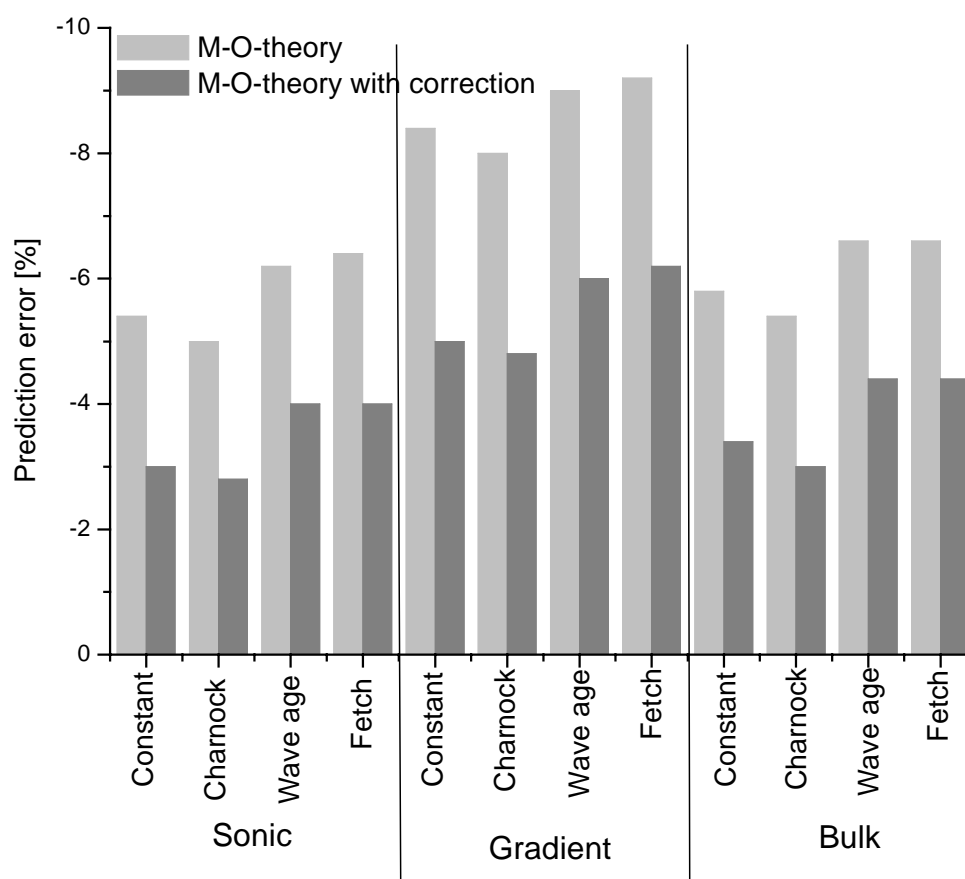


Figure 5.10: Error in power output prediction $(P_{meas}-P_{pred})/P_{meas}$ of an example turbine for the Rødsand data set; different methods to extrapolate the wind speed measurement at 10 m height to 50 m are used (see text)

The estimated production with wind speed extrapolation is lower than that using the measured wind speed at hub height in all cases with errors ranging from 3% to 9%. Significant differences are found for the performance of the different methods to derive the Monin-Obukhov length L : The results for the sonic and bulk methods are almost equal with about 3-6% and 3-7% error, respectively, but the results obtained with the gradient method show larger errors of 5-9%. For the different sea surface roughness methods it can be seen that the constant roughness assumption and the Charnock relation lead to almost equal results. Equally, there is almost no difference between the wave age and the fetch models, which show a slightly (about 1%) higher error. The correction method for the wind speed profile leads to a significant reduction in the prediction error in all cases. For the sonic and bulk methods the error is reduced by about 2%, while for the gradient method a reduction of about 3% is obtained.

The variation of the absolute prediction error with stability can be seen in Figure 5.11 for the three methods to derive L with and without applying the correction for flow with inversion layer from section 5.4. The difference between predicted and measured power output has been bin averaged with respect to the stability parameter $10/L$. Without correction, both the gradient and bulk methods show large errors for stable

stratification. This shows that situations with stable stratification are important for the estimation of the power output of an offshore wind turbine, even though the wind speeds are on average smaller than for near-neutral conditions. The simple correction for the flow modification due to the land-sea transition is shown to have an important impact on the absolute power production estimation, since it improves the estimation significantly for stable conditions.

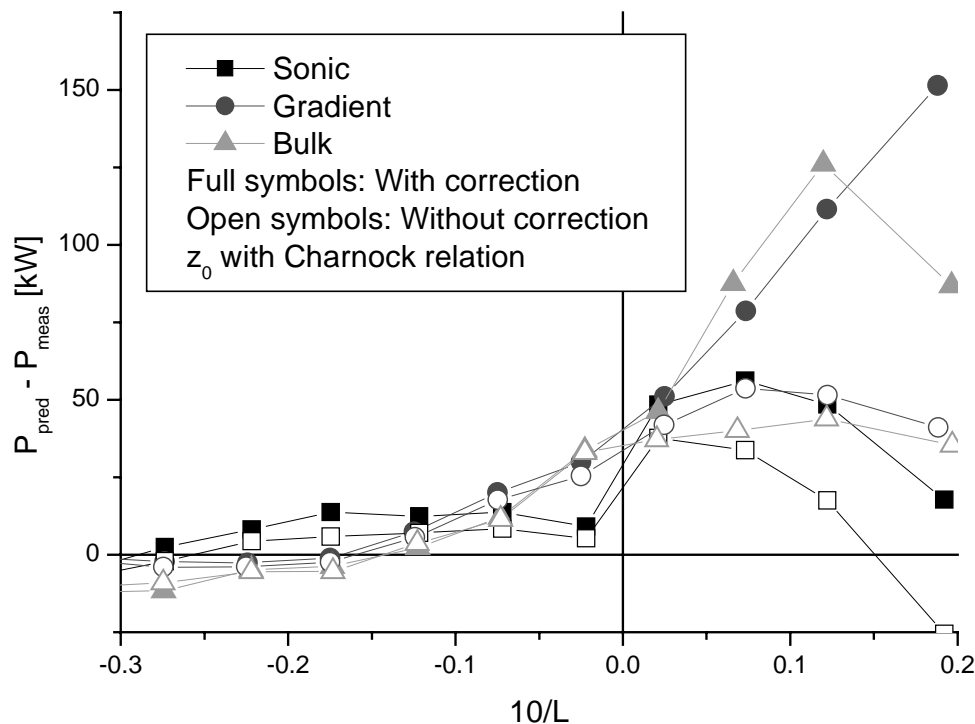


Figure 5.11: Difference between predicted and measured power output, bin averaged for stability parameter $10/L$; L derived with Sonic, Gradient and Bulk methods; Prediction with and without wind profile correction

Figure 5.12 shows the variation of the absolute prediction error with wind speed. The difference between predicted and measured power output has been bin averaged with respect to wind speed bins of 1 m/s. The four roughness models (see section 5.3.2) have been used with the bulk method to derive L with correction. The estimation errors are most important in the wind speed range 5-9 m/s, while for wind speeds in the range of 9-13 m/s both wind speed and power output estimation show only small errors. For very low and very high wind speeds no prediction error occurs, since for lower wind speeds the power production is small and so is the absolute error. For very high wind speeds above 13 m/s the decreasing steepness in the power curve reduces the impact of errors in wind speed estimation on power production estimation.

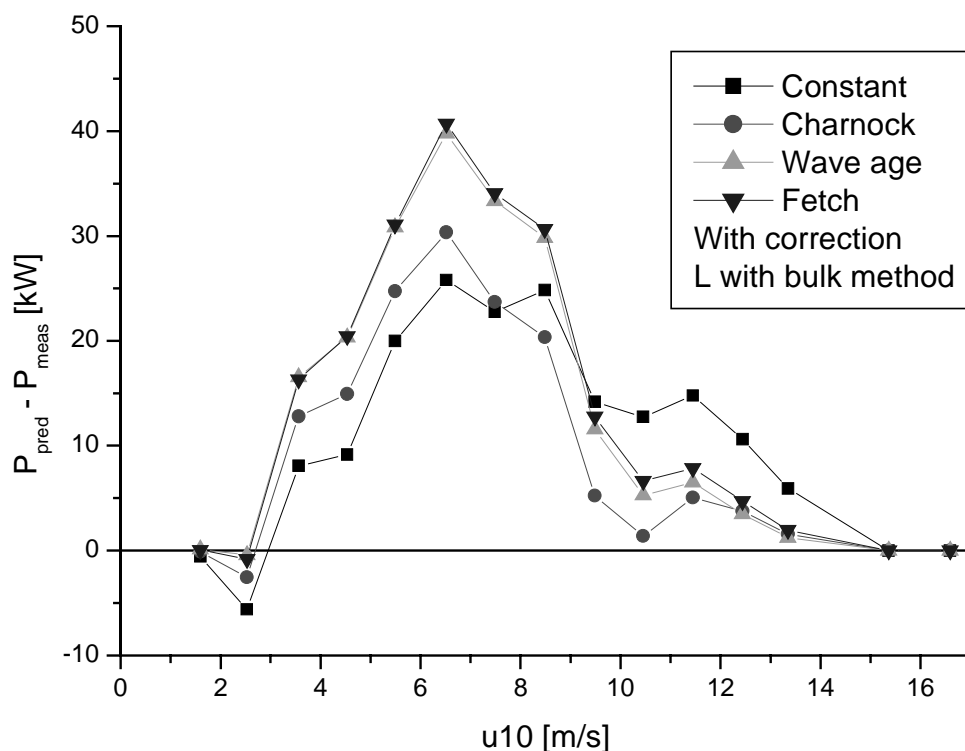


Figure 5.12: Difference between predicted and measured power output, bin averaged for 10 m wind speed; Comparison of different models for with wind profile correction

5.5.2 Comparison with results from a longer time series

The results obtained above are compared with those from a data set of a one year long time period, where only part of the measurements are available. Therefore the sonic method to derive L and the wave age model for z_0 can not be used. They are shown in Figure 5.13.

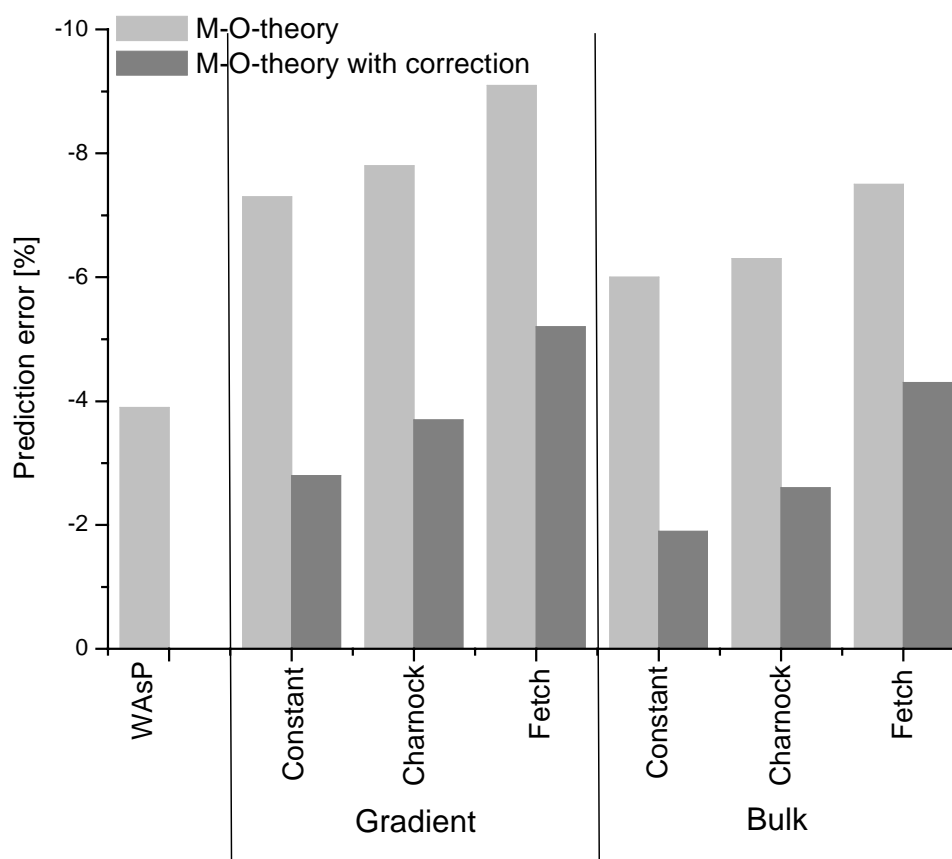


Figure 5.13: Error in power output prediction $(P_{meas}-P_{pred})/P_{meas}$ of an example turbine for the 2 year long Rødsand data set; different methods to extrapolate the wind speed measurement at 10 m height to 50 m are used (see text); the result with the WAsP method is also shown

Compared to the result of the short time series (Figure 5.10) the overall picture remains unchanged. The mean production derived from the measurement at hub height is slightly smaller. Equally, the prediction errors are slightly smaller, while the comparison of the different methods shows the same overall picture as before. This shows that the effects found are not due to unusual conditions during the measurement period, but are at least qualitatively representative.

5.5.3 Comparison with the wind resource estimation program WAsP

The results are also compared with the mean power production calculated with the wind resource assessment program WAsP in Figure 5.13. For the WAsP calculations, the same data as for the extrapolation with the different methods have been used, i.e. the wind speed measurements at 10 m height. The estimated mean production with WAsP is about 4% lower than that derived from the wind speed measurements at hub height.

When no correction is applied for wind profile correction, the extrapolation methods described above show a higher prediction error than WAsP, even though the

atmospheric stability and sea surface roughness are estimated for each record, while the WAsP method uses a mean profile.

The WAsP method assumes a constant sea surface roughness and a slightly stable mean atmospheric stability. This means that the mean stability used in WAsP for the site Rødsand leads on average to better results than the actually measured atmospheric stability.

As could also be seen from Figure 5.10, the prediction error is smaller for the bulk than for the gradient method. This is due to the influence of the flow regime with inversion layer on the profiles, which leads to a larger error in the estimation of L .

For the sea surface roughness modelling there is little difference between the constant roughness assumption, as also used by WAsP, and the use of the Charnock relation. The fetch model for the roughness leads to an increased error.

The prediction accuracy is improved greatly when the simple correction for the wind profile is applied. With this correction, the bulk method to derive L and the constant roughness assumption, the predicted mean power production error is less than 2%. This shows that a large part of the prediction error found in all methods is due to the modified wind profile stemming from a flow regime of a mixed layer with capping inversion.

5.6 Conclusion

Models to describe the flow regime in the coastal zone have been compared with data from the Rødsand measurement program in the Danish Baltic Sea. Focus of the investigation has been the description of the vertical wind speed profile for resource assessment in offshore wind power utilisation.

The vertical wind profile has been described by Monin-Obukhov theory and different models have been applied for the estimation of the two parameters used in this description: the Monin-Obukhov length and the sea surface roughness. For near-neutral and stable stratification large deviations from the measurements have been found in all cases. These are believed to be due to the inhomogeneous flow situation near the land-sea discontinuity. To investigate the importance of this effect for wind resource assessment, a simple correction method has been developed for the vertical wind speed profile.

To test the different models, the wind speed at 50 m height has been extrapolated from the measurement at 10 m height. To investigate the importance of the differences for wind power output estimations, the extrapolated wind speeds have also been converted to power production estimates. The following options have been used for extrapolation:

- Three different methods to derive the Monin-Obukhov length have been used, which utilise different measured quantities.
- Four sea surface roughness models of different complexity have been tested.
- A simple correction term has been applied in the equation of the vertical wind speed profile to account for the modification of the wind speed profile in a flow regime of a mixed layer capped by an inversion.

The three different methods to derive L from the measurements were found to disagree for stable atmospheric conditions. This is believed to be a consequence of the

flow regime with mixed layer capped by an inversion. Monin-Obukhov theory is not applicable here. The largest differences were found for the method deriving L via the Richardson number from measured profiles of temperature and wind speed. This is explained by the large difference in these profiles in the modified flow from usual Monin-Obukhov theory. Consequently, the simple correction method for the flow regime improved these results most. The derivation of L from sonic measurements (u_* and $w'T'$) or from bulk measurements ($T_{\text{sea}}, T_{\text{air}}, U$) showed less strong deviations.

The difference between the different models for the sea surface roughness is small compared to differences of other model choices. The simplest assumption of a constant roughness was found to be sufficient for the purpose of wind resource assessment. The reason is that errors of this method first become important at high wind speeds, where the power curve of the turbine is flat. Therefore the wind speed prediction errors do not lead to errors in production estimation. Compared to the assumption of constant roughness, the Charnock relation does not lead to improvements in power output prediction. The more complex sea surface roughness models based on wave age dependency were found to actually increase the prediction error.

When the usual Monin-Obukhov profile is used, the wind shear in the surface layer is under-estimated at the Rødsand site by all models for L and z_0 , when the atmospheric stratification is near-neutral or stable and the fetch is long (>30 km). In contrast, all models showed reasonable results for unstable stratification. Also for wind directions with short fetch (<20 km) the deviations for near-neutral and stable conditions are at least smaller.

This effect is believed to be due to a certain flow regime, developing when warmer air is blown from land over a colder sea. At some distance behind the coastline a flow regime develops, which consists of a mixed layer at the surface, capped by an inversion layer. In such a flow regime Monin-Obukhov theory is no longer applicable.

A simple correction term has been applied in the equation of the vertical wind speed profile (see eq.):

$$u(z) = \frac{u_*}{\kappa} \left[\ln\left(\frac{z}{z_0}\right) - \Psi_m\left(\frac{z}{L}\right) + c \frac{z}{h} \right] \quad (5.17)$$

Here h is the height of the inversion and c is an empirical constant, estimated to $c=4$ by a fit to the Rødsand data.

The predictions of the wind speed profile have been repeated with the different models for sea surface roughness and Monin-Obukhov length. For the Rødsand data it is found that this simple correction leads to a clear improvement of the predictions for stable conditions. It has also been shown that this effect occurs at wind speeds (predominantly 5-9 m/s), which are important for power production with wind turbines. More than half of the error in the prediction of the mean power output of an example turbine was due to this effect.

The mean power output estimation made by extrapolation of the wind speed measurements from 10 m to 50 m height with the different methods was also compared with the standard WAsP method. The WAsP extrapolation yielded a 4% too low mean power output. This was slightly less than for the best methods using Monin-Obukhov theory. This shows that the very simple assumption of a constant roughness made in WAsP does not lead to important errors. The assumption of a mean

atmospheric stability performed even better than the use of the actually measured time series of stability conditions. However, the flow modification at the coastline leading to a mixed layer flow with capping inversion is the main cause of the prediction error. The error was reduced to only 2% when the proposed simple correction was applied.

From these findings it is concluded that the wind resource estimation at offshore sites is more complex than usually believed. Not only the variable sea surface roughness, the determination of the atmospheric stability and the growth of the internal boundary layer complicate the situation, but also the land-sea discontinuity can lead to a special flow situation far offshore. In this flow regime the wind speed increases more rapidly with height than predicted by Monin-Obukhov theory. It should be noted that these deviations, although caused by the coastal discontinuity, were found far offshore for fetches of 30 to 100 km.

Currently these conclusions can be drawn for the site Rødsand only and need to be validated with other measurements. But from this example it can be seen that the flow modification in conditions of warm air advection from land plays an important role in the flow regime at offshore sites. At Rødsand this is the dominating uncertainty in the description of the wind conditions. Other sources of uncertainties, like the derivation of L , can not be understood without taking this into account. We expect that a better understanding of this effect is a prerequisite for future improvements in the description of the wind regime over the coastal zone.

To improve the wind resource estimation for offshore sites, a model for the flow regime in conditions of warm air advection from land over sea is needed. The simple correction method introduced in this paper is intended to show the importance of the effect, but can not be used as a general model of the flow regime. Further development with data from additional sites is needed. Until such a model is available, measurements at or close to hub height are necessary for an accurate estimation of the wind resource of an offshore location.

Acknowledgements

The original instrumentation and maintenance of the Rødsand measurement station were funded by the EU-JOULE program and the Danish Energy Ministry's UVE program 'Offshore Wind Resources'. Subsequent instrumentation, operation and maintenance were funded by SEAS Distribution A.m.b.A. The technical support team at Risø, particularly Ole Frost Hansen, are acknowledged for their contribution to the data collection. Mr Kobbarnagel of Sydfalster-El performed the maintenance and data collection at Rødsand.

References

- [5.1] Charnock H. Wind stress over a water surface. *Quart. J. Roy. Meteor. Soc.*, Vol. 81(1955) p. 639-640.
- [5.2] Johnson HK, Højstrup J, Vested HJ, Larsen SE. On the Dependence of Sea Surface Roughness on Wind Waves. *J. Phys. Oceanogr.*, Vol. 28 (1998) p. 1702-1716.
- [5.3] Taylor PK, Yelland MJ. The dependence of sea surface roughness on the height and steepness of the waves. *J. Phys. Oceanogr.*, Vol. 31 (2001) p. 572-590.

- [5.4] Lange B, Højstrup J, Larsen SE, Barthelmie RJ. A fetch dependent model of sea surface roughness for offshore wind power utilisation. Proceeding of the European Wind Energy Conference 2001, Copenhagen, Denmark (2001) p. 830-833.
- [5.5] Garratt JR. The atmospheric boundary layer. Cambridge, Cambridge University Press. (1994).
- [5.6] Edson JB. Fairall CW. Similarity relationships in the marine atmospheric surface layer for terms in the TKE and scalar variance budgets. J. Atmos. Sci. Vol. 55 (1998) p. 2311-2328.
- [5.7] Källstrand, B., H. Bergström, J. Højstrup and A.-S. Smedman: Mesoscale wind field modifications over the Baltic Sea. Boundary-Layer Meteorology Vol. 95 (2000) p. 161-188.
- [5.8] Frank, H. P., S. E. Larsen and J. Højstrup: Simulated wind power off-shore using different parameterisations for the sea surface roughness. Wind Energy Vol. 3 Issue 2 (2000) p. 67-79.
- [5.9] Csanady GT. Equilibrium theory of the planetary boundary layer with an inversion lid. Boundary-Layer Meteorol. Vol. 6 (1974) p. 63-79.
- [5.10] Troen, I. and E. L. Petersen: European Wind Atlas. Roskilde, Risø National Laboratory, Denmark (1989).
- [5.11] Mortensen, N. G., Landberg L., Troen, I., and Petersen, E. L.: Wind Analysis and Application Program (WASP) - User's Guide, Report Risø-I-666(EN) (v.2), Risø National Laboratory, 4000 Roskilde, DK, (1993) 133 pp.
- [5.12] Matthies, H.G., A.D. Garrad: Study of Offshore Wind Energy in the EC. Executive Summary. Report: Joule 1 (JOUR 0072), Part 1 of 5 Volumes. (1993) p. 1-13
- [5.13] Lavagnini, A., S. Martorelli and L. Cavaleri: The wind climatology of the Adriatic Sea deduced from coastal stations. Il Nuovo Cimento Vol. 19(C1) (1996) p. 37-50.
- [5.14] Halliday, J. A., G. M. Watson, J. P. Palutikof, T. Holt, R. J. Barthelmie, J. P. Coelingh, L. Folkerts, E. J. v. Zuylen and J. W. Cleijne: POWER - A methodology for predicting offshore wind energy resources. European Wind Energy Conference 2001, Copenhagen, Denmark (2001).
- [5.15] Enger, L.: Simulation of dispersion in a moderately complex terrain. Part A. The fluid dynamic model. Atmos. Environ. Vol. 24A (1990) p. 2431-2446.
- [5.16] Bergström, H. and R. Barthelmie: Offshore boundary-layer modelling. Global Windpower Conference 2002, Paris, France (2002).
- [5.17] Lange, B. and J. Højstrup: Evaluation of the wind-resource estimation program WASP for offshore applications. Journal of Wind Engineering and Industrial Aerodynamics Vol. 89 (2002) p. 271-291.
- [5.18] Lange B, Barthelmie RJ, Højstrup J. Description of the Rødsand field measurement. Report Risø-R-1268, Risø National Laboratory, 4000 Roskilde, DK, (2001) 60 pp.
- [5.19] Lange B, Larsen S, Højstrup J, Barthelmie R.: The influence of thermal

- effects on the wind speed profile of the coastal marine boundary layer. submitted to *Boundary-Layer Meteorol.*
- [5.20] Højstrup J.: Vertical Extrapolation of Offshore Windprofiles. Wind energy for the next millennium. Proceedings. 1999 European wind energy conference (EWEC '99), Nice (FR). Petersen, E.L.; Hjuler Jensen, P.; Rave, K.; Helm, P.; Ehmann, H., Eds., (1999) p. 1220-1223.
- [5.21] Schotanus, P.: Temperature measurement with a sonic anemometer and its application to heat and moisture fluxes *Boundary-Layer Meteorol.* Vol. 26 (1983) p. 81-93.
- [5.22] Geernaert G, Larsen S: On the role of humidity in estimating marine surface layer stratification and scaterometer cross section *J. Geophys. Res.* Vol. 98(C1) (1993) p. 927-932.
- [5.23] Larsen, SE: Observing and modelling the planetary boundary layer. Raschke E, Jacob D (eds.). *Energy and water cycles in the climate system. NATO ASI series I, volume 5, Springer-Verlag, Berlin, Heidelberg, (1993) p. 365-418.*
- [5.24] Businger JA, Wyngaard JC, Izumi Y, Bradley EF. Flux-profile relationships in the atmospheric surface layer. *J. Atmos. Sci.* Vol. 28 (1971) p. 181-189.
- [5.25] Högström, U: Nondimensional wind and temperature profiles. *Boundary-Layer Meteorol.* (1988) Vol. 42 p. 55-78.
- [5.26] Grachev AA, Fairall CW: Dependence of the Monin-Obukhov stability parameter on the bulk Richardson number over the Ocean. *J. Appl. Meteor.* Vol. 36 (1997) p. 406-414.
- [5.27] Wu J: Wind-stress Coefficients over Sea Surface near Neutral Conditions – A Revisit. *J. Phys. Oceanogr.* Vol. 10 (1980) p. 727-740.
- [5.28] Kahma KK, Calkoen CJ: Reconciling discrepancies in the observed growth of wind-generated waves. *J. Phys. Oceanogr.* Vol. 22 (1992) p. 1389-1405.
- [5.29] Smedman AS, Bergström H, Grisogono B: Evolution of stable internal boundary layers over a cold sea. *J. Geophys. Res.* Vol. 102(C1) (1997) p. 1091-1099.
- [5.30] Tjernström M, Smedman AS: The vertical turbulence structure of the coastal marine atmospheric boundary layer. *J. Geophys. Res.* Vol. 98(C3) (1993) p. 4809-4826.

6 Summary and Conclusion

An accurate estimation of the offshore wind resource requires detailed knowledge about the meteorological processes governing the wind flow in the marine atmospheric boundary layer. Models for the interaction of the wind flow with the underlying sea surface have been developed for the open ocean, where wind and wave fields only interact with each other. Offshore wind power utilisation, however, will take place in the coastal zone of the oceans. Here additionally the influence of the land-sea discontinuity on wind and wave fields has to be taken into account. It causes the wind flow to be not in equilibrium with the momentum and heat transfer at the surface. From a meteorological point of view this makes the modelling of the coastal marine boundary layer a complex and challenging task. An additional problem is that simultaneous measurements of meteorological and oceanographic data in the coastal zone are scarce. In Denmark such measurements were established as part of the offshore wind power utilisation program. In this study mainly data from the Rødsand measurement program have been used, which is located in the Danish Baltic Sea and experiences a wide range of fetch conditions from 10 to 100 km. A large database of meteorological data from a 50m high mast as well as simultaneously measured oceanographic data has been analysed.

This thesis is concerned with modelling the structure of the marine atmospheric boundary layer with an emphasis on evaluating micrometeorological models for the use in wind resource estimation for offshore wind farms. As a starting point the standard method for this has been evaluated. Two topics have been identified which are of main importance for resource estimation and where the physical conditions offshore differ from those on land: 1. The dependence of the aerodynamical roughness of the sea surface on wind speed and fetch. 2. The modification of the flow regime due to thermal effects in the coastal zone. Basic meteorological research has been undertaken to improve the knowledge about these effects. The third main topic of this thesis is the application of the results of this research to the case of offshore wind resource assessment. In the following, results and conclusions of this work are summarised first for the two meteorological aspects and thereafter for offshore wind resource modelling.

The first meteorological aspect dealt with is the modelling of the *aerodynamical roughness of the sea surface*. Most research in this area concentrates on improving the Charnock relation for conditions, where wind and waves are not in equilibrium. During the last 30 years considerable effort has been devoted to this question and a variety of model approaches have been proposed. The aim of this study is a critical analysis of the approach most often used, which is the parameterisation of the Charnock parameter with wave age.

With data from the measurement program at Rødsand an increase of the Charnock parameter with inverse wave age is found, which can be described by a power law relation. Different coefficients for this relation found in the literature can probably be explained by self-correlation effects and differences in data selection and analysis. While the existence of the trend seems clear, the significance of it is not. The parameterisation of sea surface roughness with wave age is severely influenced by spurious correlation, i.e. by self-correlation of the friction velocity, which enters into both sides of the power law relation. This questions the significance of the power law and its usefulness for improving the Charnock relation for sea surface roughness by

including wave age. The use of this relation in applications can therefore not be expected to yield large improvements compared to the Charnock relation.

Further studies with data from additional measurement sites are necessary to confirm these findings and to determine the importance of the physical information compared to self-correlation effects. The critical analysis done here for the wave age model should be extended to other proposed approaches with the aim of finding the model which best represents the physical dependencies between roughness and wave field. An aggregated data set compiled from measurements at different sites should be used for this analysis, in order to provide enough variability for all the critical parameters entering into the problem.

The second aspect of basic meteorological research treated in this thesis is the importance of *thermal effects for the wind flow in the coastal zone*. It has been shown that thermal effects, like e.g. low level jets, can modify the flow regime over large distances, e.g. over the entire Baltic Sea. So far mainly case studies using airborne as well as mast measurements have been used for the investigations. For wind resource assessment the question arises how much influence such effects have on the wind climatology, e.g. how often the wind field is significantly influenced by thermal effects.

Using the long-term measurement at Rødsand it is found that thermal effects can be important for the wind climatology and hence for wind resource assessment. The effects were found to occur systematically when warm air is advected from land over a long distance (>30km) of colder water to the site. Under this condition the wind shear is found to be larger than predicted with standard Monin-Obukhov theory. The deviations are more pronounced for large fetches (>30km) than for fetches of 10-20km, in contrary to the intuitive expectation that the importance of coastal influences decreases for increasing fetch.

A hypothesis for the qualitative explanation of this result is developed based on a published theoretical approach, which assumes that, when warm air is advected over a colder sea, an inversion lid with strongly stable stratification will develop at the top of the internal boundary layer. The heat flow through the inversion is small, while the air below the inversion is cooled continuously from the sea surface. It will eventually take the temperature of the sea and become a well-mixed layer with near-neutral stratification. In such a situation with strong height inhomogeneity of atmospheric heatflux Monin-Obukhov theory must fail. The smaller deviations for short fetches indicate that the inversion lid is less strongly developed for these fetches. The plausibility of this hypothesis has been tested with measured temperature data from eight upwind land stations and the water temperature at the site. The data support the view that the deviations found can be qualitatively explained with the proposed hypothesis. Furthermore, a simple correction method has been proposed to evaluate the magnitude of the effect for wind power applications.

Further research is needed to validate the findings and test the hypothesis. Data from different sites have to be analysed to ensure that the findings can be transferred to other locations. Upper air data are needed to evaluate the flow regime of the whole marine boundary layer and test the proposed explanation. Additionally, mesoscale modelling might help in understanding the effect. Finally, a micrometeorological model is needed, which describes the fluxes and profiles in the coastal marine boundary layer under conditions of warm air advection.

The importance of the above described physical processes for *wind resource modelling in the coastal offshore region* has been evaluated in this thesis. Despite of the complexity of the physical processes, which determine the offshore wind field, wind resource assessment for offshore wind power utilisation is currently performed with models developed for sites on land. Most commonly, the European Wind Atlas method with the wind resource estimation program WAsP (Wind atlas analysis and application program) is used. In an initial study of this thesis this method has been evaluated with measurements from three offshore sites. Deviations have been found for certain wind directions. For two sites, Rødsand and Omø Stålgrunde, this leads to deviations in the wind resource prediction. The simplified assumptions for roughness and stability used in WAsP have been compared with more complete meteorological models. For resource estimation, the effects have been evaluated in their climatological significance and influence on power production of wind turbines.

For the Rødsand site the use of more advanced models for sea surface roughness did not improve the wind resource estimation significantly. The reason is that sea surface roughness is not of main importance for wind resource estimation, at least for sites like Rødsand, where the minimum fetch is larger than 10 km. This means that the sea surface roughness will not deviate significantly from the simple models in the wind speed range important for wind resource estimation. Further validation of this result with data from other locations is necessary, especially for sites with shorter fetch. Here the influence of fetch on the wave field can be expected to be larger for the wind speed range important for wind resource estimation. Although it has been found that sea surface roughness modelling is of minor importance for wind resource estimation, it is important in other fields, like wave modelling and climate modelling. It can also be expected to be important for other questions for wind power utilisation, e.g. in the description of conditions of extremely high wind speeds.

Thermal effects caused by the land-sea discontinuity have been found to be of main importance for wind resource assessment in the coastal zone. They modify the flow in situations with warm air advection. In such situations, which have been shown to occur frequently at least at the Rødsand site, standard Monin-Obukhov theory can not be applied. To be able to quantify the importance of the deviations from Monin-Obukhov theory, a simple correction method to account for this effect has been developed and tested. It leads to a clear improvement of the wind speed and power output predictions.

Future research should be done with two complementary approaches: Flow modelling with mesoscale models is extremely costly in computation effort, but has already been demonstrated to work. The development of a simple micrometeorological model, i.e. an understanding and description of the phenomenon would allow simple calculations, but first needs to be developed.

Curriculum Vitae

- 27.9.1966 **Born in Bremen (D)**
- 1988 - 96 **Physics course** - University of Konstanz (D), University of Edinburgh (GB) and University of Oldenburg (D)
Diploma thesis (Diplomarbeit) in wind energy - University of Oldenburg: "Validation and Improvement of Wind Farm Models with Detailed Analysis of Power Output Measurements from Large Wind Farms – Comparison of a Simple Kinematic Model with a Method based on a Solution of the Reynolds Equations"
- 1994 - 97 **Work in wind power consultancy services and Teaching assistant for wind energy education** - University of Oldenburg (D)
- 1996 - 97 **Research assistant** - wind energy group at the University of Oldenburg (D)
- 1997: **Guest researcher** - Department of Wind Energy and Atmospheric Physics at Risø National Laboratory (DK)
- 1997 - 98 **Export project manager** - Wind World af 1997 A/S, Aalborg (DK)
- 1998 - 00 **Researcher** - Department of Wind Energy and Atmospheric Physics at Risø National Laboratory (DK)
EC Marie Curie Research Training Grant for the project: 'Description of the wind/wave interaction for offshore wind energy utilisation'.
Project leader for the study *Wind conditions for the offshore wind farm Utgrunden* and the Danish utilities' research project *Wind data base and wind models*.
Consultancy work in wind resource estimation and teaching experience in WAsP training courses in Denmark and Japan.
- 1998-02 **PhD study** - University of Oldenburg (D) / Risø Natinal Laboratory (DK)
- since 2000 **Freelance Consultant** - BL-Consult, Oldenburg (D)
International consulting work in data analysis and wind resource studies for wind power projects
- 2000-01 **Researcher** - Department of Energy and Semiconductor Physics at the University of Oldenburg (D)
Project leader for the EU-funded project ENDOW- Efficient Development of Offshore Windfarms

Publication List

Publications in scientific journals

Lange, B. and J. Højstrup: Evaluation of the wind-resource estimation program WAsP for offshore applications. in: *Journal of Wind Engineering and Industrial Aerodynamics*. Vol.89 (2001), issue 3-4; pp.271-291

Barthelmie, R., G. Larsen, H. Bergström, M. Magnusson, W. Schlez, K. Rados, B. Lange, P. Vølund, S. Neckelmann, L. Christensen, G. Schepers, T. Hegberg, L. Folkerts: ENDOW: Efficient Development of Offshore Windfarms. *Wind Engineering* vol. 25 (2002), no. 5; pp. 263-270

Rados, K., G. Larsen, R. Barthelmie, W. Schlez, B. Lange, G. Schepers, T. Hegberg, M. Magnusson: Comparison of Wake Models with Data for Offshore Windfarms. *Wind Engineering* vol. 25(2002), no. 5; pp. 271-280

Schlez, W, A. Umaña, R. Barthelmie, G. Larsen, K. Rados, B. Lange, G. Schepers, T. Hegberg: ENDOW: Improvement of Wake Models within Offshore Wind Farms. *Wind Engineering* vol. 25(2002), no. 5; pp. 281-288

G. Schepers, R. Barthelmie, K. Rados, B. Lange, W. Schlez: Large Off-Shore Windfarms: Linking Wake Models with Atmospheric Boundary Layer Models. *Wind Engineering* vol. 25(2002), no. 5; pp. 307-316

Lange, B., H.-P. Waldl, R. Barthelmie, A. G. Guerrero, D. Heinemann: Modelling of offshore wind turbine wakes with the wind farm program FLaP. Manuscript accepted by *Wind Energy*

Lange, B., H. K. Johnson, S. Larsen, J. Højstrup, H. Kofoed-Hansen: The dependence of sea surface roughness on wind-waves. Manuscript submitted to *Journal of Physical Oceanography*

Lange B, Larsen S, Højstrup J, Barthelmie R. The influence of thermal effects on the wind speed profile of the coastal marine boundary layer. Manuscript submitted to *Boundary-Layer Meteorology*

Recent conference publications (1999-2002)

Lange, B., H.-P. Waldl, R. Barthelmie, A. G. Guerrero, D. Heinemann: Improvement of the wind farm model FLaP for offshore applications. Proceedings of the World Wind Energy Conference, 2.-6.7.2002 Berlin, Germany (in print)

Lange, B., S. Larsen, J. Højstrup, R. Barthelmie, U. Focken: Modelling the vertical wind speed and turbulence intensity profiles at prospective offshore wind farm sites. Proceedings of the World Wind Energy Conference, 2.-6.7.2002 Berlin, Germany (in print)

Schlez, W., Barthelmie, R., G. Larsen, H. Jørgensen, K. Rados, H. Bergström, M. Magnusson, B. Lange, P. Vølund, S. Neckelmann, L. Christensen, G. Schepers, T. Hegberg, L. Folkerts: ENDOW: Efficient development of offshore windfarms. Proceedings of the World Wind Energy Conference, 2.-6.7.2002 Berlin, Germany (in print)

Lange, B., H.-P. Waldl, R. Barthelmie, A. G. Guerrero, D. Heinemann: Improvement of the wind farm model FLaP for offshore applications. Proceedings of the Global Windpower Conference, 2.-5.4.2002, Paris, France

Lange, B., S. Larsen, J. Højstrup, R. Barthelmie: Modelling the vertical wind speed and turbulence intensity profiles at prospective offshore wind farm sites. Proceedings of the Global Windpower Conference, 2.-5.4.2002, Paris, France

Barthelmie, R., G. Larsen, H. Bergström, M. Magnusson, W. Schlez, K. Rados, B. Lange, P. Vølund, S. Neckelmann, L. Christensen, G. Schepers, T. Hegberg, L. Folkerts: ENDOW: Efficient development of offshore windfarms. Proceedings of the Global Windpower Conference, 2.-5.4.2002, Paris, France

Lange, B., J. Højstrup and R. J. Barthelmie (2001). Evaluation of models for the vertical extrapolation of wind speed measurements at offshore sites. EWEA special topic conference on wind power, Brussels, 2001

Lange, B., J. Højstrup, S. E. Larsen and R. J. Barthelmie (2001). Comparison of sea surface roughness models for offshore wind power utilisation. EWEA special topic conference on wind power, Brussels, 2001

Barthelmie, R., G. Larsen, H. Jørgensen, M. Nielsen, P. Sanderhoff, H. Bergström, M. Magnusson, U. Hassan, W. Schlez, K. Rados, B. Lange, I. Waldl, P. Vølund, S. Neckelmann, T. Christensen, T. G. Nielsen, J. Højstrup, L. Christensen, G. Schepers, T. Hegberg, F. Ormel, P. Eecen, J. Coelingh, L. Folkerts and O. Stobbe (2001). Efficient development of offshore windfarms: a new project for investigating wake and boundary-layer interactions. Helm, P. and A. Zervos (eds.): Wind Energy for the new millennium. Proceedings of the European Wind Energy Conference, Copenhagen, Denmark, 2-6 July 2001; pp.657-660

Lange, B., J. Højstrup and R. J. Barthelmie (2001). Evaluation of models for the vertical extrapolation of wind speed measurements at offshore sites. Helm, P. and A. Zervos (eds.): Wind Energy for the new millennium. Proceedings of the European Wind Energy Conference, Copenhagen, Denmark, 2-6 July 2001; pp.834-837

Lange, B., J. Højstrup, S. E. Larsen and R. J. Barthelmie (2001). A fetch dependent model of sea surface roughness for offshore wind power utilisation. Helm, P. and A. Zervos (eds.): Wind Energy for the new millennium. Proceedings of the European Wind Energy Conference, Copenhagen, Denmark, 2-6 July 2001; pp.830-833

Rados, K., G. Larsen, R. Barthelmie, W. Schlez, U. Hassan, B. Lange, I. Waldl and M. Magnusson (2001). A comparison of wake model performances in an offshore environment Helm, P. and A. Zervos (eds.): Wind Energy for the new millennium. Proceedings of the European Wind Energy Conference, Copenhagen, Denmark, 2-6 July 2001; pp.781-784

Lange, B., J. Højstrup: Evaluation of empirical relations for the sea surface roughness of fetch-limited wind waves. 26. General Assembly of the European Geophysical Society, Nice (F), 19-23 Apr 1999. Geophys. Res. Abstr. (2001) vol. 3 , 4285

Lange, B. and J. Højstrup: The influence of waves on the wind resource in near-shore waters. In: Tagungsband. 5. German wind energy conference DEWEK 2000, Wilhelmshaven (DE), 2000. (Deutsches Windenergie-Institut GmbH, Wilhelmshaven), pp. 230-233

Lange, B. and J. Højstrup: The influence of waves on the offshore wind resource. In: Proceedings of the European Seminar OWEMES Offshore Wind Energy in Mediterranean and other European Seas. 13.-15. April 2000. Siracusa, Italy. pp.491-503

Lange, B.; Aagaard, E.; Andersen, P.-E.; Møller, A.; Niklasson, S.; Wickman, A., Offshore wind farm Bockstigen - installation and operation experience. In: Wind energy for the next millennium. Proceedings. 1999 European wind energy conference (EWEC '99), Nice (FR), 1-5 Mar 1999. Petersen, E.L.; Hjuler Jensen, P.; Rave, K.; Helm, P.; Ehmann, H. (eds.), (James and James Science Publishers, London, 1999) p. 300-303

Lange, B.; Højstrup, J., WAsP for offshore sites in confined coastal waters - the influence of the sea fetch. In: Wind energy for the next millennium. Proceedings. 1999 European wind energy conference (EWEC '99), Nice (FR), 1-5 Mar 1999. Petersen, E.L.; Hjuler Jensen, P.; Rave, K.; Helm, P.; Ehmann, H. (eds.), (James and James Science Publishers, London, 1999) p. 1165-1168

Lange, B.; Højstrup, J., The influence of waves on the offshore wind resource. In: Wind energy for the next millennium. Proceedings. 1999 European wind energy conference (EWEC '99), Nice (FR), 1-5 Mar 1999. Petersen, E.L.; Hjuler Jensen, P.; Rave, K.; Helm, P.; Ehmann, H. (eds.), (James and James Science Publishers, London, 1999) p. 1216-1219

Barthelmie, R.J.; Courtney, M.S.; Lange, B.; Nielsen, M.; Sempreviva, A.M.; Svenson, J.; Olsen, F.; Christensen, T., Offshore wind resources at Danish measurement sites. In: Wind energy for the next millennium. Proceedings. 1999 European wind energy conference (EWEC '99), Nice (FR), 1-5 Mar 1999. Petersen, E.L.; Hjuler Jensen, P.; Rave, K.; Helm, P.; Ehmann, H. (eds.), (James and James Science Publishers, London, 1999) p. 1101-1104

Lange, B.; Højstrup, J., Estimation of offshore wind resources - The influence of the sea fetch. In: Wind engineering into the 21. century. Vol. 3. 10. International conference on wind engineering (10. ICWE), Copenhagen (DK), 21-24 Jun 1999. Larsen, A.; Larose, G.L.; Livesey, F.M. (eds.), (A.A. Balkema, Rotterdam, 1999) p. 2005-2012

Geernaert, G.L.; Lange, B.; Astrup, P., Fetch dependent wind profile and drag coefficient over the coastal sea. 24. General Assembly of the European Geophysical Society, The Hague (NL), 19-23 Apr 1999. Geophys. Res. Abstr. (1999) 1 , 439

Recent reports (1999-2002)

Lange, B., R. J. Barthelmie and J. Højstrup: Description of the Rødsand field measurement. Report Risø-R-1268. Risø National Laboratory, DK-4000 Roskilde, Denmark. 2001

Lange, B.: Estimation of relative power production statistics for the wind farm Utgrunden. Internal report Risø-I-1665(EN). Risø National Laboratory 2000 31p.

Lange, B.: Correlation analysis for two wind measurements at Utgrunden lighthouse. Internal report Risø-I-1649(EN). Risø National Laboratory 2000 28p.

Lange, B.: One year standardised wind data of the measurement stations Risø, Tystofte, Omø Stålgunde, Gedser Rev and Rødsand. Internal report Risø-I-1632(EN). Risø National Laboratory 2000 14p.

Lange, B.: Data analysis of the Rødsand field measurement. Part I: Report & Part II: Time series plots of Rødsand measurement data. Internal report Risø-I-1631(EN). Risø National Laboratory 2000 74p. & 31p.

Lange, B., A.-M. Sempreviva, M. Nielsen: Prediction of power production and wind climate for the proposed off-shore wind farm Utgrunden. Risø internal report I-1514, 2000

Lange, B.: Estimation of the 10 m wind field behind the proposed wind farm Rødsand. Risø internal report I-1545, 2000

Lange, B.: A model study of fetch limited waves using MIKE 21 OSW (3G version). DHI internal report. (Danish Hydraulic Institute, Hørsholm, 2000) September 2000

Kofoed-Hansen, H.; Johnson, H.K.; Højstrup, J.; Lange, B., Wind-wave modelling in waters with restricted fetches (paper presented at 5. International workshop on wave hindcasting and forecasting, Melbourne, FL (US), 27-30 Jan 1998). In: Wind-wave interaction in fetch restricted coastal and shallow water environment. Final report. Kofoed-Hansen, H.; Vested, H.J.; Larsen, S.E.; Hansen, C. (eds.), (Danish Hydraulic Institute, Hørsholm, 2000) 16 p.

Lange, B.: Wind field prediction for three offshore areas as input for wave modelling. In: Wind-wave interaction in fetch restricted coastal and shallow water environment. Final report. Kofoed-Hansen, H.; Vested, H.J.; Larsen, S.E.; Hansen, C. (eds.), (Danish Hydraulic Institute, Hørsholm, 2000) 16 p.

Lange, B., H. K. Johnson, S. Larsen, J. Højstrup, H. Kofoed-Hansen: The dependence of sea surface roughness on wind-waves – Part I: Analysis of new field data. In: Wind-wave interaction in fetch restricted coastal and shallow water environment. Final report. Kofoed-Hansen, H.; Vested, H.J.; Larsen, S.E.; Hansen, C. (eds.), (Danish Hydraulic Institute, Hørsholm, 2000)

Johnson, H.K., B. Lange, H. Kofoed-Hansen: The dependence of sea surface roughness on wind-waves – Part II: Aggregated data set. In: Wind-wave interaction in fetch restricted coastal and shallow water environment. Final report. Kofoed-Hansen, H.; Vested, H.J.; Larsen, S.E.; Hansen, C. (eds.), (Danish Hydraulic Institute, Hørsholm, 2000) 16 p.

Sempreviva, A.M., B. Lange: Evaluation of power production from an offshore wind farm at Middelgrunden. Risø internal report I-1432, 1999

Barthelmie, R.J., M.S. Courtney, B. Lange, M. Nielsen, A.M. Sempreviva, J. Svenson, F. Olsen, T. Christensen: Offshore Wind Resources at Danish Measurement Sites. Internal report Risø-I-1339(EN). Risø National Laboratory 1998 89p. & 4 App.

Barthelmie, R.J., B. Lange, M. Nielsen: Wind Resources at Rødsand and Omø Stålrunde. Internal report Risø-I-1456(EN). Risø National Laboratory 1999 96p.